JPL PUBLICATION 82-78

The SIR-B Science Plan

Imaging Radar Science Working Group

December 1, 1982

National Aeronautics and
Space Administration

Jet Propulsion Laboratory
California Institute of Technology
Pasadena, California


OSTA-3
ORIGINAL PAGE
COLOR PHOTOGRAPH

JPL PUBLICATION 82-78

The SIR-B Science Plan

Imaging Radar Science Working Group

December 1, 1982

NASA
National Aeronautics and
Space Administration

Jet Propulsion Laboratory
California Institute of Technology
Pasadena, California

This publication was prepared by the Jet Propulsion Laboratory, California Institute of Technology, under a contract with the National Aeronautics and Space Administration.

National Aeronautics and
Space Administration

Washington, D.C.
20546

September 24, 1982

Reply to Attn of EL-4

Dear Colleague:

NASA has historically conducted pioneering research in the development of space technology for earth and planetary exploration. NASA's R&D efforts in earth applications are designed to understand the variety of information that can be derived from orbital measurements, and to apply proven space techniques to more basic studies of the Earth's resources and its environment. Earth applications research in the early and mid-1970's concentrated primarily upon the development of imaging techniques that obtain measurements in the visible and infrared portions of the electromagnetic spectrum. More recently, there has been increased interest in the development of radar imaging methods that can provide fundamentally different types of information about surface conditions on our planet. We currently view visible, infrared, and microwave techniques as being highly complementary, and expect to pursue future development of all three imaging methods.

Earth applications research in the 1980's will make extensive use of the Space Shuttle as an experimental platform for instrument development and data collection. The Shuttle is ideally suited for remote sensing research because it provides easy access to space and offers a convenient means of collecting experimental data throughout the world. The successful flight of the Shuttle Imaging Radar-A (SIR-A) on the second orbital mission of the Space Shuttle provided a conclusive demonstration of the utility of the Shuttle for remote sensing R&D.

Based in part on the results of the SIR-A experiment, NASA plans to launch an upgraded radar system called SIR-B during the summer of 1984. SIR-B will possess a new and unique set of orbital measurement capabilities that differ substantially from those of earlier sensor systems. The data collected by SIR-B is expected to have a wide variety of potential scientific applications in the fields of geography, geology, hydrology, oceanography, agronomy, and botany.

This Science Plan outlines various types of experiments that could potentially be performed with the SIR-B system. These different classes of experiments are designed to exploit SIR-B's measurement capabilities and the maneuvering capabilities of the Space Shuttle. This document is intended to stimulate creative thinking about how we can employ the SIR-B experiment to advance the current state-of-the-art of microwave remote sensing for earth applications. I invite you to share in the planning and execution of this exciting scientific project.

Jesse W. Moore
Director
Earth and Planetary Exploration Division
Office of Space Science and Applications

Abstract

The Shuttle Imaging Radar-B (SIR-B) will be the third in a series of spaceborne SAR experiments conducted by NASA which began with the 1978 launch of Seasat and continued with the 1981 launch of SIR-A. Like Seasat and SIR-A, SIR-B will operate at L-band and will be horizontally polarized. However, SIR-B will allow digitally processed imagery to be acquired at selectable incidence angles between 15 and 60 deg, thereby permitting, for the first time, parametric studies of the effect of illumination geometry on SAR image information extraction. This document presents a science plan for SIR-B and serves as a reference for the types of geoscientific, sensor, and processing experiments which are possible.

Executive Summary

The National Aeronautics and Space Administration (NASA) shuttle imaging radar experiments planned for this decade will greatly expand our understanding of the utility of radar imagery in relation to visible and infrared imagery and also will identify optimum configurations of future radar sensors for earth resources applications research. The next spaceborne radar mission will be the Shuttle Imaging Radar-B (SIR-B), scheduled for launch on the Shuttle Transportation System (STS-17) in the summer of 1984, as a part of the Office of Space and Terrestrial Applications (OSTA-3) experiment package.

This document presents a science plan for SIR-B and provides a general description of some novel and potentially very useful geoscientific, sensor, and processing experiments that will be possible. This plan is intended to not only serve as a reference for the types of experiments which are possible, to also but provide broad guidelines for the organization of the mission.

SIR-B will be the third in a series of spaceborne synthetic aperture radar (SAR) experiments conducted by NASA, which began with the 1978 launch of Seasat and continued with the 1981 launch of SIR-A. Like Seasat and SIR-A, SIR-B will operate at L-band and will be horizontally polarized. However, SIR-B will allow *digitally processed imagery* to be acquired at *selectable incidence angles between 15 and 60 degrees*, thereby permitting for the first time parametric studies of the effect of illumination geometry on SAR image information extraction. Since the incidence angle is a very important parameter in determining information content in SAR images, SIR-B will be a significant step in understanding the optimum viewing geometries for various applications.

This summary outlines some important scientific and technological experiments which can be conducted with SIR-B, including those in the geoscientific disciplines (Section 3), those concentrating on sensor performance and capabilities (Section 4), and those dealing with data processing and information extraction (Section 5). Due to the limited duration of the mission, it will not be possible to conduct all of these experiments, but the scope of potential experiments can be seen.

I. Geoscience Experiments

The geoscientific experiments are grouped according to discipline: geography, geology, hydrology, oceanography, and vegetation.

A. Geography

1. **Cartography.** Understand planimetric limitations of SIR-B; evaluate stereo-mode contour mapping and conformality (shape accuracy) of data; determine registration possible with multiple data sets; assess accuracy of SIR-B maps relative to National Map Accuracy Standards.

2. **Forest monitoring.** Estimate location and extent of clear-cutting and deforestation in developing areas where maps do not exist or are inaccurate; assess changes in forestation over 6-year period covered by Seasat, SIR-A, and SIR-B; assess utility of and assimilation techniques for radar data in global climate models.

3. **Geomorphology.** Quantitative assessment of potential of radar data for characterizing human impact on landscapes, as evidenced by changes in topography, drainage, roughness scales, landscape textures, etc.

4. **Land cover.** Identification of gross changes in rural and urban land cover; determine accuracy of detection of urban/rural fringe and urban expansion into farmland; provide quantification of radar backscatter from urban scenes.

B. Geology

1. **Structural mapping.** Regional structural studies using SIR-B multiangle images; optimum radar viewing geometry for structural studies and topographic mapping; comparison of structural information obtained by different sensor systems; extent of subsurface penetration in hyperarid regions.

2. **Lithologic mapping.** Discrimination and identification of surficial geological materials; combined utility of microwave and visible-infrared techniques for lithologic mapping; analysis of microwave image texture; regional variations in surface electrical properties.

C. Hydrology

1. **Surface water.** Study optimum illumination geometry for mapping of watershed boundaries; conduct stereo observations of watershed relief; determine extent and location of reservoirs, lakes, and ponds; provide regional overview of flood impact and damage; delineate drainage patterns for fluvial morphology studies; monitor shoreline and stream channel positions and immigrations.

2. **Water surface.** Discrimination of oil slicks and spills, and of floating and emergent vegetation areas such as coastal kelp beds; radar observations of surface manifestations of underwater obstructions and subsurface flow in rivers, river outflows, and shallow coastal waters.

3. **Soil moisture.** Determine optimum viewing geometry for observation of soil moisture over large areas, taking into account the confusing effects of slope, surface roughness, and vegetation cover.

4. **Glaciers.** Determine utility of SAR imagery to reveal glacial snowlines which provide estimates of glacial growth; differentiate between glacial ice, rock debris, and snow.

D. Oceanography

1. **Surface winds.** Use SIR-B as a pulse scatterometer to assess L-band response to surface winds.

2. **Wave structure.** Assess utility of spotlight-mode radar to measure full directional wave spectrum by observation of a limited portion of the 2-dimensional wave spectrum; use short-pulse range compression.

3. **Internal structure, upwelling, currents, and fronts.** Use multiangle radar imagery for observation of internal waves, including suitable surface truth; test sites for upwelling, currents, and fronts experiments should be selected independently.

4. **Bottom morphology.** Acquire extensive surface truth at several points in the tidal cycle for near-shore test sites to assess radar response to surface manifestations of bottom topography.

5. **Slicks and entrained materials.** Determine radar response to various incidence angles to natural slicks; use simultaneous surface observations and scatterometer observations to indicate degree of suppression of small waves.

6. **Coastal refraction and morphology.** Assess utility of multiangle radar imagery for measurement of refraction and diffraction for coastal morphology studies.

E. Vegetation

1. **Agricultural crops.** Acquire multiangle radar imagery to assess the effects of crop-canopy morphology on radar response, including the confusing effects of soil background, regional topography, regional planting and management practices, wind, and confusion crops; illumination geometry on crop separability.

2. **Forestry and rangeland.** Use multiangle SIR-B data to study effects of backscatter from tree and rangeland vegetation over soil backgrounds; illumination angles on separability of forest and rangeland vegetation; detection of occurrence of certain stages of growth in forest and rangeland vegetation; confusion effects due to topography; diurnal changes.

II. Sensor Experiments

SIR-B will offer an opportunity to conduct a number of controlled sensor experiments, which would provide valuable information for future sensor designs. These experiments include:

(1) Radiometric calibration

(2) Geometric calibration

(3) Target statistics

(4) Spotlight mode

(5) Squint mode

III. Correlation and Image-Processing Experiments

The digital processing of SIR-B data into image form will allow several valuable data processing experiments to be conducted, among them:

(1) Multilook processing

(2) Cartographic rectification

(3) Latitude-longitude resampling

(4) Data merging (of multiangle sets)

(5) Image domain filtering

The SIR-B Science Working Group

This science plan for SIR-B has been developed as a result of the first phase of activity of the NASA Imaging Radar Science Working Group (IRSWG), chartered on March 16, 1982 by authorization of the Associate Administrator for Space Science and Applications. The Charter requests that the IRSWG:

(1) Document the present state of knowledge with respect to radar imaging of the earth at variable incidence angles, frequencies, and polarizations.

(2) Identify areas where further fundamental research is needed in radar backscatter signatures of cover types and measurement of topography.

(3) Define a candidate series of radar remote sensing scientific experiments which take advantage of multiparameter imaging radars on a shuttle and other platforms.

(4) Evaluate the need for parallel developments in SAR image processing and image calibration, and information extraction techniques.

The first phase of the IRSWG activity has focused on SIR-B and the team supporting this study has been called the SIR-B Science Working Group. The purpose of the SIR-B SWG has been to produce a science plan which provides the information requested above, as it pertains to SIR-B.

The SIR-B SWG structure is shown below:

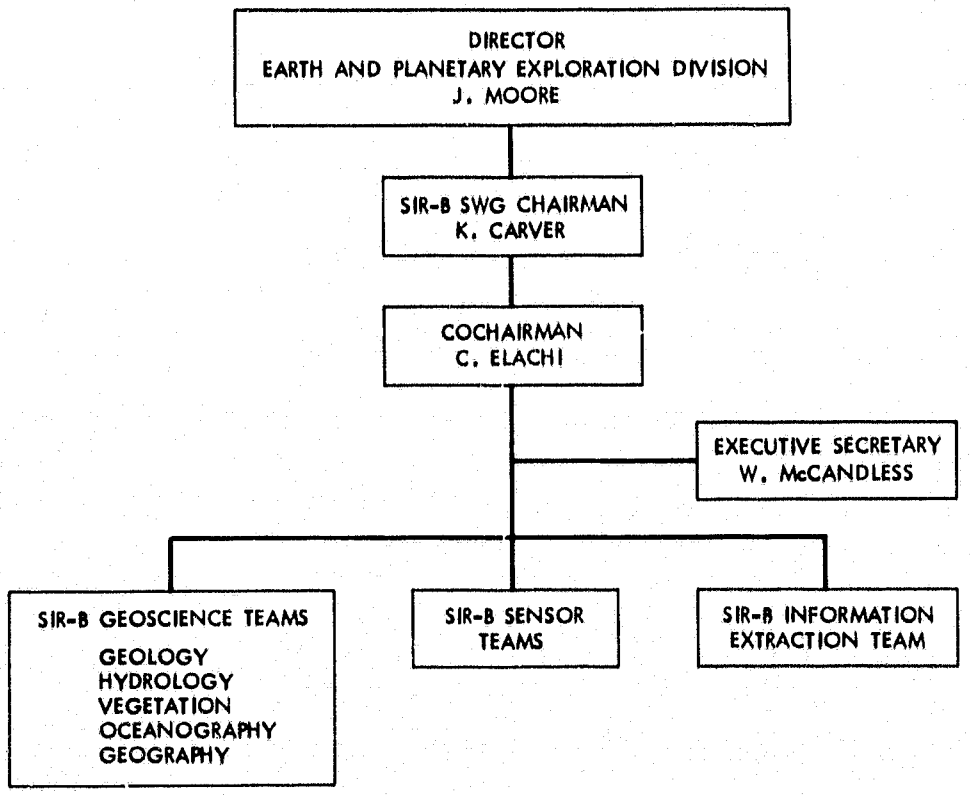

The SIR-B SWG was chaired by Keith Carver (NASA Headquarters) and cochaired by Charles Elachi of the Jet Propulsion Laboratory (JPL). Walt McCandless (User Systems, Inc.) served as Executive Secretary. Five geoscientific disciplines teams were formed:

Geology Team	Leader: Mark Settle, NASA HQ
Hydrology Team	Leader: Tom Schmugge, NASA Goddard Space Flight Center (GSFC)
Oceanography Team	Leader: Dick Moore, University of Kansas
Vegetation Team	Leader: Jack Paris, NASA Johnson Space Center (JSC)
Geography Team	Leader: Len Bryan, JPL

In addition, a SIR-B Sensor Team and a SIR-B Information Extraction (Data Processing) Team were formed:

Sensor Team	Leader: Dan Held, JPL
Information Extraction Team	Leader: Tom Bicknell, JPL

Three meetings of the SWG were held:

April 22-23, 1982	California Institute of Technology, Pasadena, California
May 10-11, 1982	Airlie House, Warrenton, Virginia
July 15, 1982	NASA Johnson Space Center, Houston, Texas

The first two of these meetings were used to develop a candidate series of SIR-B experiments, and the third to refine the resulting draft of the SIR-B science plan. The SIR-B SWG disbanded on October 1, 1982.

SIR-B SWG Team Members and Observers who actively participated are listed below:

SIR-B Science Working Group

Team Members

Bob Beal	Johns Hopkins University
Tom Bicknell	Jet Propulsion Laboratory
Len Bryan	Jet Propulsion Laboratory
Frank Carsey	Jet Propulsion Laboratory
Keith Carver	NASA Headquarters
Charles Elachi	Jet Propulsion Laboratory
Tony England	NASA Johnson Space Center
Ted Engman	U.S. Department of Agriculture
Jack Estes	University of California, Santa Barbara
John Ford	Jet Propulsion Laboratory
Jim Head	Brown University
Dan Held	Jet Propulsion Laboratory
Verne Kaupp	University of Arkansas
Mike Kobrick	Jet Propulsion Laboratory
Maurice Long	Private Consultant
Walt McCandless	User Systems Engineering, Inc.
Dick Moore	University of Kansas

Jack Paris	NASA Johnson Space Center
Gerry Schaber	U.S. Geological Survey
Tom Schmugge	Goddard Space Flight Center
Mark Settle	NASA Headquarters
Fawwaz Ulaby	University of Kansas
Chialin Wu	Jet Propulsion Laboratory

Observers

Nevin Bryant	Jet Propulsion Laboratory
Bill Cannell	Defense Mapping Agency
JoBea Cimino	Jet Propulsion Laboratory
Mike Daily	Mobil Oil R&D
Diane Evans	Jet Propulsion Laboratory
Tom Farr	Jet Propulsion Laboratory
Peter Ford	Massachusetts Institute of Technology
Yoshinori Ishii	University of Tokyo (Japan)
Gordon Keyte	Royal Aircraft Establishment (U.K.)
Ed Langham	Radarsat Project (Canada)
Dave Lichy	U.S. Army Corps of Engineers
Steve Mango	Naval Research Laboratory
Hal Masursky	U.S. Geological Survey
Gordon Pettengill	Massachusetts Institute of Technology
Dave Pieri	Jet Propulsion Laboratory
Vince Pusateri	Naval Oceans Systems Center
Keith Raney	Radarsat Project (Canada)
Floyd Sabins	Chevron Oil Field Research
Alois Sieber	Federal Republic of Germany (DFVLR)

Abbreviations

ARS	Agricultural Research Service
CIR	color infrared
CZCS	coastal zone color scanner
EST	eastern standard time
GSFC	Goddard Space Flight Center
HCMM	heat capacity mapping mission
HDDT	high density digital tape
HH	polarization (horizontal transmit, horizontal receive)
HV	polarization (horizontal transmit, vertical receive)
IDP	interim digital processor (at JPL)
IEEE	Institute of Electrical and Electronics Engineers
IRSWG	Imaging Radar Science Working Group
JPL	Jet Propulsion Laboratory
JSC	Johnson Space Center
MSS	multispectral scanner (Landsat)
NASA	National Aeronautics and Space Administration
NOAA	National Oceanic and Atmospheric Administration
OSSA	Office of Space Science and Applications
OSTA	Office of Space and Terrestrial Applications (now OSSA)
RBV	return beam vidicon (Landsat)
RSS	root sum square
SAR	synthetic aperture radar
SIR	shuttle imaging radar
SLAR	side-looking airborne radar
SNR	signal-to-noise ratio
STALO	stable local oscillator
STS	shuttle transportation system
TDRS	tracking and data relay satellite
TIR	thermal infrared radiometer
TM	thematic mapper (Landsat–4)
VV	polarization (vertical transmit, vertical receive)

Contents

Figures

Tables

Section 1
Introduction

I. NASA Shuttle Imaging Radar Missions

NASA shuttle imaging radar missions planned for this decade are a vital element of America's program of remote sensing research for earth applications. These missions will greatly expand our understanding of the utility of radar imagery in relation to visible and infrared imagery collected by satellites such as Landsat. They will also permit us to identify the optimum configuration of future radar sensors that could be used for routine data collection from advanced platforms in space. Even though 1-week shuttle SAR missions do not allow continuous earth observations over periods of months or years, many of NASA's applications research objectives can be readily addressed by shuttle-based experiments. In fact, several points can be made in favor of a shuttle as a logical platform for remote sensing.

First, some important potential geoscientific applications of SAR data do not require continuous observations over periods of months or years. These include radar stereo missions for topographic or cartographic mapping, observations of urban morphology, geologic mapping missions, monitoring of clear-cutting, glaciological observations, etc. Repetitive shuttle missions may be completely satisfactory for studying phenomena which remain relatively constant or change slowly.

Such missions obviously exclude SAR studies of phenomena that change much more rapidly, such as crop distributions, soil moisture variations, ice dynamics, etc. The importance of obtaining continuous data for these and other such geoscientific studies which demand daily or weekly observations should not be underestimated. For the foreseeable future, sources of data for these studies may be limited to aircraft SAR data or SAR data obtainable from earth resources observations missions sponsored by other countries.

Second, a shuttle-based SAR experiment costs about an order of magnitude less than a free-flyer SAR satellite plus associated ground segment. NASA should be able to fly several 1-week SAR missions in the decade of the eighties at a total cost less than that of one free-flying satellite.

Third, the flexibility offered in flying, retrieving, modifying, and reflying SAR sensors has a significant advantage since it means that each new shuttle SAR flight can incorporate additional degrees of sophistication with minimum cost and risk. Furthermore, this series of shuttle SAR missions will offer an extraordinary opportunity to conduct scientific research on the optimum radar parameters of incidence angle, wavelength, and polarization for various applications. The results of this research will be of considerable interest not only to American geoscientists, but also to the worldwide remote sensing community, since the optimum parameters for particular applications are but poorly understood in many cases. This understanding becomes crucially necessary in order to justify and design future free-flyer SAR satellites with price tags in the several hundred million dollar range. Research of this nature may entail high scientific or technological risk, but it is accompanied by a commensurately high potential payoff.

Finally, from a practical point of view, the ability to continue acquiring space SAR research data within the next two years or so is much preferred to a delay of seven years or more while waiting for a free-flying SAR satellite. In particular, this means that SIR-B data can be co-registered with Landsat-4 Thematic Mapper (TM) data or other such visible/infrared space data, thereby permitting some very exciting studies of the more accurate classification of many surface features expected to result from this technique. Such experiments will be possible by 1984.

II. The SIR-B Mission

The SIR-B mission is the next evolutionary step in the sequence of NASA spaceborne imaging radars which began in 1978 with the Seasat SAR and continued in 1981 with SIR-A. SIR-B will be the largest instrument of the OSTA-3 experiment pallet (Fig. 1-1) on the seventeenth flight of the Space Shuttle. It is currently scheduled for launch during the summer of 1984. Unlike Seasat and SIR-A, SIR-B will for the first time provide the ability to control the angle of incidence at the earth's surface by mechanically tilting the antenna.

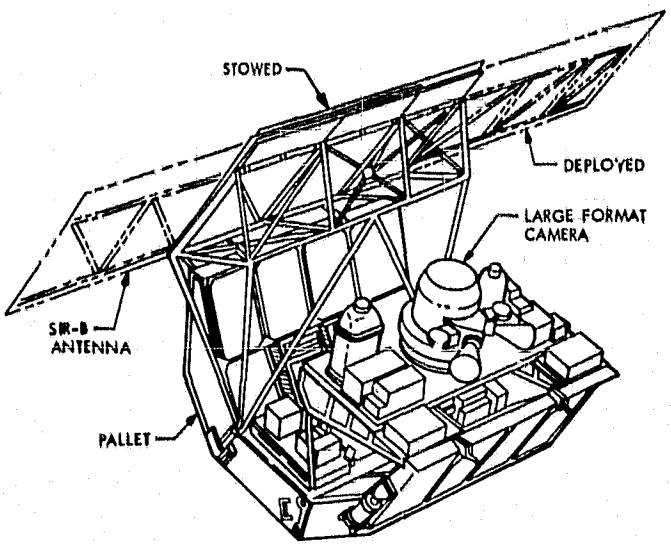

Fig. 1-1. OSTA-3 experiment pallet

This controllable angle capability of SIR-B will allow three major types of experiments, illustrated in Figs. 1-2, 1-3, and 1-4. Figure 1-2 illustrates the possibility of imaging a specified area at up to six different incidence angles ranging from 15 to 60 deg. This configuration also gives stereo imagery. Figure 1-3 shows the capability of imaging a specific area at several different azimuth angles. Figure 1-4 illustrates the capability of acquiring images contiguously for large-scale mapping. Appendix B gives further details on data-taking scenarios for SIR-B.

SIR-B will provide digitally processed images for 25 hours of data acquisition in addition to optically processed images for eight of those hours. Other performance characteristics of SIR-B are listed in Table 1-1.

The SIR-B instrument will be mounted on the OSTA-3 pallet, which will also carry the Large Format Camera (LFC), the Feature Identification and Location Experiment (FILE), the Measurement of Air Pollution Satellite (MAPS), and

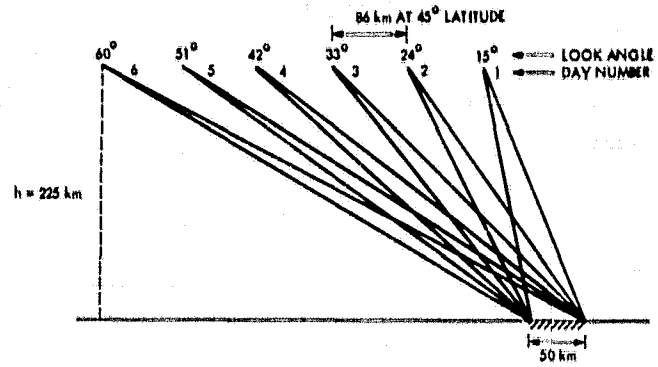

Fig. 1-2. Multiple incidence angle (stereo) mode for SIR-B; at 45° latitude and 225-km altitude, the shuttle drifts westward by 86 km in one day

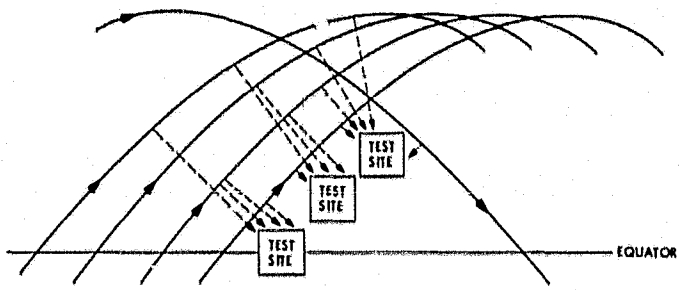

Fig. 1-3. SIR-B configurations for multiple azimuth angle imaging of selected test sites

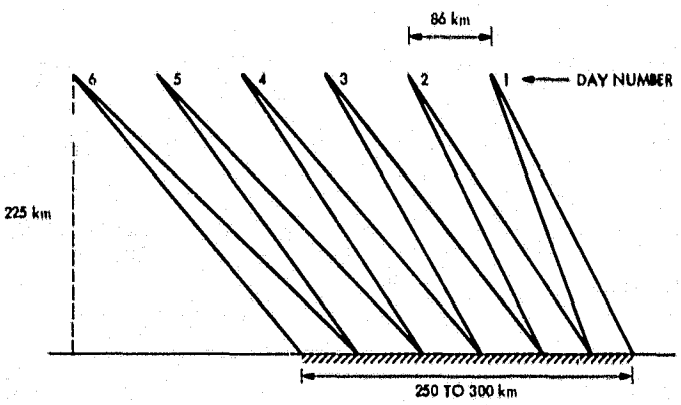

Fig. 1-4. SIR-B mapping mode for wide swath coverage showing 86 km per day westward drift of orbit

possibly other instruments. OSTA-3 will be placed in a 57-deg inclination circular orbit at a nominal altitude of 225 km. Using its optical recorder, SIR-B will be able to provide imagery of any selected areas of the earth between 57 deg south latitude and 57 deg north latitude. With the digital

Table 1-1. Characteristics of SIR-B

Mission characteristics
OSTA-3 experiment package on STS-17
Expected launch date: August 1984
Orbital inclination: 57 deg
Orbital altitude: 225 km
SIR-B performance characteristics
Frequency: 1.28 GHz
Wavelength: 23 cm
Polarization: HH
Angles of incidence: 15-60 deg, nominal
Swath width: 40-50 km, nominal
Azimuth resolution: 25 m (4 look)
Range resolution at 60 deg: 17 m
Range resolution at 15 deg: 58 m

shuttle-to-tracking and data relay satellite (TDRS)* link, the areas of coverage are restricted to those where a shuttle K_u-band antenna is in view of the TDRS, as further explained in Appendix B.

Optically recorded SIR-B data will be processed within months after the mission. Digitally recorded data will be processed on the JPL Interim Digital Processor (IDP), which will have a throughput rate of approximately 200 minutes of processing time for each minute of data acquisition. It is planned to digitally process about two hours of SIR-B data during the first year following the mission, with the capability to process an additional 12 hours of data in 1985 and 1986.

III. Science Plan Organization

This SIR-B science plan is designed to provide broad guidelines for the organization of the SIR-B mission and a general description of geoscientific experiments which are possible with SIR-B. Experiments outlined in this plan are arranged into generic discipline areas and should be very useful in designing specific experiments. The experiment outlines presented here are not intended to restrict the scope of SIR-B investigations. *It is certainly possible that meaningful SIR-B experiments may be conducted that are not specifically discussed in this plan.*

The second section of this document begins with a short history of the development of imaging radar through Seasat and SIR-A. A succinct discussion is then presented on the status of research in the science of radar remote sensing, with summaries of key results in geography, geology, hydrology, oceanography, vegetation, and ice applications. Key findings from Seasat and SIR-A are summarized and the rationale for future spaceborne SAR missions is presented.

The third section discusses basic SIR-B experiments organized by geoscientific discipline (geology, hydrology, etc.). This section is the heart of the science plan and seeks to answer the following questions for each discipline:

(1) What are the scientific or applications objectives for remote sensing data in this discipline?

(2) What role does radar imagery play in these objectives?

(3) What is the potential contribution of SIR-B and what kinds of experiments would be useful?

(4) What data are needed which is ancillary to SIR-B and how can SIR-B be used synergistically with other data sources such as TM?

A more detailed description of the SIR-B sensor is provided in the fourth section, which includes details on such image quality factors as the signal-to-noise ratio (SNR), dynamic range, quantization, and radiometric calibration. Various SIR-B sensor evaluation experiments are outlined, including experiments on calibration, target statistics, squint and spotlight modes, etc.

The SIR-B information extraction process is discussed in Section 5 with emphasis on the two major aspects of data processing, namely SAR signal correlation and postcorrelation image processing. Quick-look and standard image products are described for both digital and optical processing. Signal correlation and image-processing test experiments, possible with SIR-B, are outlined.

The sixth section provides recommendations for the ancillary data support of the SIR-B mission through aircraft underflights and *in situ* ground truth data collection.

*The TDRS will be used to relay high data rate information via a K_u-band antenna onboard the shuttle to the ground at White Sands, New Mexico. The TDRS system consists of two satellites in geosynchronous orbit. The satellites will also be used to relay commands and engineering data.

Section 2
Imaging Radar Science: Status and Plans

I. Introduction

Imaging radars were first developed in the early fifties as incoherent side-looking airborne radars (SLAR) for high-resolution all-weather military reconnaissance. In the sixties, these radars were further developed by earth scientists for land remote sensing, and by 1969 SLAR surveys were available on a commercial basis. In parallel with SLAR exploitation, the coherent imaging radar or SAR was in the making first with the early fifties experiments by Carl Wiley of the Goodyear Aircraft Corporation, and later at the Universities of Illinois and Michigan. The SAR makes use of the Doppler phase history of the backscattered radiation from natural targets to synthesize an effective along-track aperture which is much larger than the real aperture, thereby permitting fine along-track resolution without the need for an impractically long antenna. Tone, texture, and context in images from both real and synthetic aperture radars were and are still used by photo-interpreters to reveal valuable information useful in geology, land use studies, urban geography, and a host of current and emerging interest areas.

On June 26, 1978, Seasat was launched into a 108-deg inclination orbit at an altitude of 786 km. In addition to an L-band SAR (the first in space), Seasat carried an altimeter, scatterometer, and microwave radiometer. On October 10, 1978, Seasat failed as a result of a massive short circuit in its electrical power system. However, during its 100-day lifetime, the Seasat SAR collected almost 42 hours of data equivalent to about 100 million square kilometers areal coverage of the earth. Nearly all of the Seasat data were optically processed, and certain selected 100 km × 100 km scenes were also digitally processed at JPL as well as by other digital processors that have since been developed.

On November 12, 1981, at 10:10 a.m. eastern standard time (EST), the second Space Shuttle (STS-2) was launched into a circular orbit at a 38-deg inclination and 260-km altitude. The major payload was the OSTA-1 experiment pallet, which included SIR-A in addition to various other remote sensing instruments. Due to technical problems, the Shuttle was forced to abbreviate its mission and landed at Edwards AFB at 1:23 p.m. EST, on November 14. However, during this short 2-day mission, SIR-A optically recorded nearly eight hours of data, equivalent to 10 million square kilometers areal coverage. SIR-A data was optically processed into image format at JPL. The SIR-A sensor was derived from the Seasat development and used the same type of antenna panels, transmitter, modulator, and receiver. However, whereas the angle of incidence was 20 deg for Seasat, it was 50 deg for SIR-A. Figure 2-1 illustrates the various angles commonly used to specify radar illumination geometry.

Both Seasat and SIR-A were fixed-parameter imaging radars, i.e., the frequency, polarization, and incidence angle were constant. Much of the work with these images has been and still is being accomplished using the photo-interpreters' tools of tone, texture, and context.

SIR-B will be the first spaceborne imaging radar providing control of the illumination geometry (incidence angle). Furthermore, SIR-B will provide digitally processed images at these selectable incidence angles. These are potentially very significant advantages, since it will now be possible to enter an entirely *new era of radar image analysis in which quantitative methods and mathematical models of backscatter will provide a powerful enhancement to the traditional photo-interpretive methods.* Of course, tone, texture, and context will continue to play an important role, but the use of quantitative scattering models along with controllable illumination geometry and digitized images will greatly expand the utility of radar imagery for the assessment of topographic relief, surface roughness, geomorphology, and land cover classification.

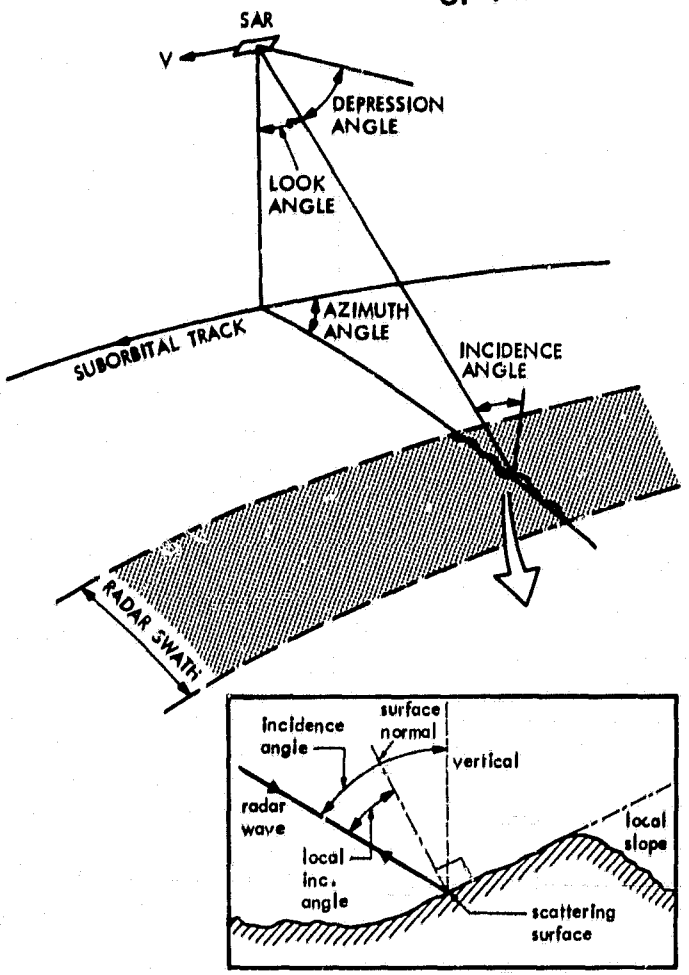

Fig. 2-1. Definition of angles. The look angle is the look from nadir to the radar beam measured at the orbiter. The incidence angle is the angle the beam makes with the surface, where the vertical at the surface is measured from the center of the earth. The local angle of the incidence is the angle between the beam and the normal to the local surface.

II. Status of Radar Science Research

Radar science deals with the relationships between scene parameters and illumination parameters. It seeks to find the best illumination parameters of wavelength, incidence angle, and polarization for remote sensing of such scene parameters as soil moisture, oceanic significant wave heights, lithologic units, etc. The past decade of radar science research has demonstrated the proper roles to be played by imaging radars, scatterometers, and altimeters in exploiting the microwave spectrum. Scatterometers and altimeters operating at K_u-band on Skylab, GEOS-3, and Seasat have been found to be particularly useful for remote sensing of oceanic winds and wave heights, respectively. Spaceborne SARs flown on Seasat and SIR-A have revealed the potential benefits of SAR application in geology, agriculture, hydrology, ice mapping, geography, etc. When airborne real aperture imaging radars were first made available for civilian use, geologists were quick to seize upon their potential value for structural and lithologic mapping; photo-interpretive techniques were used with reliance on tone, texture, and context as a means of classification. Although traditional methods will continue to be used, imaging radar science is clearly evolving toward a much more quantitative and analytical approach as multiparameter calibrated SARs become available. Radar images demonstrate a unique sensitivity to surface geometry, plant morphology, and the presence of water in either liquid or frozen form. Radar scientific research of the past decade has revealed a number of key relationships between scene parameters and illumination parameters. A few of the more important of these are summarized below as they pertain to the SIR-B science plan. Also, Appendix C presents further references and suggested reading.

A. Geography

Geography, as a discipline, may be subdivided into physical and cultural geography.

The application of radar remote sensing techniques to physical geography concentrates on three major areas of research: hydrology, geomorphology, and vegetation geography. Hydrologic research in the physical geography context is oriented primarily toward understanding drainage patterns and their variability within the climatic context, with the goal being to determine the optimum radar parameters for hydrologic mapping. Geomorphic studies, closely allied to hydrologic studies, concentrate on the understanding of the effect of topographic slope, look direction, and depression angles on the final radar image. The use of orbital radar for vegetation analysis in the physical geography context seeks to identify large, regionally oriented vegetative associations and ecoregions rather than specific crops.

Cultural geographers are interested in monitoring the spatial and temporal morphology of the impact of urban populations on the earth's surface. For example, radar imagery provides a means of delineating urban-rural boundaries and further classifying land use patterns (Fig. 2-2). This classification is accomplished by the use of tone and texture. Tone, or intensity of backscatter, in urban areas is determined by those specular facets of buildings, transportation networks, open surfaces, etc., that are oriented orthogonally to the radar direction. Texture is related to the spatial distribution of scattering centers and has been used to infer urban land use patterns. Both tone and texture are also influenced by the radar operating parameters of wavelength, polarization, and illumination geometry as well as resolution and number of looks. Two-dimensional Fourier analyses of radar imagery may be useful for inference of land cover spatial distributions when the radar operating parameters are known.

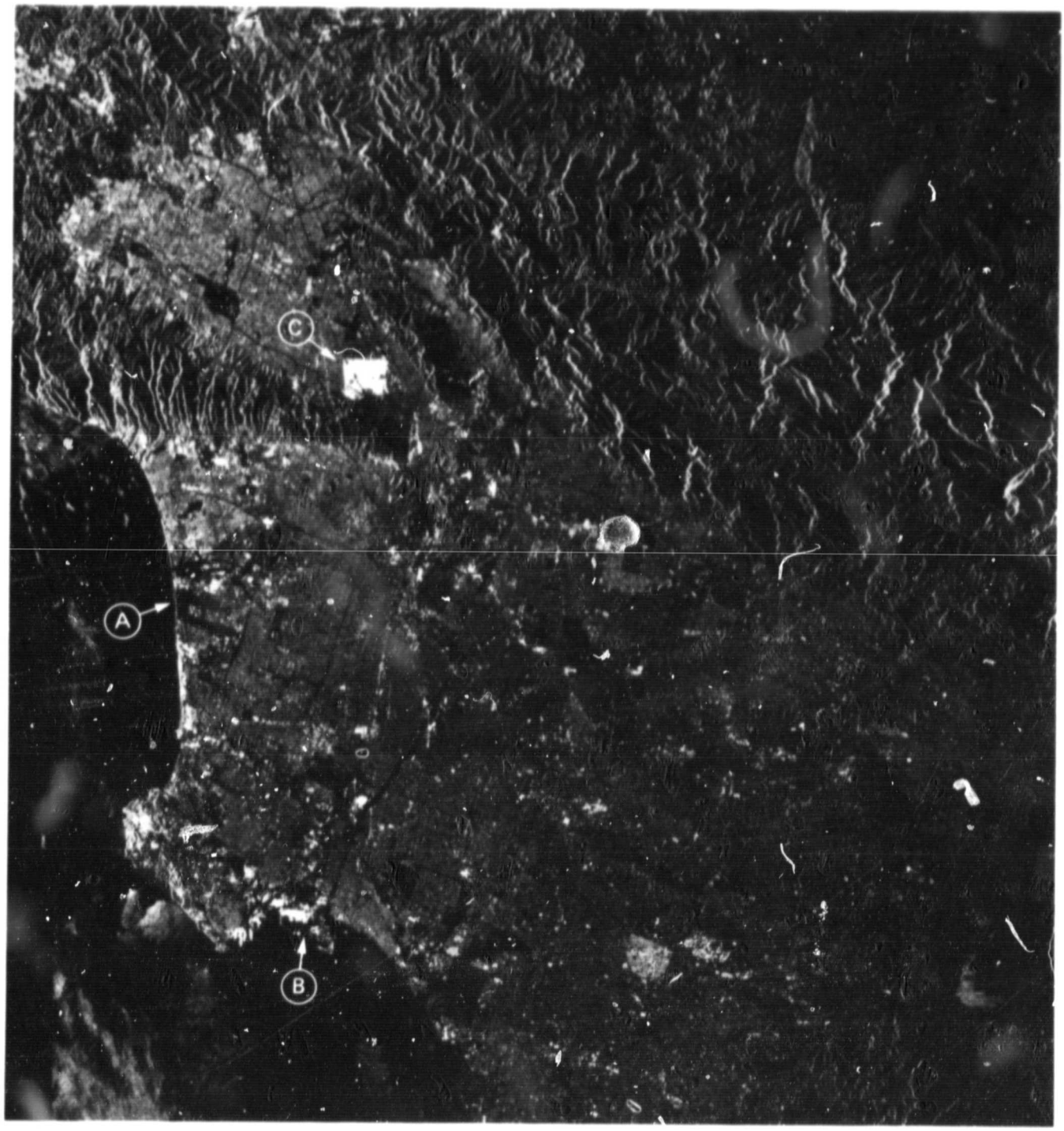

ILLUMINATION DIRECTION

Fig. 2-2. Seasat SAR image of the greater Los Angeles area: (a) Los Angeles International Airport; (b) Long Beach Harbor; (c) Burbank

Previous studies have suggested that cross-polarized imagery may be more useful for urban mapping than like-polarized because the HV data eliminate the artifically bright returns associated with quasi-specular reflectors perpendicular to the radar beam.

B. Geology

Geologists have made extensive use of radar imagery in the past primarily for purposes of terrain analysis and structural mapping. At incidence angles of 5 to 25 deg from the local vertical, large variations in backscatter are produced by relatively small changes in surface slope. Geologists have exploited this capability of imaging radars to detect subtle variations in surface topography which, in turn, can be related to the presence of underlying crustal structures such as folds and faults.

Radar imaging techniques have proved to be particularly useful for structural studies of tropical regions which are characterized by low topographic relief and extensive vegetation. Radar's sensitivity to changes in surface slope is particularly useful for highlighting topographic variations in this type of environment. Photographic surveys of tropical areas are complicated by cloud cover conditions which can persist through most seasons. Radar imaging techniques are superior to photographic methods in this regard, in that they can be used to collect data under any weather conditions. Extensive airborne radar surveys have been conducted in many tropical areas of the world for purposes of oil and mineral exploration.

The controllable illumination geometry of radar systems has also been exploited by geologists for purposes of structural mapping. Natural solar radiation tends to preferentially illuminate surface terrain in an east-west direction. This illumination bias highlights north-south trending features perpendicular to the solar azimuth. In many cases, major geologic structures may be oriented parallel to the direction of solar illumination, which complicates the analysis and interpretation of photographic imagery. Radar systems provide an active, controllable source of surface illumination which can be used to overcome this biasing problem. Airborne radar surveys are commonly designed to illuminate natural terrain in a direction perpendicular to major topographic trends.

Seasat afforded geologists their first opportunity to obtain large-scale radar imagery at a constant angle of surface illumination. Previous attempts to relate tonal and textural variations observed in aerial radar imagery to surface geological boundaries had been complicated by the relatively large variation in illumination angles that occurs across an aerial radar swath (typically on the order of 20 deg or more). Under these circumstances it is extremely difficult to distinguish differences in surface backscatter produced by variations in incidence angle from those that are related to the structure and composition of surficial materials. Variations in the lithology of surficial rocks and soils have been successfully detected in Seasat imagery. Analysis of Seasat data has tentatively suggested that orbital radar imagery can be used to detect lithologic boundaries between different geological materials in certain types of environments.

Seasat's orbit was designed in such a fashion that radar imagery could be obtained during both ascending and descending satellite passes. At middle latitude regions within the U.S., this permitted the collection of radar imagery from two distinct azimuthal directions that were nearly orthogonal. Analysis of large-scale Seasat imagery acquired from perpendicular directions has extended our appreciation of how radar illumination conditions introduce biases in studies of crustal structure. Research currently in progress seeks to develop new methods of combining lineament information derived from radar imagery acquired from independent look directions (see Fig. 2-3).

SIR-A data are still in a preliminary stage of analysis, although several interesting and encouraging results have already emerged. SIR-A imagery obtained in hyperarid regions of northern Africa has revealed the presence of subsurface stream channels and other drainage features in an area uniformly covered with windblown sand (see Fig. 2-4). Theoretical models suggest that the attenuation of a radar signal in a moisture-free medium should be quite low. However, this is the first documented instance of large-scale radar penetration. SIR-A imagery has also proved to be useful for mapping surficial drainage features in areas which are characterized by uniform spectral properties. It is frequently difficult to detect ephemeral stream channels in visible and infrared imagery of semi-arid regions because these areas possess relatively uniform spectral characteristics at visible and infrared wavelengths. Such channels may be preferentially highlighted in radar imagery due to the presence of fine grained sand, rocky boulders, or surface vegetation along stream beds.

Comparison of Seasat and SIR-A acquired data has provided insight into the utility of multiple incidence angle imagery for geologic mapping. Imagery acquired at low local incidence angles (less than about 30 deg) emphasizes variations in surface relief although geometric distortions due to layover and foreshortening in mountainous regions can be severe. Imagery taken at higher angles greatly reduces the geometric distortion and furthermore highlights variations in surface roughness, although radar shadows increase. New methods of combining, displaying, and classifying radar imagery obtained at multiple angles of incidence are currently being developed. These methods will be directly applicable to geological analysis of SIR-B data.

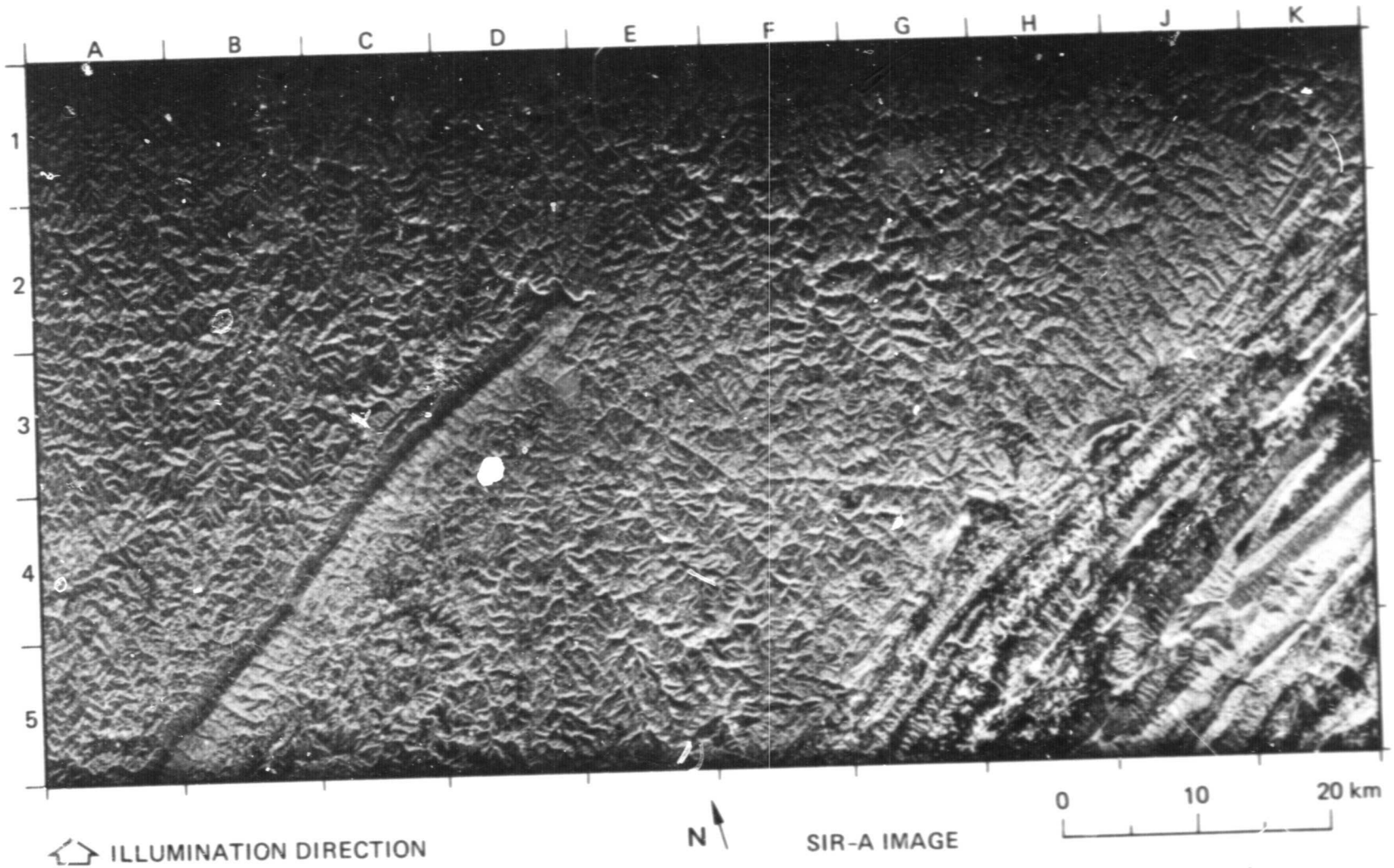

Fig. 2-3(a). The Appalachian Plateau in eastern Kentucky and adjacent Virginia is a steeply sloping, deeply and extensively dissected, forested terrain. The local incidence angle of SIR-A illumination is very low at slopes that face toward the radar. This produces strong returns that appear bright on the SIR-A image. Correspondingly the high local incidence angle at the backslopes results in dark tones on the image. The strong image contrast enhances linear topographic features that are normal or oblique to the radar illumination; features that are nearly parallel to the illumination are scarcely perceptible on the image.

Fig. 2-3(b). The steep slopes of the Appalachian Plateau produce mostly specular reflections (0° incidence) or layover (negative incidence angle) from foreslopes that appear very bright on the Seasat SAR image. Despite strong image contrast between foreslopes and backslopes the compression of the former and stretching of the latter distorts or obliterates all but the largest topographic features on the image, regardless of the illumination direction.

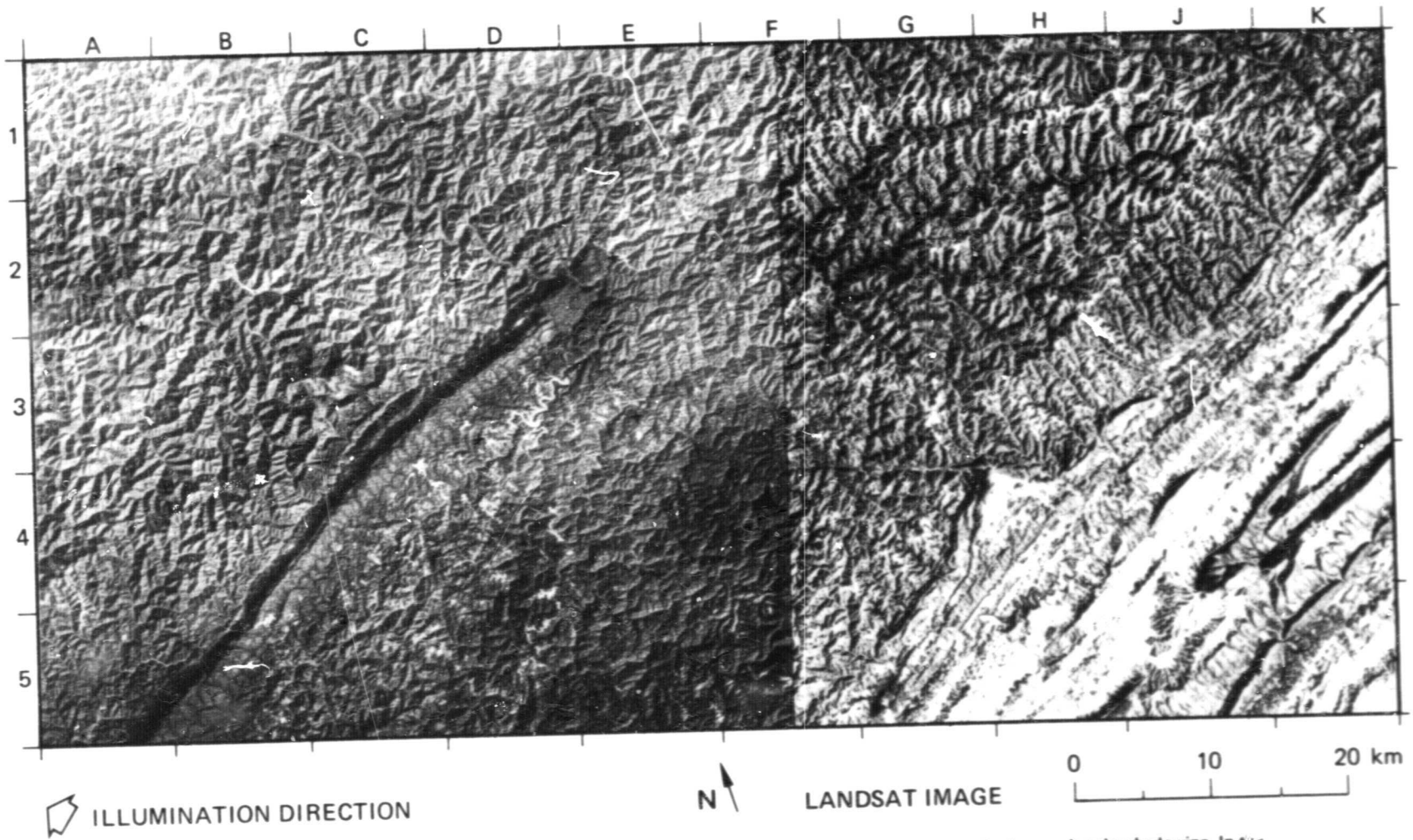

Fig. 2-3(c). Topographic features and especially small-scale topography are enhanced on Landsat images by low-angle solar shadowing. In the Appalachian Plateau this occurs on cloud-free images acquired between November and February. Major and minor topographic features and especially linear features are enhanced on these RBV and MSS images by solar shadowing, except in a narrow sector within about ±5° of the sun illumination direction. In this sector the linear topography is suppressed on the images due to insufficient image contrast.

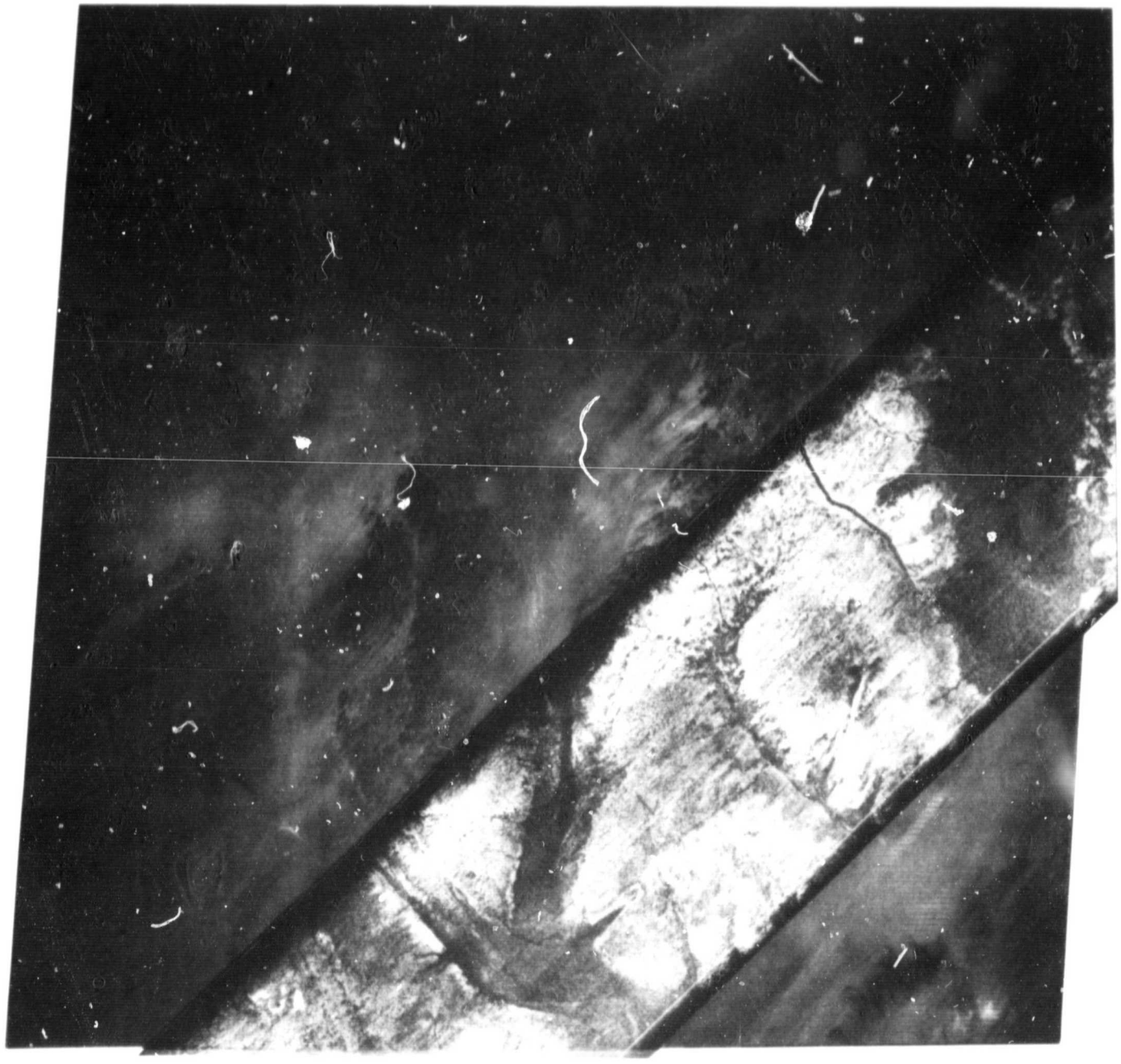

Fig. 2-4. Landsat image of hyperarid region of Libyan desert, with SIR-A image crossing lower right corner. Drainage features observed in this image are blanketed by surface deposits of windblown sand and are not readily apparent in Landsat or photographic imagery. Radar penetration of surface deposits in this area extends to depths of several meters.

C. Hydrology

Less than three-quarters of a percent of the water on the earth is directly usable, and of this only about one-half is readily accessible in the form of surface water. Surface water supply results primarily from precipitation runoff, so that watershed runoff determination is fundamental to hydrologic forecasting. Soil moisture may also be useful in crop yield predictions, even though currently used United States Department of Agriculture (USDA) yield models use antecedent precipitation rather than direct soil moisture.

Since the microwave dielectric constant of water at L-band wavelengths is about 80, whereas that of dry soil is about 3, the presence of water in the top few centimeters of soil can be detected in radar imagery. Soil moisture and surface wetness become particularly apparent at the longer wavelengths (L-band and C-band) and at incidence angles of 10 to 15 deg.

Radar imagery does not directly measure soil moisture even though the presence of water is a strong determinant of backscatter intensity. The factors of surface roughness, slope, and vegetation cover must also be included in an algorithm which uses radar imagery to estimate soil moisture. Results obtained by using a truck-based radar scatterometer show that the effects of surface roughness are minimized when a C-band radar with a 10- to 15-deg incidence angle is used; the polarization is not critical, although HH polarization is preferred. This is an important finding, although it should be noted that this truck radar result has not yet been confirmed using either aircraft or spaceborne radar imagery. The truck-based results included both bare and vegetated fields which had essentially zero slope; for bare fields, a linear regression analysis of the data gives the following linear dependence of the radar scattering coefficient (dB) on soil moisture M (top 5 cm, expressed as a percent of field capacity):

$$\sigma^\circ \text{ (dB)} = 0.148\,M - 15.96$$

For vegetated fields (corn, wheat, beans, milo), the relationship is not greatly different:

$$\sigma^\circ \text{ (dB)} = 0.133\,M - 13.84$$

These relations are for C-band, HH, 15-deg incidence data over essentially flat terrain with a normal range of roughnesses expected in plowed fields. The significant finding here is that not only is there a strong relationship between radar backscattering and soil moisture, but that for these parameters the effect of vegetation and surface roughness is minimized. Similar linear relationships have been found for L-band, HH, 15-deg data, but surface roughness is a larger confusion factor at this longer wavelength.

What happens if the fields are in gently to moderately rolling terrain? It is known that for surfaces with low to moderate surface roughnesses, the radar backscattering coefficient is strongly dependent on incidence angle, especially for near-nadir angles. For such surfaces, a 5-deg change in slope could easily modulate the backscattering coefficient by 10 dB, which might then mask the changes caused by soil moisture. To the first order, these topographic effects can be removed through the use of digital topographic map data when it is available, although this can be a difficult processing task.

The Seasat SAR demonstrated that elevated soil moisture associated with rainfall events was easily seen over large regions of the midwestern farm belt of the U.S. where the terrain is fairly flat, as shown in Fig. 2-5. Analysis of this imagery shows that a 20 percent increase in soil moisture corresponds to an approximate 7-dB increase in radar backscatter.

Radar imagery is ideal for the detection of landform changes and drainage patterns associated with watersheds. Both SIR-A and Seasat images clearly show the landform morphology associated with watersheds. Both watershed geometry and soil wetness are needed to improve yield information on watershed storm runoff and the size of water control structures. A data set taken at 2- to 3-day intervals over a several-week period is ideal for understanding runoff. This suggests that change detection procedures may be useful for detecting the change in soil moisture from co-registered radar images taken over the 7- to 10-day period associated with the SIR-B mission.

For completeness, it should be mentioned that snowpack parameters are very important to hydrologic modeling and forecasting. Snow state, depth, and snow water equivalent are of primary interest. Research has shown that microwave response to snow water is strongest at the millimeter wavelengths where volume scattering from liquid water is so strong that surface scatter is minimized. Radar backscatter sensitivity to snow water equivalent in the 0- to 80-cm range is very strong at 37 GHz and becomes less strong as the frequency is reduced, according to truck scatterometer measurements. Although there is a moderate sensitivity to snow water at C-band, it is not expected that at L-band there will be any appreciable response to snow since even the thickest packs would exhibit little volume scattering in relationship to the underlying surface scatter.

D. Oceanography

L-band SAR imagery of the surface has been shown to be sensitive to the short gravity waves on the ocean surface. To understand the radar signal properties, therefore, one must understand the phenomenological behavior of the short gravity waves—how they are generated and modulated by the wind,

Fig. 2-5(a). Seasat image of Ames, Iowa. The light toned areas result from increased soil moisture due to a rain event.

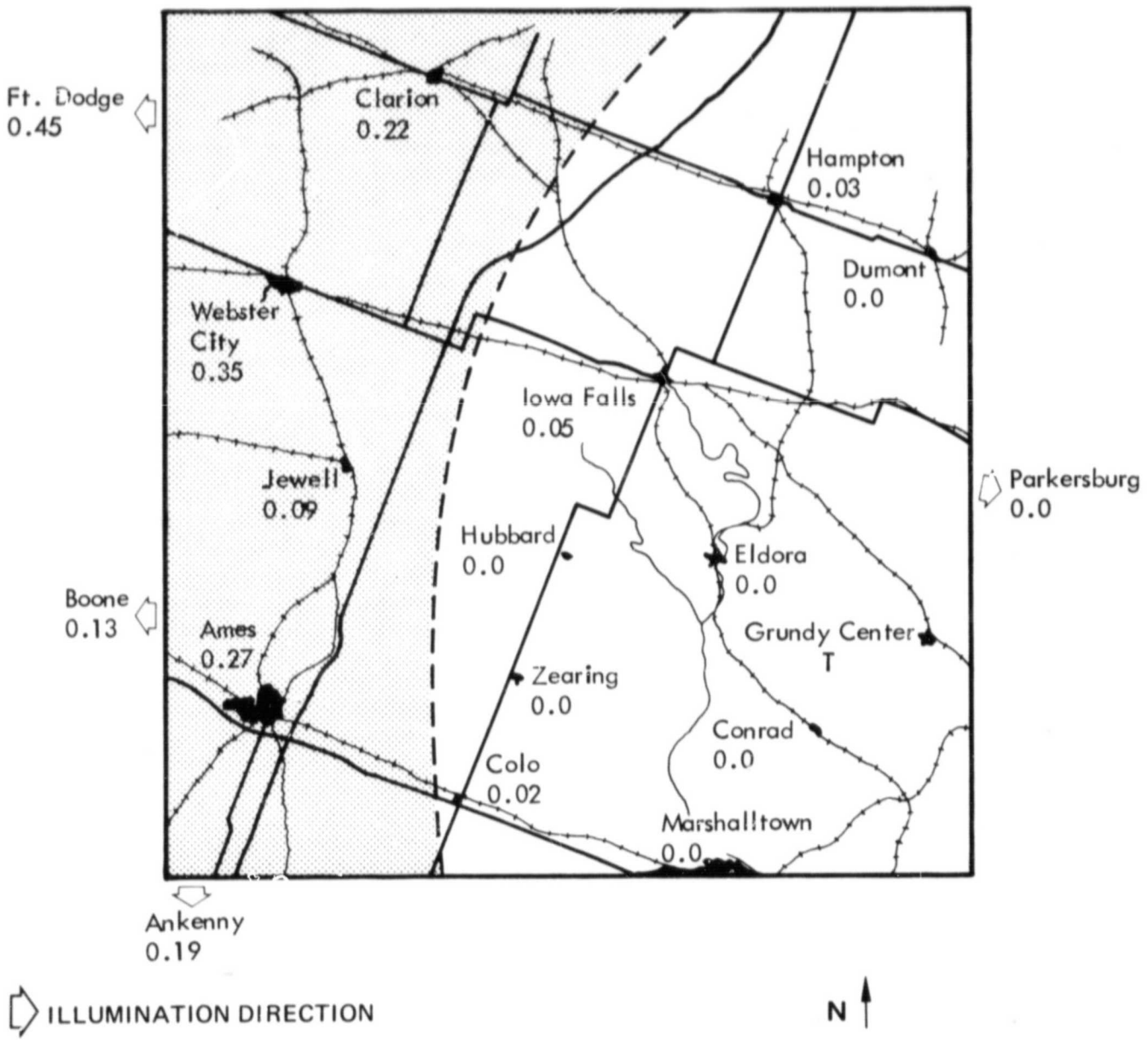

Fig. 2-5(b). Ames, Iowa. Rain gauge readings (in./day) acquired during the 24-hour period preceding acquisition of the radar imagery are given at several points. The stippled area represents rainfall greater than 0.1 in./day.

currents, and long gravity waves. Bright points on a SAR image of the ocean may be due to steep slopes, the larger amplitudes of the short gravity waves (caused by increases in local wind or by modulation due to the larger waves), or by phenomena associated with the synthetic aperture imaging process dependence on the differing drift velocities of different components of the surface.

SAR images of the ocean often show wave structures, such as those in Fig. 2-6. When the SAR is pointed normal to the direction of wave travel, the representation of wavelength of the ocean waves on the image is correct. As the angle at which the SAR observes the ocean is varied toward the direction parallel to the crests of the waves, the image representation of the wavelength is distorted. Thus, the apparent direction of the waves on the surface is not the true direction, and the wavelengths observed are not always the correct ones for the ocean waves. Recent progress in the theory of synthetic aperture imaging of the ocean, however, has indicated that the correct wavelength and direction can be extracted from the images in many cases.

The Seasat and SIR-A images of the ocean show many features that are probably related to local wind variations, internal waves, oceanic fronts, etc. Moreover, clear manifestations of surface phenomena related to features of the ocean bottom have been observed in shallow water, and perhaps in water over 100 m deep. The exact causes of these effects are not understood, and more research is needed even to describe many of them. Nevertheless, they are of great interest in that they indicate the potential of the SAR to determine kilometer-scale features of the ocean never before observed.

The directional properties of ocean backscatter intensity have been extensively observed in the 2-cm wavelength region, but little observation has been conducted at the 23-cm wavelength of the Seasat, SIR-A, and SIR-B imaging radars. At 2-cm wavelengths, the backscattering has been found to be described approximately by a model of the form

$$\sigma^\circ = a_0 u^{b_0} + a_1 u^{b_1} \cos\phi + a_2 u^{b_2} \cos 2\phi$$

where

u = wind speed at a specified height (usually about 20 m)

b_i = wind speed exponents

a_i = angular coefficients

ϕ = direction of the radar beam relative to upwind

The coefficient a_1 describes the magnitude of the upwind-downwind variation, and the coefficient a_2 the much larger magnitude of the upwind-crosswind variation. The coefficients b_i are, as are the a_i, functions of angle of incidence. Depending upon polarization and angle of incidence, b_0 and b_2 are of order between 1.5 and 2.5, with maximum (reasonably constant) values in the 35- to 55-deg range. The coefficient b_1 has a behavior that is not as well defined, but is comparable with the others for angles not exceeding 45 deg.

At a 25-cm wavelength, the upwind-downwind ratio may be small enough to be ignored. This is based on interpretations of images from Seasat and L-band aircraft radars. Furthermore, the backscatter coefficients b_0 and b_2 were found to be of the order of 0.4 to 0.5, a value much less than those observed at shorter wavelengths, but still possibly useful for wind-speed determination.

E. Vegetation

A microwave radar sees a vegetation canopy as a cloud of volume scatterers composed of a very large number of discrete plant components (leaves, stalks, fruits) all underlain by a soil which may contribute surface scattering to the energy which penetrates the canopy, as suggested in Fig. 2-7. When the wavelength approximates the mean size of a plant component, discrete volume scattering is enhanced and if the plant canopy is dense, there may be strong backscatter at these wavelengths. Experiments with both scatterometers and imaging radars have shown that the entire microwave spectrum (1 to 30 GHz) is useful for discrimination of vegetation. Longer wavelengths (10 to 30 cm) appear to be preferable for larger plants such as trees and shorter wavelengths (2 to 6 cm) for smaller crop plants (corn, soybeans, wheat, etc.).

Radar backscattering from trees is evidently related strongly to the tree, trunk, and limb sizes and to a lesser degree to the leaves. For example, a recently published study showed that an L-band radar could be used to discriminate the ages of pine trees.

Crops are best discriminated in the 5- to 15-GHz range, where the wavelength is short enough so that volume scatter predominates and surface scatter from the underlying soil is minimal. One recent experiment used airborne scatterometer data taken over a large number of fields in Webster County, Iowa to show that corn and soybeans are easily separated at C-band using both 50-deg angle of incidence, cross-polarized (HV) data, and 10-deg angle of incidence, like-polarized (HH) data. The HV-polarized backscatter is strongly influenced by volume multiple scattering which in turn depends on the size and orientation of the corn and soybean plant components. Another recent experiment in southern Germany used airborne C-band SAR imagery to show that rye fields stand out very clearly against surrounding fields of sugar beets and

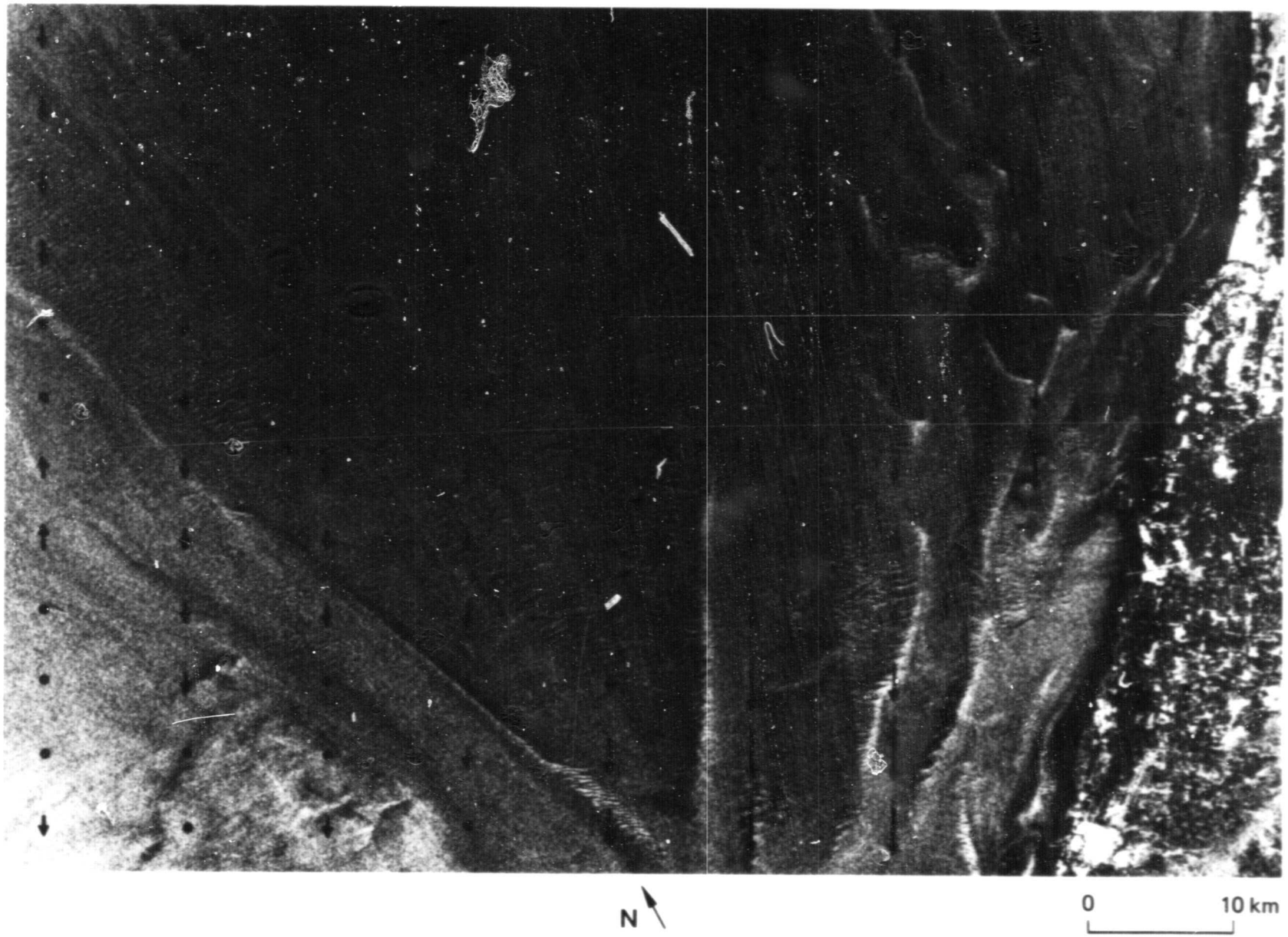

Fig. 2-6. Seasat ocean image over English Channel showing wave structure bottom morphology, surface ships, and wakes. Arrows indicate Doppler shift measurements.

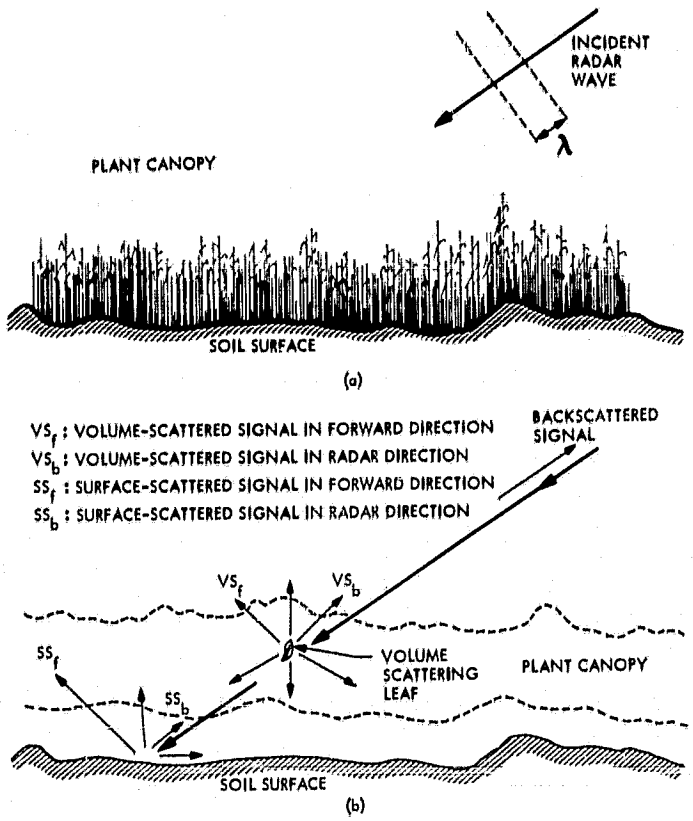

Fig. 2-7. Model of radar scattering from plant canopy. (a) Crop-type plant canopy illuminated by radar wave. (b) Volume scattering (VS) from leaves, fruits, stalks in plant canopy, plus surface scattering (SS) from underlining soil.

potatoes. Since the rye heads are approximately 5 to 6 cm in length, the same as the wavelength, it is presumed that the bright returns from the rye fields are due to volume scattering from the heads.

F. Ice

Radar backscatter from sea ice is dependent on the dielectric properties and spatial distribution of the ice. Below about 10 GHz, the real part of the dielectric constant for ice is essentially frequency-independent, but is dependent on the salinity S (parts per thousand):

$$\epsilon_r' = \frac{3.5}{1 - 3S}$$

so that for a salinity S of 15 parts per thousand, $\epsilon_r' = 3.6$. The imaginary part of the dielectric constant is a strong function not only of the salinity but also frequency and ranges typically from 1 to 5 over the 1- to 10-GHz region.

Radar backscatter from sea ice is dependent on the age, geometric properties, and temperature of the ice, as well as on the amount of snow cover. The fact that 2- to 3-cm wavelength radars can differentiate between ice types, and by inference between ice thicknesses, has been known for over a decade. In fact, the Soviet Union has used an airborne radar to prepare operational maps of the ice cover north of the Eurasian continent for application to convoys of shipping. More recently Canada has begun to use such a radar operationally.

The phenomenology of radar backscatter from sea ice is quite complex, and much research remains before it is fully understood. The operational systems make use of empirical image interpretation schemes without full knowledge of the scientific basis. Backscatter from sea ice is a combination of surface and volume scatter, with the relative degrees of the two depending on the relative salinities of the different kinds of ice. Ice morphology and composition are very complex; newly formed ice has a high brine content, with this concentrated in vertical "tubules," whereas older ice is less saline because the brine has, over the season, diffused downward. Multiyear ice, in fact, has very little salinity in its upper layers. Moreover, the situation is complicated by both the history of freezing and melting and by the phenomenon of rafting, in which one ice sheet rides up over another. Nevertheless, one can show experimentally that the multiyear ice gives strong backscatter compared with first-year ice when it is very cold, with less contrast during the summer months, at the shorter wavelengths.

At L-band, ice backscatter measurements during the cold season show little contrast, if any, between first-year and multiyear ice. This was borne out by the observations with both Seasat and the various L-band aircraft SARs. Ice edges could usually be distinguished, but ice types could not, as shown in Fig. 2-8. Thus, the use of L-band radar for ice monitoring can be helpful in showing the total extent, but not in showing the types and thicknesses.

Thus, even if SIR-B were able to image sea-ice areas within its coverage, available evidence suggests that it would be difficult to discriminate ice age, although pressure ridges should be easily detected.

III. Summary of Seasat and SIR-A Results

The Seasat SAR and SIR-A were the first two synthetic aperture imaging radars to be put in earth orbit by NASA. These experimental programs demonstrated that spaceborne SAR techniques could be used to achieve high-resolution (25-m) imagery over moderate swaths (50 to 100 km), allowed the further development of SAR technology, and have shown

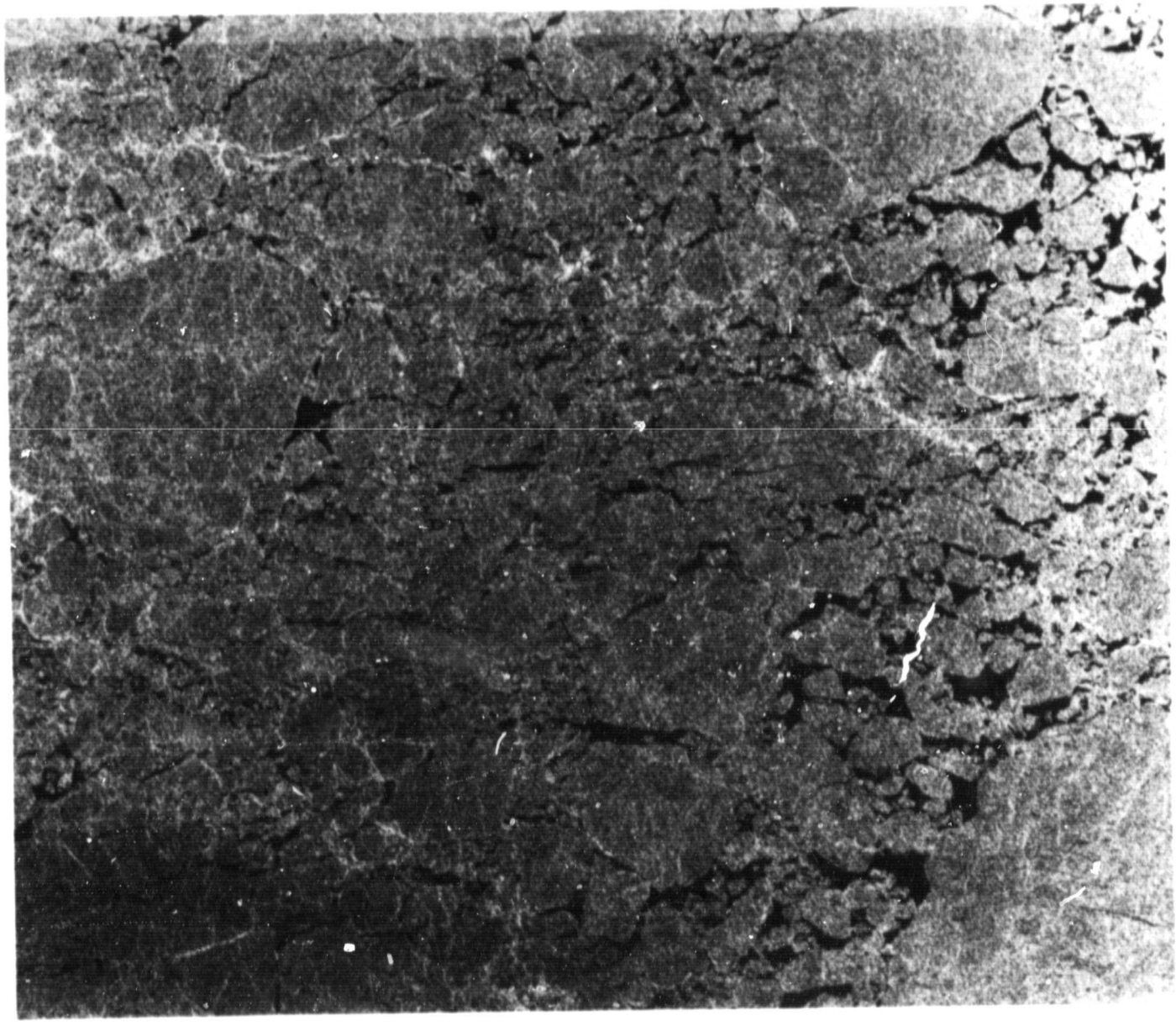

Fig. 2-8. Seasat image of Beaufort Sea orbit 780, July 16, 1978

that spaceborne SAR imagery is a valuable complement to Landsat imagery for earth applications.

The scientific results obtained from Seasat and SIR-A have been discussed in the literature (see Appendix C for recommended further reading), but a few key findings can be pointed out:

(1) Seasat imagery showed the feasibility of large-scale polar ice mapping and tracking with an accuracy of better than 100 m.

(2) Both Seasat and SIR-A demonstrated the capability of spaceborne SAR for imaging ocean surface waves and their patterns.

(3) Seasat showed that internal waves are much more common than previously thought.

(4) SIR-A and Seasat showed that a wide variety of patterns (not all well understood) are observed on the ocean surface which are related to bathymetry, currents, wind, and rain.

(5) SIR-A and Seasat demonstrated that radar provides complementary information (relative to Landsat) for structural and lithological mapping.

(6) SIR-A acquired, for the first time, images of subsurface features in the hyperarid regions of Africa.

In all of these examples, it is seen that radar has a unique sensitivity to surface geometry and the presence of surface water. In very dry desert terrains, there can be radar signal penetration on the order of centimeters to meters.

IV. The Role of Future Space Radar Missions

It should also be pointed out that, although much was learned from the Seasat and SIR-A experiments, much more has yet to be discovered using SAR as a remote sensing tool. Both Seasat and SIR-A were fixed-parameter SAR designs, i.e., the wavelength, incidence angle, and polarization parameters were not controllable. However, it is known that the utility of SAR is greatly enhanced when long, medium, and short wavelengths (L-, C-, and X-bands) are available, with multiple polarizations (HH, VV, HV) and at controllable incidence angles. The ability to control each of these parameters would greatly increase the potential information content from spaceborne SAR. Practically, however, this ideal 3-parameter radar is more expensive and complex than either a fixed-parameter radar (Seasat or SIR-A), or even one with a single controllable parameter such as SIR-B with its selectable incidence angle.

SIR-B represents the first step toward an eventual radar research instrument which exploits the full information content in backscattered microwave energy. It is a very significant first step since the ability to control the illumination geometry is quite important in a wide variety of potential research applications.

Beyond SIR-B, additional shuttle-based and independent platform imaging radar experiments are being planned by NASA which will add the additional controllable parameters of wavelength and polarization to space-based radar remote sensing research. Both SIR-B and these advanced radars will be increasingly put to use in combination with satellite imagery from optical sensors such as the Landsat-4 TM, as well as solid-state linear array pushbroom scanners of the future.

Section 3
SIR-B Geoscientific Experiments

I. Introduction

This section discusses the geoscientific experiments which are generally feasible with SIR-B. The discussion is organized according to five major disciplines: geography, geology, hydrology, oceanography, and vegetation.

Each of these five will be individually described in more detail in the following subsections, by answering the following questions:

(1) What are the thematic objectives of the use of remote sensing for this discipline?

(2) What role does radar play in meeting these objectives and what is the scientific basis for a SIR-B role in particular?

(3) What generic categories of SIR-B experiments appear to be reasonable?

The major scientific interests ascribed to each area are shown in Table 3-1. The experiment categories, while suggestive of what is possible with SIR-B, should not be construed as comprehensive or all-inclusive.

The geographic coverage of the Seasat, SIR-A, and SIR-B missions is shown in Fig. 3-1. The SIR-B mission will have the additional benefit of allowing extended temporal observations of demographic, morphologic, and other thematic changes that have taken place since the launch of Seasat in 1978. Seasat covered most of North American and adjacent bodies of water as well as sections of northern Europe during its 100-day odyssey. Over 100 million square kilometers of the earth's surface were imaged by the Seasat SAR, as roughly indicated by the dashed area on Fig. 3-1. The SIR-A instrument imaged many of these same areas within its 10 million square kilometers of coverage. In 1984, the SIR-B mission will have the opportunity to image an additional 40 million square kilometers over selected swaths from about 60 deg north to 60 deg south latitude. It is therefore important that the SIR-B mission plan consider the prior data collected by Seasat and SIR-A in order to allow extended temporal observations of selected sites. The central challenge for the SIR-B mission design is to wisely use the 25 hours of mission data for carefully chosen experiments designed with knowledge of prior investigations, data sources, and a practical understanding of what is possible in each of these terrestrial science areas.

Table 3-1. SIR-B experiment categories: partial list

Geography	Geology
Cartography	Structural mapping
Deforestation and clear-cutting	Lithologic mapping
Cultural geomorphology	
Land cover	Oceanography
	Oceanic wind experiments
Hydrology	Oceanic wave structure
Soil moisture experiments	Internal structure experiments
Surface water mapping	Bottom morphology experiments
Snow experiments	Slicks and entrained materials
Watershed drainage experiments	Coastal refraction and morphology
Vegetation	Sea ice and icebergs
Agricultural crop experiments	
Forestry and rangeland experiments	

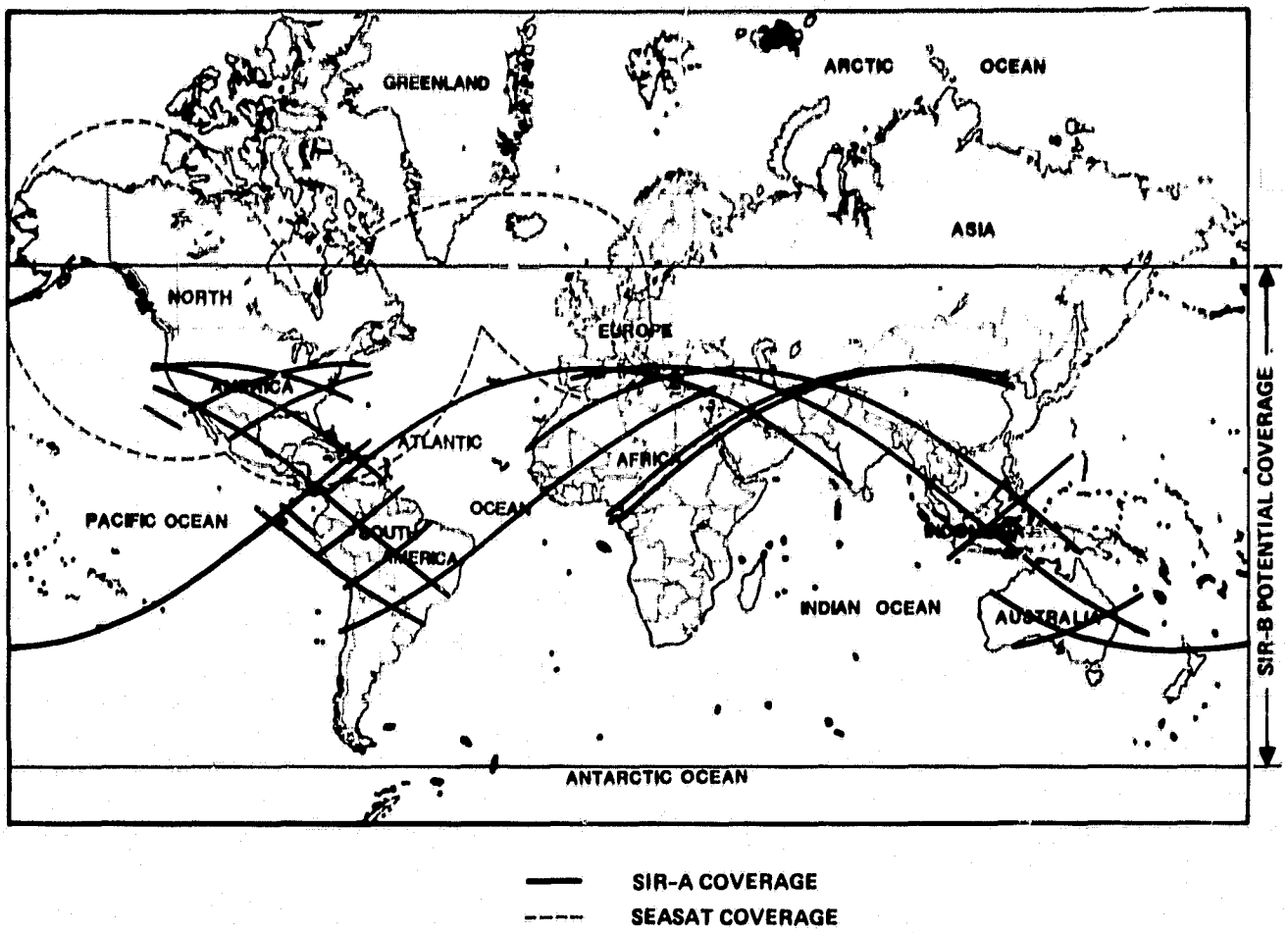

Fig. 3-1. Coverage obtained by Seasat and SIR-A, and the region of potential SIR-B coverage

II. Geography

A. The Objectives of Remote Sensing in Geography

Remote sensing applied to geography furnishes information about the spatial and temporal distribution of physical and cultural features of the earth's surface and provides a synoptic and interactive perspective of the earth. As such, it is concerned with understanding the nature of the changes of the earth's surface, which may be physically and/or culturally induced. A major problem arising out of the continuing advances in technology is the rate of the environmental changes and modifications which generally outstrip our ability to monitor and understand the location, extent, and ultimate impact of such changes. Examples are the expansion of urban areas into prime agricultural land, the location of industry and the possibility of industrial impact in distant localities through such processes as pollution (e.g., acid rain, down-stream deposition, and pollution), and the extraction of resources such as timber and mining. Remote sensing from space offers a means of acquiring consistent regional and global data sets over extended time scales. These data provide fundamental inputs to models which demonstrate the effect of human-induced changes at a variety of scales.

B. The Scientific Basis for SIR-B Geography

High-resolution visible and infrared sensors on satellite platforms have demonstrated their utility for monitoring geographically important phenomena. These data also have limitations. The synthetic aperture radar adds a special significance by providing measurements of geometrically important aspects of the earth's surface (for example, surface roughness, shapes, and orientation of objects). It is also possible to measure surface slopes and orientation and allow the quick identification of major and minor types of surface cover. All of these measurements can be obtained at times and locations which are independent of meteorological variables.

SIR-B observations will cover many different regions, each having a wide variety of surface features. SIR-B will not allow repeated observations of individual areas but can rely on the valuable correlation information from Seasat, SIR-A, and other space-based imagers to support evaluations of regional or local changes. The sensitivity to surficial roughness may also provide evidence of very broad cultural revisions in surface characteristics such as deforestation or conversion of rough underdeveloped areas into ploughed land. Demographic analyses can be performed on a broad scale as cities and towns are readily observable in both Seasat and SIR-A data sets. Human-made changes that relate directly to city size, density, composition, and gross technological status can be observed. The relative orientation of the city layout and the radar look directions (aspect angle) strongly influences the resulting image, and this factor may yield important information from the multiple aspect viewing made possible by the squint feature provided exclusively by SIR-B. It may also be useful to view representative demographic areas at several incidence angles, a utility afforded by the SIR-B sensor. There are many demographic indicators such as expanding lines of communications (vehicular roads, railroads, navigable seaways or canals, power distribution patterns, etc.) that can readily be analyzed from radar data. Land tenure indicators (fences, boundaries, etc.) are also frequently observed. A common attribute of these features is that they generally have a linear form. The SIR-B squint mode provides a method for obtaining data from angles other than orthogonal to the satellite navigation track which will prove helpful for detection and identification of linear features which are critically oriented.

Although airborne camera acquisition of cartographically accurate and valuable data is well established, extensive coverage of large areas to map accuracy standards is very expensive. Spaceborne radars may be able to assist in topographic mapping of sparsely mapped regions, as there are many areas of the world that are either remote or of currently low interest to planning or development organizations and administrations.

The data-taking and processing techniques associated with radargrammetry need to be determined, and the basic limitations on this process need to be established as well. SIR-B incidence variability should be a valuable asset in quantitatively probing this unresolved area of experimentation.

C. SIR-B Geography Experiments

Some suggestions for geography experiments with SIR-B have been developed in (1) cartography, (2) deforestation and clear-cutting, (3) cultural geomorphology, and (4) land cover.

1. Cartography experiments. The purpose of cartography experiments would be to further our understanding of the planimetric limitations of SIR-B, to evaluate stereo-mode contour mapping and conformality (shape accuracy) of the radar data, and to determine the relative and absolute registration possible with multiple SAR sets (SIR-B data from crossover points) and with ancillary data (e.g., Landsat, Seasat-A, SIR-A, maps, and other geographic grids).

Registration is the spatial realignment (rotation, expansion or contraction, and local adjustment), or geometric "rubber-sheeting" of individual pixels to match a reference image or map base. Hence, one of the objectives of the cartographic experiments is to assess the accuracy (relative and absolute) of SIR-B images relative to National Map Accuracy Standards on a geographic grid.

A primary concern for potential users is an understanding of the inherent planimetric limitations for SIR-B and future missions. These limitations on position and derived elevation will constrain both the mapping efforts and co-registration of data obtained on separate SIR-B passes or from other experiments and applications.

Experiments in digital and optical SAR processing need to assess the platform ephemeris and attitude data precision necessary for SAR image radargrammetry. These experiments could also determine the registration techniques and tolerances required for multiple SAR pass data registration under different relief conditions. An understanding of the SIR-B planimetric potential under flat, hilly, and mountainous terrain will also help to define the potential limits to the use of the spaceborne SAR systems for projects that may require mapping, integration with ancillary data, and multisensor data registration.

2. Deforestation and clear-cutting monitoring experiments. Deforestation is an important area of investigation which can address the accuracy of vegetation maps in areas of active deforestation. Clearing is widespread, particularly in the tropics, and there are large variations in current estimates of clearing rates and areal extent. Scientists are forced to use small-scale maps on which to base calculations of biomass and models of biogeochemical fluxes. A specific justification for accomplishing this study would be to demonstrate that deforestation information based on data from satellite-borne synthetic aperture sensors can be provided with a higher degree of reliability than those currently available. Sample information relative to localized rates of deforestation could be derived from areas of active deforestation covered by a combination of either Seasat, SIR-A, and/or SIR-B overpasses.

Experiments can be developed to estimate the location and extent of clear-cutting and deforestation in developing areas

where maps are nonexistent, old, or highly inaccurate to assess changes in forestation over the 6-year period spanned by Seasat, SIR-A, and SIR-B, and to assess the utility and assimilation techniques of radar data in global climate models.

3. **Geomorphological experiments.** Because the data obtained by synthetic aperture radars are especially sensitive to geometric features, they are ideal for obtaining high-resolution information concerning the forms of small- and large-scale geomorphic features on the earth's surface. It has been demonstrated that very-low-angle viewing (e.g., near-grazing angle) creates shadows which enhance very subtle features (e.g., drumlins), whereas high-angle viewing (e.g., Seasat-A 20 deg off nadir) can be equally valuable for identifying the same and similar features. This is due to the increase in radar backscatter as the local incidence angle approaches being normal to the surface. Because SIR-B provides an opportunity to view the earth's surface at a wide variety of depression angles, the importance for obtaining geomorphic information could be studied and assessed.

Experiments in cultural geomorphology consist of quantitative assessments of the potential of radar data for characterizing the human impact on landscapes in a variety of environments, as evidenced by changes in topography, drainage, roughness scales, landscape textures, etc. The experiments could also consider land utility or capability studies, time revision of erosion indices, and desertification induced by human action.

Imaging radar data allows us to rapidly gather regional planimetric and topographic data in a format which can be processed by computer. This allows, for the first time, the acquisition and compilation of large area data sets. Specific geomorphological parameters and parametric distributions can be extracted and compared with other data sets (e.g., optical imaging, geologic maps, land use patterns), as well as with radar parameters (e.g., terrain texture and backscatter characteristics). Both the natural environment and the effects of development, channelization, dams, road networks, overgrazing, soil destabilization, and erosion can be assessed. Quantitative analysis of patterns and the intercomparison of pattern characteristics between affected and nonaffected areas over time may bring to light subtle differences which can be relevant to understanding the effects of human intrusions into the ecosystems. Related topics might also include the effects of major natural disasters on the environment (e.g., floods, volcanic eruptions, dust bowls, aeolian stripping of soil, etc.). The emphasis here should be on acquiring a quantitative data set amenable to computer manipulation, which could allow characterization of quantitative parameters for land characteristics.

4. **Land cover experiments.** Land cover experiments which include identification of gross changes in rural and urban land cover as an input to major statistical studies of crop potential and environmental quality within selected regions should be considered. These studies will provide the data needed to provide baseline inventories and to access the cumulative impact and contribution of land use to forecast models.

Specific subjects of interest are to determine the accuracy of detection of the urban/rural fringe, to assess the urban expansion into farmland, to provide quantification of the effect of urban morphology on radar backscatter, and to provide for mapping of small settlements in poorly mapped areas.

Land use mapping provides the data base upon which a variety of environmental modeling and forecasting systems depend. For example, crop yield estimates for a state or country require statistics on the location, area, and type of crop lands, and hydrologic runoff models apply different infiltration and surface flow rates to different land cover types. Land cover areas experiencing significant changes over the 4- to 5-year time interval between SAR missions, particularly due to deforestation, urban land area expansion, and diminished rangeland capacity associated with desertification, provide test sites for change detection using satellite-borne radars. These changes, over decades, significantly affect regional agricultural potential and environmental quality.

In many of the suggested experiments, the strength of the radar backscatter, as related to the preferential look direction and the orientation of the cultural activities, will be of major importance. The SIR-B instrument has the unique ability to operate at a variety of look direction (squint mode) for any given geographic site, in addition to the previously mentioned variation in incidence angle. Thus, it will be possible to capitalize on the geometric aspects of the region, which is not possible using other satellite-borne sensors. Data obtained which show preferential expression of trends on the ground such as geologic morphology, tilling practices (e.g., contour ploughing), or city grids, will enhance the utility of the remote sensing data.

III. Geology

A. The Objectives of Geological Remote Sensing

Modern industrial economies which form the basis of twentieth century society are critically dependent upon mineral and energy resources that are extracted from the earth's crust. Geologists study the earth in both a basic and applied sense to gain an improved understanding of the processes that shape the crust and the manner in which mineral

deposits form. Basic geological research is concerned with learning more about how rocks form and deform, how continents nucleate and grow, and how crustal processes have changed during the past few billion years of earth history. Applied research is concerned with the emplacement of geological resources, the study of geological hazards such as earthquakes and volcanic eruptions, and man's ability to exploit and manage the geological environment in which he lives.

Remote sensing is one of a variety of tools that has been employed by geologists to study crustal structure and composition. There is a growing realization within the geological community that certain types of unique information can be derived from remote sensing measurements that cannot be obtained with conventional field mapping or geophysical survey techniques. Remote sensing methods tend to complement conventional techniques and can potentially contribute to the creation of new, more sophisticated types of geological maps. Remotely sensed imagery obtained at synoptic scales has proved to be particularly useful for regional evaluation of oil and mineral potential. Remote sensing can play an important role in developing regional exploration strategies and targeting localized areas for detailed field mapping and geophysical studies. Current research in geological remote sensing seeks to determine the various types of geological information that can be obtained through the analysis of remotely sensed data and how space techniques can be combined with conventional methods for improved geological analysis.

Space-acquired data have provided new insight into the geological structure of many remote and inaccessible areas which have not been extensively studied in the past. The unique ability of orbital sensor systems to acquire data on a global basis at uniform scales and accuracies holds great promise for the study of mineral frontier regions situated in polar, tropical, and arid areas. The availability of remotely sensed data acquired by orbital sensors also enables geologists to conduct comparative studies of crustal structure and composition on a worldwide basis to an extent which has not been possible in the past. Research of this nature can potentially contribute to improved understanding of crustal processes that operate at continental and global scales.

B. The Scientific Basis for SIR-B Geology

The principal research objectives of the SIR-B geology experiments are to determine what types of geological information can be extracted from radar imagery, and to apply such space-derived information to the study of the earth's crust. Previous orbital sensors have obtained radar imagery at a constant angle of incidence. Surface coverage from more than one azimuthal direction (aspect angle) has only been collected in areas where the ground tracks of earlier sensor systems have intersected. SIR-B will be able to illuminate the earth's surface over a wide range of incidence angles (15 to 60 deg). In addition, the maneuverability of a shuttle platform can be exploited to obtain radar imagery of selected areas from several different azimuthal aspects. The SIR-B antenna can be oriented to the left or the right of a shuttle flight direction. The shuttle can also be yawed left or right to "squint" the radar beam forward and aft of the nominal broadside ground track.

In light of the limited duration of the SIR-B mission and the innovative measurement capabilities of the SIR-B sensor, primary emphasis will be placed on using SIR-B for experimental study of the geologic utility of radar remote sensing techniques. Technique related research will specifically focus upon determining what types of geological information can be extracted from radar imagery obtained under different illumination conditions, and comparing this with information obtained with other sensor systems (e.g., Landsat) and conventional methods (e.g., aerial photography, field mapping). The results of the SIR-B mission will be invaluable in attempting to optimize the design of future orbital radar systems for geological applications. These results will also prove useful in evaluating the complementary nature of different remote sensing techniques, and in formulating recommendations concerning sensors that could eventually be placed on a permanently orbiting space platform.

The secondary geological objective of the SIR-B mission involves the use of SIR-B data in an applied sense to study the regional structure and geological characteristics of specific crustal provinces. Radar coverage of the earth's surface provided by earlier orbital sensors has been constrained by a variety of factors including the data acquisition capabilities of ground receiving stations, onboard data recording capabilities, and the orbital inclination of the sensor platform. The high orbital inclination and digital data transmission capabilities of SIR-B will permit researchers to obtain radar imagery of many geologically interesting regions for the first time (see Fig. 3-1). The ability to change antenna look angle during the SIR-B mission will also enable researchers to obtain overlapping coverage of adjacent areas which can be combined to form large area mosaics of selected regions. SIR-B will provide an unparalleled opportunity to apply orbital radar imagery to regional geological studies in a wide variety of geological settings.

Extended coverage of specific regions will necessitate the acquisition of SIR-B imagery from various azimuthal directions and incidence angles during successive orbital passes of the shuttle. Scene-to-scene variations in surface illumination conditions will introduce complications in the analysis and interpretation of image mosaics. Furthermore, there will invariably be gaps in the coverage that can be obtained over

large areas during a 7-day shuttle mission. For these reasons, the use of SIR-B data for large-scale mapping and crustal research is considered to be the secondary geological objective of the mission. Nevertheless, it is essential that extended coverage of selected areas be acquired to demonstrate how orbital radar imagery can be used for global crustal studies, and to underscore the need for global radar data sets.

C. SIR-B Geology Experiments

Radar imaging techniques can be used to detect areal variations in surface relief and roughness, and in the intrinsic electrical properties of surficial materials. Information of this nature has a wide variety of potential geological applications in terms of analyzing crustal structure, detecting lithologic variations in sedimentary rock strata, studying regional geomorphology, and detecting petrologic variations within surficial rocks and soils. Proposed SIR-B experiments are categorized here in terms of their applicability to structural and lithologic mapping.

1. Structural mapping experiments. Structural mapping experiments are concerned with the use of radar methods to obtain information concerning the relief or topography of natural surfaces. Detailed knowledge of surface relief is essential for classifying landforms, determining the alignment and orientation of particular topographic features, and mapping regional variations in surface slope. Geologists employ areal variations in landform distribution and orientation, and observed relationships between surface slope and regional drainage patterns to infer the attitude of sedimentary rock units, the presence of crustal folds and faults, the style and intensity of regional tectonic deformation, etc.

a. Regional geological studies. Extended SIR-B coverage should be obtained over selected areas in which the availability of radar imagery would make a significant contribution to improved understanding of regional crustal geology. Candidate terranes include, but are not limited to, tropical areas which are frequently cloud covered and difficult to observe with visible and infrared imaging systems such as Landsat, arid areas containing widespread deposits of windblown sand, and remote mountainous areas which have received limited study in the past due to their inaccessibility.

Tropical regions have received comparatively little attention from exploration geologists due to logistical problems, health hazards, and the large cost of field operations. Airborne radar imagery has been collected over a limited number of tropical areas, notably within Panama, Brazil, Venezuela, and Nigeria. While these aerial data sets have proved useful, they are limited in size and have severe shortcomings in terms of their geometric fidelity and radiometric control. The acquisition of SIR-B imagery over tropical areas would enhance the geologic utility of existing aircraft imagery, and also provide new insight into the regional structure of major mineral frontier areas.

Many arid areas are characterized by low regional relief and widespread variations in surface roughness. Deflation surfaces formed by the removal of windblown sand generally contain rocks of varying size that have been locally exhumed. Areas of active sand deposition are relatively smooth in comparison. Radar imagery acquired at carefully selected incidence angles can potentially be used to distinguish areas of sand erosion and deposition on the basis of their roughness characteristics, and to detect incipient desertification of semi-arid regions.

Soil moisture normally attenuates microwave radiation over a depth of a few centimeters; however, radar penetration to depths of several meters can be achieved in hyperarid environments that contain surficial deposits of dry windblown sand. Subsurface geological features have been detected in earlier orbital imagery obtained in areas of extreme aridity. Extended SIR-B coverage of hyperarid regions would potentially provide new insights into the bedrock geology of the eastern Sahara desert, and portions of China, Australia, and the Middle East.

SIR-B coverage can potentially be obtained in a variety of remote mountainous areas which are currently sites of active tectonic deformation. For example, the Andes Mountains of South America have been constructed in recent geological time by the collision of the South American continent and the Pacific Ocean tectonic plate. In contrast, the Himalayan Mountains of Asia have been produced by the collision of two continental landmasses (the Asian continent and the Indian subcontinent). Comparative study of the style and extent of tectonic deformation in these different geological settings could potentially contribute to improved understanding of plate tectonic processes.

These examples do not represent specific targets for SIR-B data acquisition. Extended coverage should be acquired to address specific geologic problems in any area where regional radar imagery could lead to a significant improvement in current understanding of crustal geology.

b. Optimum radar viewing geometry for structural studies and topographic mapping. Previous research has clearly demonstrated that radar imaging techniques can be used to highlight subtle topographic variations in different types of terrain. However, the detection of particular topographic features within a radar image is critically dependent upon the direction of radar illumination and the local angle of radar incidence. Backscatter from natural terrain is very sensitive to changes in surface slope at incidence angles of 0 to 30 deg

(measured from the local vertical). At higher incidence angles radar backscatter is primarily governed by surface scattering effects (30 to 70 deg) and shadowing (70 to 90 deg).

Seasat imagery has proved to be extremely useful for detecting subtle drainage features in areas of low regional relief because small changes in surface slope produce large variations in radar backscatter at low incidence angles. The utility of Seasat data acquired in mountainous areas of high relief is quite limited, however, due to extensive superposition of adjacent terrain elements (i.e., image layover). In contrast, SIR-A imagery acquired at 47-deg incidence possesses much less geometric distortion in areas of high relief. It is generally superior to Seasat imagery for identifying drainage features in mountainous areas. By acquiring multiple radar imagery at different look angles, SIR-B will be able to achieve low incidence angle coverage of a wide spectrum of topographic features in different geomorphic environments. Comparative studies of slope effects and feature perception within multiple SIR-B imagery will permit geologists to determine the combination of radar look angles that is best suited for structural mapping in different geomorphic settings (e.g., basins, plains, mountain belts, etc.). Figure 3-2 illustrates the type of variations that are observed in low and high incidence angle imagery of mountainous terrain.

The sensitivity of radar backscatter to variations in surface slope can also be used, in principle, to map the topography of the earth's surface. Multiple radar images acquired at different look angles from a constant azimuthal direction can be viewed stereoscopically. Stereoscopic convergence can also be achieved with image pairs acquired from different azimuthal directions at a constant look angle.

Radar imagery differs in several fundamental respects from conventional photography, and these differences can affect the utility of radar data for topographic mapping. Layover is commonly observed in radar images of mountainous areas acquired at low look angles (i.e., less than 30 deg). Layover is similar to shadowing in that it results in the loss of topographic information within selected areas. In addition, SAR images inevitably contain some degree of speckle because they employ a geometrically coherent source of scene illumination. Speckle represents a source of noise in radar imagery that can lead to erroneous estimates of local elevation. Topographic features that appear in two stereoscopic radar images are illuminated in a slightly different manner as they move through the ground coverage pattern of a SAR system. This effect (referred to as specular point migration) occurs because the source of surface illumination moves with the sensor, and it places an upper limit on the vertical exaggeration that can be achieved within stereoscopic image pairs.

Theoretical studies indicate that topographic mapping accuracy generally increases with decreasing radar look angle due to reduction in shadowing effects. However, accuracy deteriorates at very small look angles due to extreme foreshortening and layover. Computer modeling procedures have also been developed to simulate radar imagery for stereoscopic analysis. Computer simulation studies have been performed for a limited number of geomorphic terrains for which digital topographic data is readily available. These studies have proven the feasibility of using multiple look angle imagery for topographic mapping. However, they also suggest that optimum combinations of radar look angles for topographic mapping may vary significantly among different types of terrain.

SIR-B will provide a unique opportunity to empirically verify theoretical and computer simulation studies performed in the past. Multiple look angle imagery obtained by SIR-B can be used to extend the results of earlier computer simulation studies to a wider diversity of terrains, and to determine the optimum radar illumination conditions for topographic mapping in specific geomorphic settings.

c. Comparison of structural information obtained by different sensor systems. Various types of orbital remote sensing imagery have been employed in the past for regional scale structural mapping. The utility of orbital imagery for structural studies is governed by image spatial resolution, the geometric relationship between the radiation source and the orbital sensor, and the manner in which radiation of varying wavelength is reflected or emitted from the earth's surface. Past attempts to compare the utility of visible, infrared, and microwave imagery have been complicated by variations in the former two parameters listed above.

For example, the series of multispectral scanners carried on the Landsat series of satellites have obtained measurements of reflected solar radiation with a pixel resolution of 80 m, whereas the Seasat radar system obtained measurements of backscattered microwave radiation with a pixel resolution of 25 m. In areas of subdued relief, Seasat imagery has generally proved to be superior to Landsat for detecting small-scale landforms, resolving detailed bedding features in stratified rock exposures, and identifying higher order stream channels in regional drainage networks. Improvements in mapping capabilities realized with Seasat are undoubtedly related to the improved spatial resolution of the Seasat SAR. However, fundamental differences in the manner in which solar and microwave radiation are reflected from natural surfaces may also influence the detectability of specific surface features.

Planar surface features which directly face a radar's antenna provide a strong return signal and appear bright in radar imagery, whereas features which parallel the direction of signal

ORIGINAL PAGE
BLACK AND WHITE PHOTOGRAPH

NOVEMBER, 1981

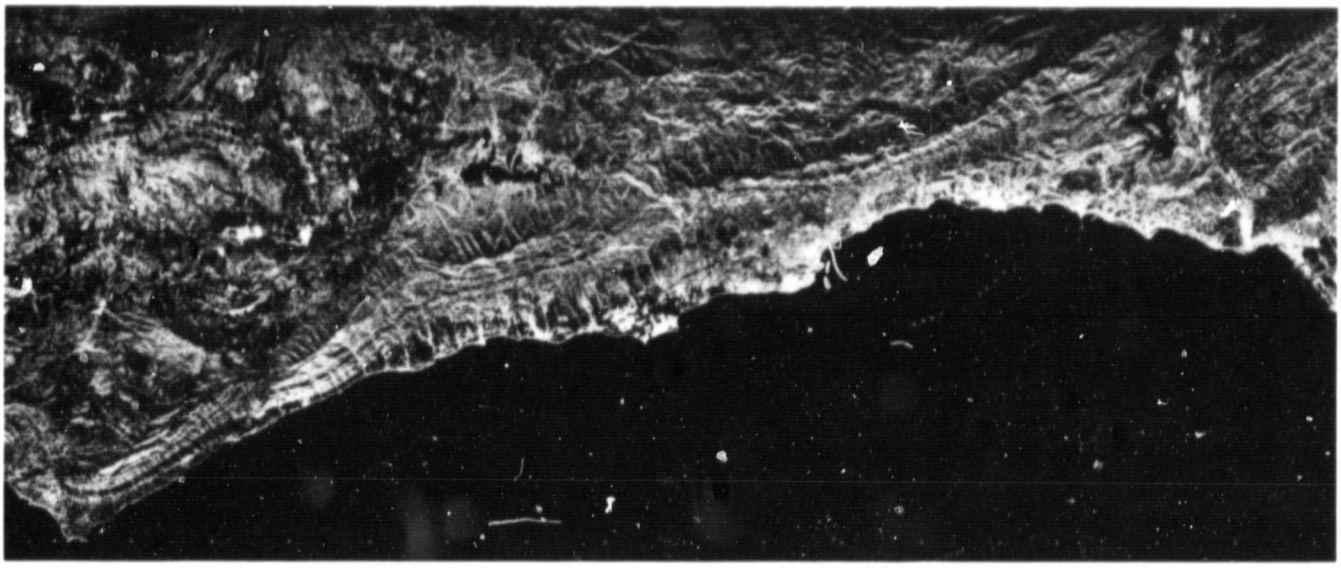

ILLUMINATION DIRECTION

N

0 10 20 km

SIR-A
50° INCIDENCE ANGLE

JULY, 1978

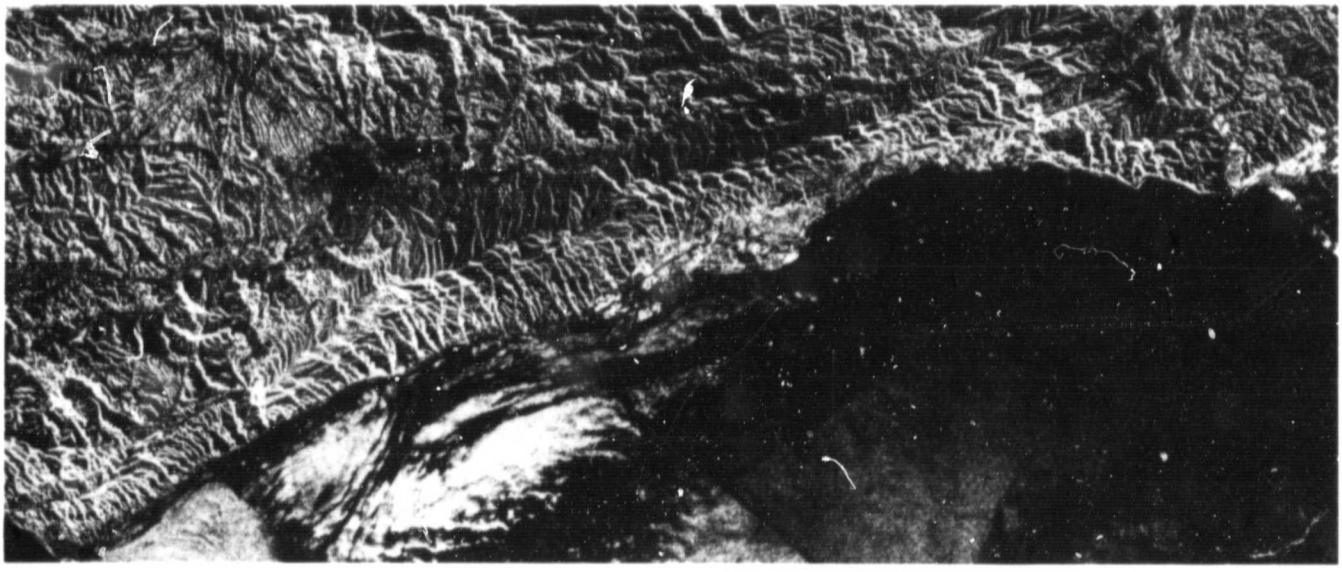

ILLUMINATION DIRECTION

N

0 10 20 km

SEASAT
20° INCIDENCE ANGLE

Fig. 3-2(a). Comparison of Seasat and SIR-A imagery of the Southern California coastline near Santa Barbara. Individual rock units within the coastal mountain range can be detected as alternating dark and light bands and traced over distances of several kilometers in the SIR-A image. These units cannot be readily detected in the Seasat imagery due to the sensitivity of radar backscatter to variations in surface slope at lower angles of incidence. (Note that variations in ocean surface roughness produce features in the seasat image that resemble clouds)

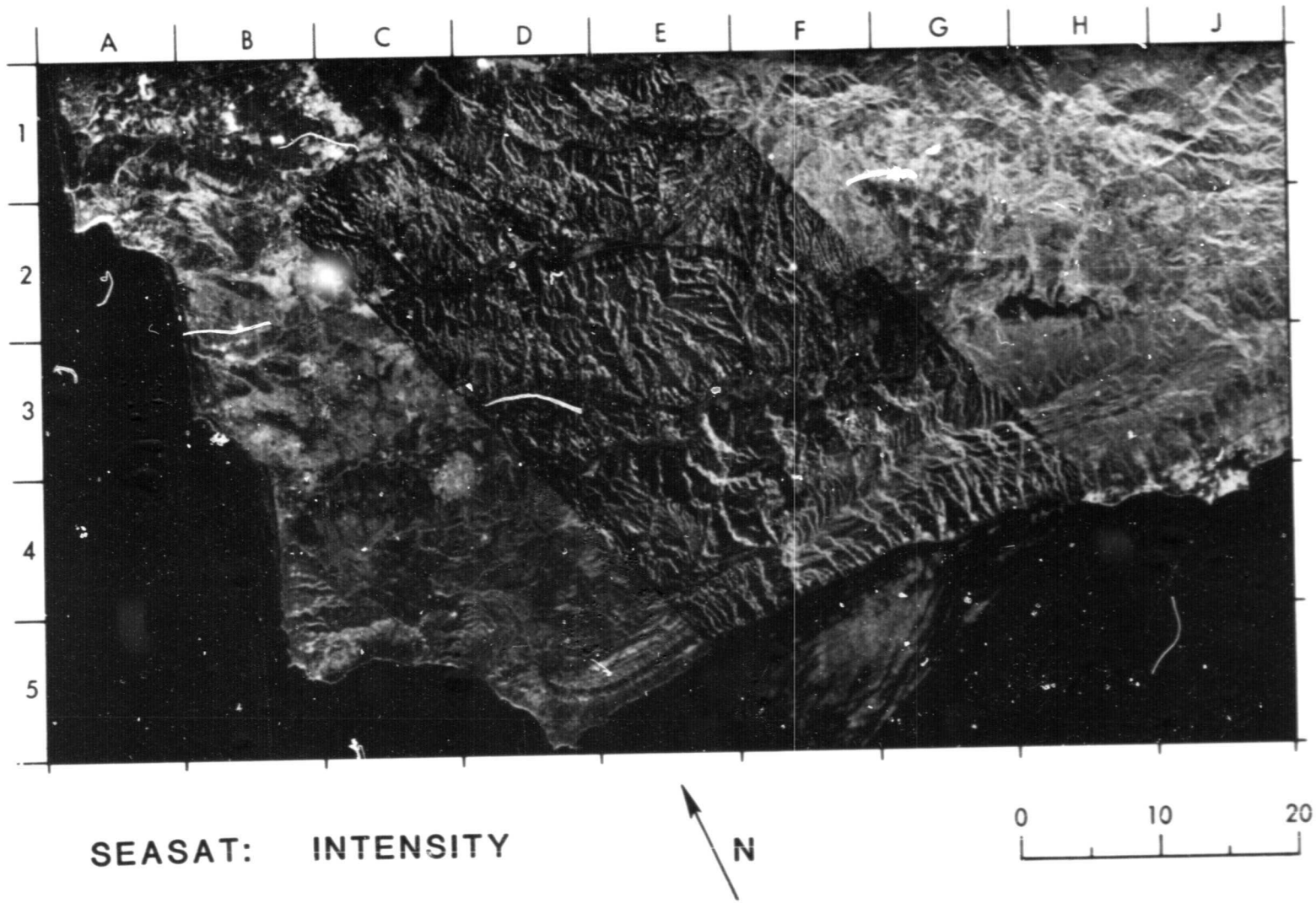

ORIGINAL PAGE
COLOR PHOTOGRAPH

Fig. 3-2(b). Co-registered SIR-A and Seasat SAR images of the Santa Ynez Mountains, California

propagation tend to provide weaker radar returns. Scarps, hillsides, and stream banks which are much smaller in width than individual picture elements may nevertheless be highlighted within a radar scene because they directly face the radar's antenna. Geologists normally desire improved spatial resolution in orbital imaging systems in order to detect smaller scale landforms and topographic features. However, in the case of radar, the ability to acquire multiple images of a given area at variable look angles may prove to be more valuable for structural mapping than further improvements in image spatial resolution.

Geometric relationships between the source of scene illumination and sensor system can introduce biases into structural interpretations based upon orbital imagery. Over the course of a typical day natural solar radiation preferentially illuminates the earth's surface in an east-west direction. This directional bias in solar illumination highlights linear topographic features aligned in a north-south direction within visible-infrared imagery, and it tends to obscure features with east-west alignments. A similar effect occurs in radar imagery with respect to the direction of radar illumination. Ideal test sites for evaluating the effect of illumination geometry upon structural interpretations will be situated near the north and south extremes of the SIR-B orbital track (i.e., in the vicinity of ±50 deg latitude). In these regions SIR-B will illuminate the earth's surface primarily in the north-south direction, whereas the sun will preferentially illuminate the surface in the east-west direction. In principle, it should be possible to merge structural information derived from visible-infrared and microwave imagery to overcome these directional biases. However, no rigorous procedures have been developed in the past for this purpose.

The potential ability to acquire Landsat-D TM data in conjunction with the SIR-B mission will provide a unique opportunity to evaluate the relative utility of orbital imagery acquired at different wavelengths for purposes of structural mapping. In middle- and high-latitude regions, it will be possible to obtain SIR-B imagery at radar look angles and azimuths that exactly correspond to solar zenith angle and azimuth during selected seasons. Comparative analysis of SIR-B and TM imagery acquired under similar illumination conditions with comparable spatial resolution will permit researchers to study the intrinsic utility of visible-infrared and microwave techniques for terrain analysis and structural mapping.

2. **Lithologic mapping experiments.** Lithologic mapping experiments involve the use of radar methods to obtain information concerning the roughness or dielectric properties of natural surfaces. Variations in radar backscatter related to these parameters can be employed to detect areal variations in the physical structure, mineralogy, and bulk chemistry of surficial rocks and soils. In certain circumstances, it may be possible to map lithologic boundaries between different types of rocks and soils on the basis of their textural and/or dielectric properties. The use of multiple look angle imagery for lithologic mapping represents a pioneering application of orbital microwave techniques. Similar experiments have not been attempted with aerial radar data because of the large variations in incidence angle that occur as a function or range (i.e., across the radar swath).

a. Discrimination and identification of surficial geological materials. The microrelief of natural surfaces is a complex function of the size, shape, and distribution of surficial geological materials, and the size, structure, and distribution of surface vegetation. Geological materials tend to weather in distinctive fashions in different climatic environments to produce surficial deposits of soil, sand, gravel, talus, etc. The physical and chemical characteristics of surficial geological materials can also influence the distribution and development of plant species. For example, the local availability of soil moisture may be constrained by the porosity of underlying rock units, or the chemical weathering of rocks and soils may produce concentrations of metallic ions in local groundwater which cannot be tolerated by certain plant species.

Areal variations in the morphology of rock weathering products and the architecture of the overlying vegetation canopy produce areal variations in surface roughness which may be diagnostically related to the lithology of surficial rock units. For example, sandstones, mudstones, siltstones, and shales commonly found in sedimentary terrains consist of fine particles of varying size cemented together in a chemical matrix. These sedimentary rocks tend to weather in slightly different fashions when exposed at the earth's surface, and they may individually support slightly different assortments of vegetation. The weathering products and plant species that develop on the surface of these different types of rocks may produce subtle variations in surface roughness that could potentially be detected in measurements of radar backscatter.

Multiple SIR-B imagery of selected test site areas can, in principle, be used to determine the radar reflectivity of pixel-sized areas within the critical 30- to 70-deg range of incidence angles that is most sensitive to variations in surface roughness. Pixels characterized by similar brightness values at different angles of incidence can be digitally identified and classified (see Fig. 3-3). This procedure potentially provides a means of discriminating surficial materials on the basis of their roughness and intrinsic dielectric properties. Layover and foreshortening effects introduce geometric distortions which complicate the precise identification of common pixel-sized areas in radar images acquired at multiple look angles. Im-

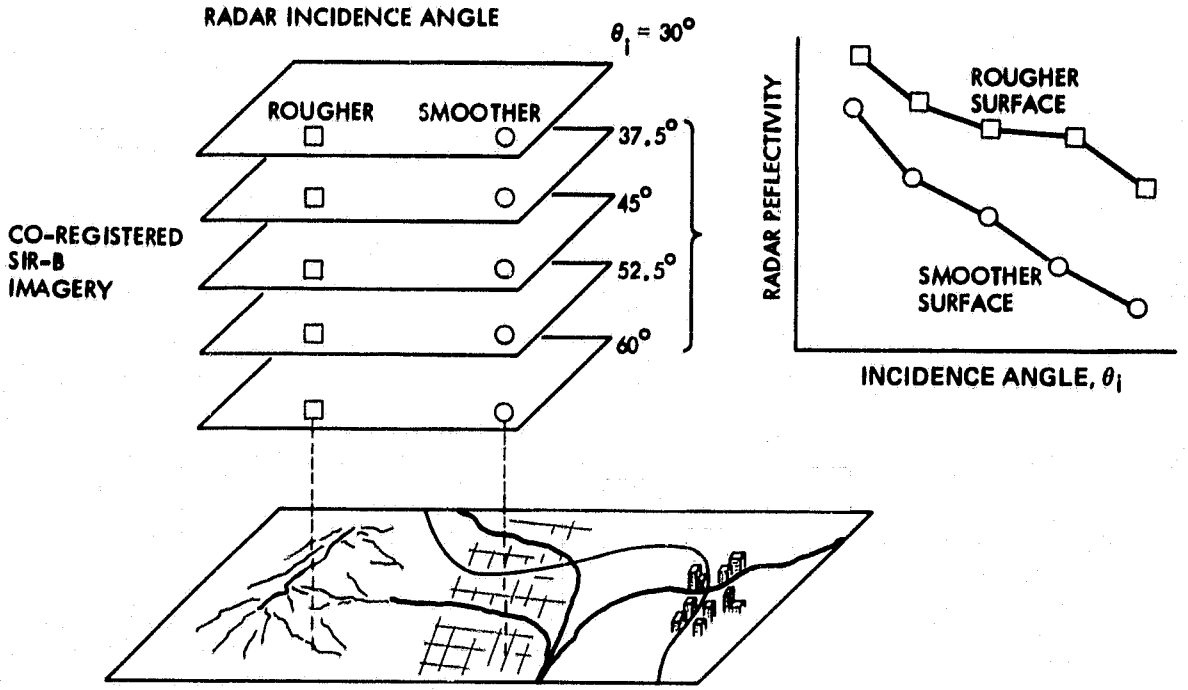

Fig. 3-3. Use of multiple incidence angle radar imagery to map surficial materials

proved methods for geometric rectification and digital co-registration of radar scenes will be required to map consistent variations in radar reflectance as a function of incidence angle within an extended area. In addition, prior knowledge of surface topography will be required to determine the average angle of radar incidence on a local scale within pixel-sized areas.

The pattern recognition procedure described above bears some resemblance to the classification of multispectral imagery collected at visible and infrared wavelengths. Reflectance variations observed in different spectral bands are used to discriminate surficial materials in the same way that backscatter variations observed at different incidence angles might be used to recognize lithologic boundaries. *In situ* measurements of surface reflectance obtained with portable field spectrometers have been used in the past to calibrate orbital multispectral surveys. Field measurements provide a means of relating variations in surface reflectance measured at orbital altitudes to an absolute reflectance standard, so that they can be directly compared with laboratory spectra. In principle, image calibration enables geologists to identify specific types of rocks and soils exposed at the surface.

In an analogous fashion, microwave scatterometer measurements may potentially be used to calibrate orbital radar imagery. Field measurements of surface backscatter are routinely obtained with truck-mounted and airborne scatterometers. In arid regions, field scatterometer measurements provide a means of relating variations in radar reflectivity observed at orbital altitudes to the actual radar scattering coefficient of the ground surface. In dry environments, it may be possible to identify particular geological materials within multiple look angle orbital imagery on the basis of field scatterometer measurements performed in localized areas. In temperate and tropical regions, spatial and temporal variations in moisture conditions can produce large, transient variations in surface backscatter. In these environments, field scatterometer data must be acquired simultaneously with orbital radar imagery for purposes of image calibration and may only be representative of the limited areas in which they are obtained.

b. Combined utility of microwave and visible-infrared techniques for lithologic mapping. Unique types of lithologic information can be obtained through the analysis of remote sensing surveys performed in different portions of the electromagnetic spectrum. Backscatter variations observed in radar imagery are primarily related to the morphology and physical structure of natural surfaces, whereas radiance variations observed in visible and infrared imagery are related to surface reflectance, emissivity, and temperature. The types of information that can potentially be derived from radar imagery differ significantly from those which can be obtained in these other spectral regions. The use of different imaging techniques for lithologic mapping could prove to be highly complementary, and further analysis of multiple image data sets is clearly warranted.

A variety of orbital and aerial imaging sensors will potentially be available for contemporaneous data collection during the SIR-B mission. These include but are not limited to:

(1) Thematic Mapper (orbital) – Landsat-D instrument which can obtain imagery in seven discrete spectral channels within the visible, reflected infrared, and thermal infrared portions of the spectrum (30-m spatial resolution; 185-km swath width).

(2) Large Format Camera (orbital) – A nadir pointing, photographic camera that will obtain imagery in the visible and near infrared (10-m spatial resolution; 160-km swath width); this instrument is scheduled to fly on the same shuttle flight as the SIR-B instrument.

(3) Thermal Infrared Scanners (aerial) – A variety of airborne scanners are available which can obtain broadband measurements of thermal emission (8 to 12 μm); diurnal surveys of apparent ground temperature can be used to estimate areal variations in apparent thermal inertia (variable spatial resolution, generally $\geq$ 10 m).

(4) Multispectral Thermal Infrared Scanner (aerial) – A 6-channel airborne scanner which obtains multispectral measurements of thermal emission in the 8 to 12 μm wavelength region (variable spatial resolution, generally $\geq$ 15 m).

(5) Real and Synthetic Aperture Radars (aerial) – Airborne radar systems (C-, L-, and X-band) with variable antenna look angles ranging from approximately 10 to 55 deg (5- to 15-m spatial resolution; 20-km swath width).

c. Analysis of microwave image texture. Various image texture studies have been performed in the past employing digital Seasat radar imagery. Different procedures have been employed to characterize image texture, such as calculating brightness variations in the vicinity of individual pixels and 2-dimensional spatial filtering of entire scenes. Preliminary results have been encouraging. Measures of local brightness variance have improved the accuracy of rock-type classifications based on Landsat data in selected test site areas. Spatial filtering procedures have served to highlight subtle variations in surface morphology in other areas which could be correlated with known boundaries between surficial rock units.

Variations in the brightness of a radar image are heavily modulated by surface topography. Spatial filtering methods provide a means of suppressing or enhancing brightness variations that occur over a particular horizontal distance within a radar scene. Consequently, spatial filtering can be used to accentuate broad scale variations in image brightness which may be obscured by smaller scale topographic variations. Conversely, filtering procedures can be used to accentuate small-scale variations in backscatter which may be observed by large-scale topographic undulations. Apparent variations in image brightness are highly dependent upon radar illumination conditions. Selective filtering of radar imagery acquired at different look angles provides an empirical means of highlighting brightness variations that occur over specific horizontal scales. Recombination of filtered image products derived from multiple look angle imagery may prove to be useful for discriminating lithologic boundaries in areas in which surface relief varies over a wide range of horizontal scales.

It may also be possible to develop new measures of image texture based upon multiple look angle imagery. Cartographic co-registration of multiple scenes will permit estimation of brightness variations in the vicinity of an individual pixel at different radar look angles. The rate at which brightness variance in the vicinity of a pixel changes with incremental changes in radar look angle may prove to be useful for detecting subtle boundaries between areas of varying surface roughness.

d. Regional variations in surface electrical properties. In most instances, backscatter variations related to surface relief and roughness are of much higher amplitude than those associated with the intrinsic electrical properties of surficial materials. Unexpected variations in radar reflectivity have been noted in earlier orbital imagery obtained over smooth, relatively flat areas. These variations have been largely attributed to ephemeral changes in soil moisture conditions which can significantly alter the bulk electrical properties of surficial materials. SIR-B could provide a meaningful test of our ability to detect variations in surface electrical properties related to soil moisture through repetitive imaging of areas where rainfall is likely to occur. *In situ* measurements of surface roughness, dielectric constant, and moisture conditions at carefully selected test sites will be essential for definitive detection of electrical property variations during the SIR-B mission.

IV. Hydrology

A. The Objectives of Remote Sensing in Hydrology

Hydrologic conditions play an important role in the world ecosystem because they influence both natural and cultural resources as well as the economies that vitally depend on these resources. Figure 3-4 illustrates the hydrologic cycle and the factors of precipitation, runoff, infiltration, irrigation, evapotranspiration, etc. Hydrologic models which are currently used to evaluate these complex and interrelated factors make use of point data sources. Design and planning procedures based on these point data sources have not changed

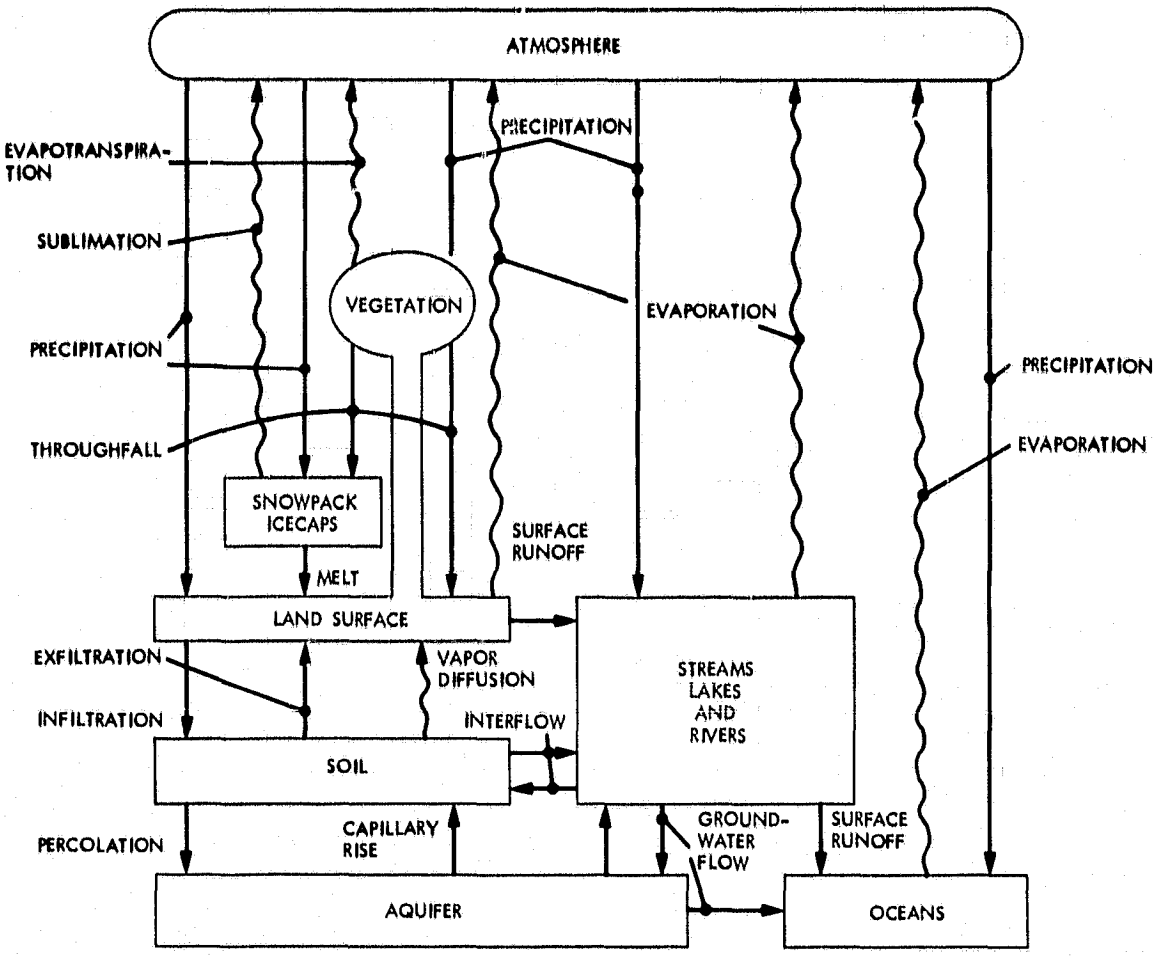

Fig. 3-4. The hydrologic cycle from an engineering viewpoint (after Eagleson, 1970)

appreciably over the last two or three decades. Major benefits will eventually be realized by developing procedures based on the use of distributed data such as obtained from remote sensors, which can provide improved water supply and flood forecasting and hydrologic evaluation of land use changes. Synoptic remotely sensed data describing drainage networks, topography, and soil type are needed at intervals ranging from months to years. More frequent data (hours, days) are needed to describe such things as soil moisture, snowpack extent and wetness, freeze/thaw lines, and runoff coefficients for small watersheds.

Landsat MSS and return beam vidicon (RBV) data, although limited by cloud cover, have been used for visible/infrared (IR) observations of both surface and ground water. Measurements from NOAA/TIROS-N (atmospheric water vapor, and temperature profiles), NIMBUS-7 (surface temperature), and HCMM (albedo) have provided thermal IR and passive microwave data which have been used for evapotranspiration estimates. TM data from Landsat-D will provide surface water observations of improved spatial and spectral resolution which will allow the inventory of smaller bodies of water, better flood plain delineation, improved separation of snow from clouds, etc.

Microwave remote sensing at longer wavelengths (e.g., L-band or C-band) is particularly promising as a technique for soil moisture monitoring and for observation of hydrodynamics. The pronounced sensitivity of emitted or reflected microwave radiation to moisture in the top few centimeters of the soil results from the fact that the dielectric constant of water is at least an order of magnitude higher than that of dry soils at these frequencies. Both radars and radiometers are sensitive to soil moisture, although from orbital altitudes L-band or C-band SAR images provide better spatial resolution than obtainable from practical radiometers operating at the same frequency.

Radar imagery is complementary to both visible/infrared imagery and passive microwave data, and it may have the potential to produce fine scale classification information about

surface soil moisture, surface water areal extent, and watershed characteristics, such as drainage patterns or snowpack water equivalent. The 7-day length of the SIR-B mission supports research experimentation but precludes the acquisition of longer term or seasonal hydrologic data at regional scales that could be valuable in distributed modeling and forecast activities.

The SIR-B mission will offer the opportunity to acquire an abundance of data which can lead to a better understanding of the radar response to a variety of hydrologic conditions. This experimental approach recognizes that the dominating influence on the radar signature of hydrologically varied scenes is not solely that of water or dielectric constant. Surficial roughness and slope both contribute significantly to a composite signature and in many cases can either mask or render ambiguous the presence of water.

B. The Scientific Basis for SIR-B Hydrology Experiments

The spatial and temporal distributions of soil moisture content represent a key input parameter to meteorological, hydrological, and crop yield models. Microwave sensors are well suited for the observation of these distributions because of the strong dependence of the soil's dielectric constant on its moisture content at microwave frequencies. The real part of the dielectric constant for a soil changes from 3 or 4 for dry soils to greater than 20 for wet soils resulting in an increase in the L- or C-band backscatter coefficient of greater than 19 dB as the soil goes from dry to wet. Seasat SAR's sensitivity to soil moisture (see Appendix C) compared with ground measurements of the soil moisture in fields with a variety of surface covers, was about the same as that observed by an airborne L-band scatterometer. There was an approximate 10-dB range in backscatter intensity for the useful soil moisture detection range. On the basis of truck and aircraft radar experiments, it appears that radars operating at C-band and at near-nadir incidence angles (10 to 20 deg) are best suited for soil moisture sensing in the presence of a wide range of surficial roughnesses. Radars operating at L-band were found to be just as sensitive to soil moisture variations but were more sensitive to surface roughness variations than at C-band. SIR-B variable incidence observations offer the opportunity to further quantify the effect of roughness, slope, and vegetation on the ability to infer soil moisture.

Maps of surface water are important in water resources management. Since surface water acts basically as a specular or forward reflector to the radar signal, discrimination between land (brighter and rougher) and water (smooth and dark) is easily accomplished with the SAR. Surface stress (wind) on the hydrosurface can produce significant backscatter, which can make discrimination more difficult, but the water surface is still more homogenous in tone than surrounding land areas.

The longer wavelength of SIR-B makes it well suited for surface water extent observation because of its reduced sensitivity to canopy vegetation. Accurate delineation of coastal wetlands boundaries depends on the ability of the radar to penetrate vegetative cover and then to indicate whether the underlying surface is land or water. Both surface and standing water identification are significant in estimating estuarine productivity. The combination of Seasat, SIR-A, and SIR-B radar data could be useful for monitoring long-term and storm-induced rapid shoreline changes in environments frequently shrouded by cloud cover.

Flood damage estimates are needed for water management and control purposes so that land use plans can be intelligently devised. Updating land use information can be accomplished through utilization of satellite-acquired data, especially for large geographic regions. The ability of active microwave sensors to map flood inundated areas under cloudy conditions is extremely important since such a capability can be used for conducting relief efforts, assessing loss of life and property, and delineating the extent of the flood plain. Observations of basic shape, stream network characteristics, land use, and drainage density permit one to infer the general characteristics of the water yield. Landsat data have been used successfully to delineate and monitor hydrological features, and radar data have proved to be excellent for this purpose as well. Cloud cover independence, better resolution, and increased sensitivity to surface relief allows radar imagery to show the relief and slope changes of the river bends permitting detection of tributaries quite easily, even if water is not in the channels year-round.

The 23-cm SIR-B wavelength is too long to allow monitoring of either free water in snow or a water equivalent measurement, both important for prediction of runoff. The soil state beneath the snow is also important for runoff predictions because permeability influences the quantity of snowmelt that will run off.

C. Hydrology Experiments

1. **Surface water experiments.** Seasat, SIR-A, and SIR-B data can be used to determine the extent and utility, and the location of reservoirs, lakes, and ponds. This information can also be used to estimate changes in water volume. SAR surface water experiments can (1) provide a regional overview of flood impact and damage, (2) delineate drainage patterns for fluvial morphology studies, and (3) monitor shoreline and stream channel positions and migrations. The gathering of quantitative data on normal or extra normal drainage networks (e.g., link-length distributions, link-slope correlations, junction angle

distribution/correlations) with drainage basin topography, longitudinal profiles, etc., is notoriously difficult and time-consuming and the fundamental studies of basic drainage networks have been limited and local in character. SIR-B will collect broad area coverage of important watershed and drainage areas, and the incidence variability of SIR-B will be very useful in determining drainage basin contours.

SIR-B imagery taken at different incidence angles will allow a study of the optimum illumination for mapping of watershed boundaries. Stereo observations of watershed relief may also be possible with the different incidence angle images. The ability of an imaging radar to map the areal extent of surface water through a vegetation canopy is a function of radar wavelength, angle of incidence, and vegetation type and amount. The latter two effects are directly amenable to study during the SIR-B mission with a proper selection of test sites. Since a SAR responds to surface soil moisture variations, the effectiveness of a SAR to determine the moisture state of a watershed as an index of its runoff potential could be assessed.

Groundwater discharge/recharge areas are usually identified as being wet for long periods of time. The ability of long wavelength SARs to observe these types of areas could be evaluated by making observations of a number of known recharge areas which exhibit a range of observing conditions. These areas under certain circumstances become saline seeps.

By using the Seasat, SIR-A, and SIR-B data, it should be possible to perform regional studies of land use and the environmental effects of water use development and management. Subjects of interest in this area include (1) determination of the increase or decrease of water use for irrigation (including center pivot irrigation systems that are very obvious in SAR images), (2) estimates of the percentage of impervious areas, (3) location of nonpoint source pollution, and (4) inventory of sediment source areas.

2. **Water surface experiments.** In addition to estimates of the extent and transport of surface water, natural and human-induced hydrologic surface features can be observed using SAR data. Seasat and SIR-A data provide clear evidence of surface pollutants including oil slicks and spills, and can also monitor large areas of floating and emergent vegetation such as coastal kelp beds and vegetated shallow estuarine and wetland areas. Although the SAR cannot determine coloration, SAR data in combination with Landsat-type sensors provide a complementary data set with respect to water surface features (SAR) and physical water quality (Landsat sensors).

Detection and classification of vegetation, sediment loading, oil slicks, etc., depend on a discerning modification of surface roughness scales and patterns, and can be confounded by competing modulations of surface features such as wind stress. Nevertheless, Seasat and SIR-A data provide ample evidence of natural and human-induced surface oil slicks, vegetation, and sediment loading classifications using SAR data and combinations of SAR and visible and infrared imagery. Classifications include both the evidence and transport (patterns) of these surface features.

Seasat and SIR-A images have shown striking evidence of a correlation between sea-surface features and bottom morphological features. SAR bathymetry interactions are most commonly observed in rivers, river outflows, and shallow coastal waters. Such observations suggest that SAR has great potential for remotely measuring surface manifestations of underwater obstructions and subsurface flow. These measurements are not related to water clarity as they would be for visible sensors, but apply in turbid sediment-laden areas. This potential cannot be evaluated qualitatively because of the limited number of observations currently available. To achieve such an assessment it is possible to combine available models of subsurface hydrodynamics, their effect on surface waves, and SAR sea-surface response to predict the SAR bathymetry observations. The model should define the range of environmental and radar parameters for which bottom topography produces surface features. Such a model would be invaluable to geoscientists and mission planners engaged in analyzing existing data and designing new SAR experiments for SIR-B. This subject is also addressed in the oceanography section to follow.

3. **Soil moisture experiments.** The need for a measurement or estimate of soil moisture that represents the areal extent of moisture has been recognized by climatologists, agriculturalists, and hydrologists for several decades. Until the advent of the computer and space remote sensing, there was not a reasonable way to collect and then handle the massive volumes of data that would be required to estimate a distribution of moisture in regional areas. Practicing hydrologists and agriculturalists in particular have been so accustomed to relying on point measurements, or no measurement at all, that the lack of technology for the application of moisture measurements over large areas is sometimes not even recognized. In addition, moisture data may be required in underdeveloped countries where gages are nonexistent or in nations where limited access is allowed. The dielectric properties of a soil are strong functions of its moisture content and determine the propagation characteristics for electromagnetic waves in the medium. They will also affect the emissive and reflective properties at the surface. As a result, these latter two quantities for a soil will depend on its moisture content, which can be measured in the microwave region of the spectrum by radiometric (passive) and radar (active) techniques. The presence of a vegetation canopy over the soil surface reduces

the sensitivity of the radar backscatter to soil moisture by attenuating the signal as it travels through the canopy down to the soil and back, and by contributing a backscatter component of its own. Moreover, both factors are, in general, a function of several canopy parameters, including plant shape, height and moisture content, and vegetation density.

For large area estimates of soil moisture by remote sensing, two general approaches have been proposed. One approach would require estimation of moisture in each of a number of sampling fields. The other approach would integrate the sensor return from a large cell and empirically estimate the average moisture over the area.

The first method, looking at individual samples of field size, would aid in reducing the data volume that would need to be used from high-resolution instruments such as the SAR. Data from the SAR would have to be modified to account for roughness in each sample area (see Appendix A). In addition, this method would require significant data handling and relatively precise registration of data to provide assurance that the same field was being sampled in sequential scenes. The second method would be based on the use of repeated looks at a single large cell. This system would not be usable for a mission of limited duration, such as SIR-B.

Another type of SIR-B soil moisture experiment would be to quantify the ability of the SAR to observe recent rainfall. Several test sites could be chosen so that there will be a high probability of a significant rain event occurring at one of them during the SIR-B flight. This probability can be assessed from the precipitation climatology for the prospective sites. Promising candidates include the 200-gage USDA/ARS network located around Chickasha, Oklahoma and extensive cooperative network (2000 gages) in the state of South Dakota.

In summary, soil moisture experiments using SIR-B data could be designed to extend our knowledge of the capabilities of spaceborne imaging radars for monitoring surface soil moisture variations. These experiments should describe how to account for confusion factors in radar response such as surface roughness and/or tillage patterns, slope vegetation cover, and incidence. Several test sites exhibiting varying conditions of soil moisture, surface characteristics, and vegetation covers could be selected to insure the possibility of observing soil moisture variations during the SIR-B mission. Multiple observation of these sites using diverse incidence viewing could be coordinated with induced moisture adjustments.

4. Glacier experiments. Seasat's 108-deg inclination orbit collected data in many glacial regions and SIR-A observed equatorial glaciers around the world. At the present time the backscattering mechanism in the glaciers is not clearly understood and could be the subject of a SIR-B investigation involving looks at multiple incidence and aspect angles. Several different test sites can be selected to insure coverage by the SIR-B and comparison with prior data collected by Seasat and SIR-A.

There have been some studies of glaciers using combined sets of Seasat SAR and Landsat MSS data that provide helpful indications about potential geophysical interpretations. In general, the SAR image shows greater relief and textural complexity. The ruggedness of the terrain is emphasized by the radar in comparison to the Landsat's rather "flat" rendering of the scene relief. Landsat data emphasizes snowlines and with the SAR can reveal ice-type boundaries.

When the glacial SAR scene is compared with a Landsat image of the same area, a variety of contrasts is evident. Scene comparisons in glaciated areas must be considered with qualification due to the persistence of cloud cover in many glacial regions and the difficulty in acquiring a reasonably cloud-free Landsat image coincident with the date of the SAR coverage of the area. The ice fracturing and surface ridges and other irregularities of the ice surface are well exposed in the SAR image. At least some of the differences may, of course, be due to the possibility of snow in the Landsat scene that is not observed in the same way by the L-band SAR. These comparisons will reveal snowlines. The contrast in radar response is due to the higher specular to backscatter ratio from the smoother snow surface as compared to the coarse, highly crevassed and probably debris-covered older glacial ice. Landsat images show even clearer evidence of snowlines. The snowline is of particular interest to glaciologists and climatologists in that they provide estimates of a glacier growth. Hydrologists use snowlines to estimate volumes of meltwater which will be added to local watersheds.

An interesting demonstration of the differential returns of glacial ice, rock debris, and snow are offered by the SAR by itself. The uppermost portion of a glacier exhibits a dark return from the glacial ice marked with narrow light bands from the medial moraines. Nearer the snout of the glacier, the ratio of high to low returns changes markedly in favor of the high backscatter from the now highly debris-laden and crevassed lobe of the glacier terminus. The contrast is, thus, largely due to textural changes in the glacial ice contributed by both the down-glacier increases in the debris content of the ice as well as surface roughness of the ice due to surface debris and fracturing of the ice. Evaluation of these features at various incidence angles could reveal information about glacier slope and contours.

SIR-B provides an excellent opportunity to expand our limited knowledge about SAR remote sensing of glaciers as observation of a few typical and high-interest glaciers will be possible.

V. Oceanography

A. The Objectives of Remote Sensing in Oceanography

Traditional methods of investigating oceanic processes have relied on *in situ* instruments which yield data that are intermittent in space and time. These samples are often inadequate when trying to describe the space-time variability in oceanic conditions. The potential of satellite remote sensing of the ocean is based on the ability to acquire global coverage of mesoscale surface features (sea-level wind stress, temperature, etc.) over short time intervals so that a temporal and synoptic view is obtained of near-surface processes.

The instruments of satellite visible/infrared remote sensing in ocean science research include the Coastal Zone Color Scanner (the CZCS is a multiband color imager which enhances certain features such as chlorophyll concentrations) and the Thermal Infrared Radiometer (TIR) (which can be used for modest accuracy sea-surface temperature estimates from the upper microns of the ocean surface). In the microwave spectrum, useful instruments are the microwave radiometer (for sea-surface temperature and salinity estimates), the radar scatterometer (for inference of surface wind stress and velocity from the backscatter of surface capillary waves), the radar altimeter (for measuring the height of the ocean surface to an accuracy of about 30 cm), and the SAR (for the depiction of internal waves, surface-wave spectra, surface current artifacts, and sea ice).

The principal objectives of satellite remote sensing in oceanography are:

(1) Surface Stress Measurement – Surface-wind stress is a major driving force of large-scale oceanic circulation, and it represents the lower boundary conditions for models of the atmospheric circulation over the ocean– an important input to global weather forecasts; a global long-term data set of surface winds and waves is therefore needed.

(2) Sea Level Observations – Radar altimetry of sea-surface heights to a precision of about 10 cm would allow many inferences about geostrophic currents and tides. Radar altimeters can also be used to determine properties of the oceanic geoid when monitored over many tidal cycles. The geoidal information can then be used to improve the current measurements.

(3) Sea-Surface Temperature Observations – An important factor in the heat energy exchange between the atmosphere and ocean is the sea-surface temperature, which can be a measure of the upper layer heat content.

(4) Biological Observations – Data from the CZCS on Nimbus-7 and the Ocean Color Experiment on the Shuttle STS-2 are being used to depict the distribution of biological and other scattering agents such as chlorophyll, and organic and inorganic suspended or entrained materials. This is potentially useful for global marine ecology studies and resource management.

(5) Sea-Ice Observations – Synoptic, timely data are needed on ice extent, type, thickness distribution, drift velocity, internal stress, properties, roughness, growth and melting rates, and snow cover. These data are useful not only for arctic and antarctic offshore operations, but are also crucial to climatological research on albedo, insulation, latent heat export, surface stress, and ice growth/oblation rates. Spaceborne SAR imagery appears to be very promising for ice-pack measurements, since the current aircraft monitoring is too limited in coverage for logistic reasons.

Microwave remote sensing of the sea surface from space has great potential, as convincingly demonstrated by Seasat. Although the SIR-A mission was primarily dedicated to geologic remote sensing, the imagery nonetheless revealed some important potentials for oceanic remote sensing research and expanded the work begun by Seasat. The full application of these techniques to oceanography requires long-duration missions because of the spatial and temporal variability of oceanic phenomena. Experiments with SIR-B can, however, make significant contributions to the remote sensing science needed to exploit fully the capabilities of future long-duration missions, and, indeed, to specifying the sensors for such missions. In fact, both Seasat and SIR-A results uncovered several apparent but unresolved scientific and applications questions. For example, empirical data confirms that a link exists between radar imaging and ocean bottom topographic mapping, entrained substances such as sediment loading, and other geophysical and human-induced phenomena for which no controlled experiments were conducted on either Seasat and SIR-A. The existence of these and other questions forms the basic theme for SIR-B oceanography which is to take advantage of the earlier Seasat and SIR-A experiences to carefully select and design the SIR-B oceanographic mission. Also, continuing basic research in sensor science is required to aid in developing sensors and their applications for expected future long-duration missions.

B. The Scientific Basis for SIR-B Oceanographic Remote Sensing Radar Experiments

Measurement of the wind vector with high-frequency (K_u-band) scatterometers has been shown successful by the Seasat experiment, but little information is available about the possibility of using L-band for such measurements. SIR-B may be

useful in a nonimaging squint mode to simulate the performance of a scatterometer for this purpose. This operating mode is described in Section 5 as the pulse scatterometer mode.

The spatial variability of the wind over the sea at scales comparable with the resolutions of imaging radars has been inferred primarily by temporal measurements made at single spots. Use of the imaging radar should allow determination of the nature and scales of these patterns on a 2-dimensional basis.

Measurement of wave spectra was the primary initial goal of the Seasat SAR. The technique can be tried out from space using the SIR-B type of system. The wave spectra obtained from images by Fourier transformation have been shown not to be wave-height spectra. The exact quantity whose spectrum is provided remains to be established. Nevertheless, the directions of the wave trains can be determined from these spectra as well as the predominant wavelengths. Use of the different angles of incidence on the proposed SIR-B should allow interesting comparisons, since the Doppler effects on the image formation may be different at the different angles.

Internal waves have always been of great interest to oceanographers who wish to understand the exchange processes taking place in the sea. Upwelling is of particular economic significance because many of the most productive fisheries are located in regions of upwelling of cold water from the deep ocean. The Seasat imagery, as well as aircraft radar images produced earlier, showed strong evidence that the regions of upwelling could be identified, and apparent internal waves showed up quite clearly. Little is known about the reasons that these show in radar images, and both, fundamental research on the causes and controlled experiments with the SIR-B, are needed to establish the reliability with which these phenomena can be identified.

Indications that radar images of the sea surface can indicate bottom morphology were first observed by de Loor in the early 1970s (de Loor and Hoogeboom, 1982). Little interest was shown until the spectacular evidences in many locations on Seasat images became clearly visible as shown in Fig. 3-5.

In view of the difficulties in updating bathymetric charts by conventional methods, this capability of the radar is a promising tool for shallow-water identification of bottom features and their changes. However, the actual mechanisms involved are unknown and must be studied using well-instrumented controlled experiments to help establish the reliability of the technique.

Operational aircraft systems for use of radar to observe human-induced oil slicks are in use in several countries, but the study of natural slicks has been minimal. The mechanism is known to be the suppression of the capillary and short-gravity waves that the radar responds to. SIR-B may offer an opportunity to map some of these natural slicks. Vegetation floating on the surface, such as that in the Sargasso Sea and the various kelp beds around the world, may also be observable on SIR-B. At 3-cm and shorter wavelengths, the kelp beds (of considerable economic importance) have been observed on aircraft radar images, but the ability to observe them at L-band needs to be tested. Many arctic and subarctic rivers containing heavy sediment loads from glacial action affect surface tension enough to cause them to show up on Seasat SAR images. SIR-B should provide an opportunity to study the ability of radar to observe coastline and embayment modification when they are compared with Seasat data.

The morphology of shorelines is continually changing and is of interest to many user communities. Repeated radar observations would allow monitoring of these changes. Seasat, SIR-A, and SIR-B provide an opportunity to obtain baseline data for several regions of interest.

C. SIR-B Oceanographic Experiments

1. Wind experiments. The ability of the L-band system to measure winds can be tested by taking the output of the radar prior to SAR processing, detecting it, and using the radar as a pulse scatterometer. This can be done over wide areas, using the hindcast data from ship reports as surface truth, as was done with the Skylab S-193 experiment. At least one experiment could be conducted with observations in the vicinity of weather ships and buoys.

2. Wave structure experiments. Use of the "short-pulse radar" technique for determining the spectrum of long gravity waves with wavelengths ranging from several hundred meters and up requires that the signal be spectrally analyzed over several kilometers of range. To achieve more than a single cut through the 2-dimensional wave spectrum, an azimuth spotlight mode could be used. Thus, by observing the same area of the sea from a range of azimuth angles, a portion of the 2-dimensional spectrum should be observable.

A continuation of the experiments performed with Seasat in evaluating directional spectra from images could be carried on with SIR-B, in part to determine the effect of angle of incidence on these observed spectra and in part to continue development of the technique. Both of these experiments require some alternate means for obtaining the directional wave spectrum.

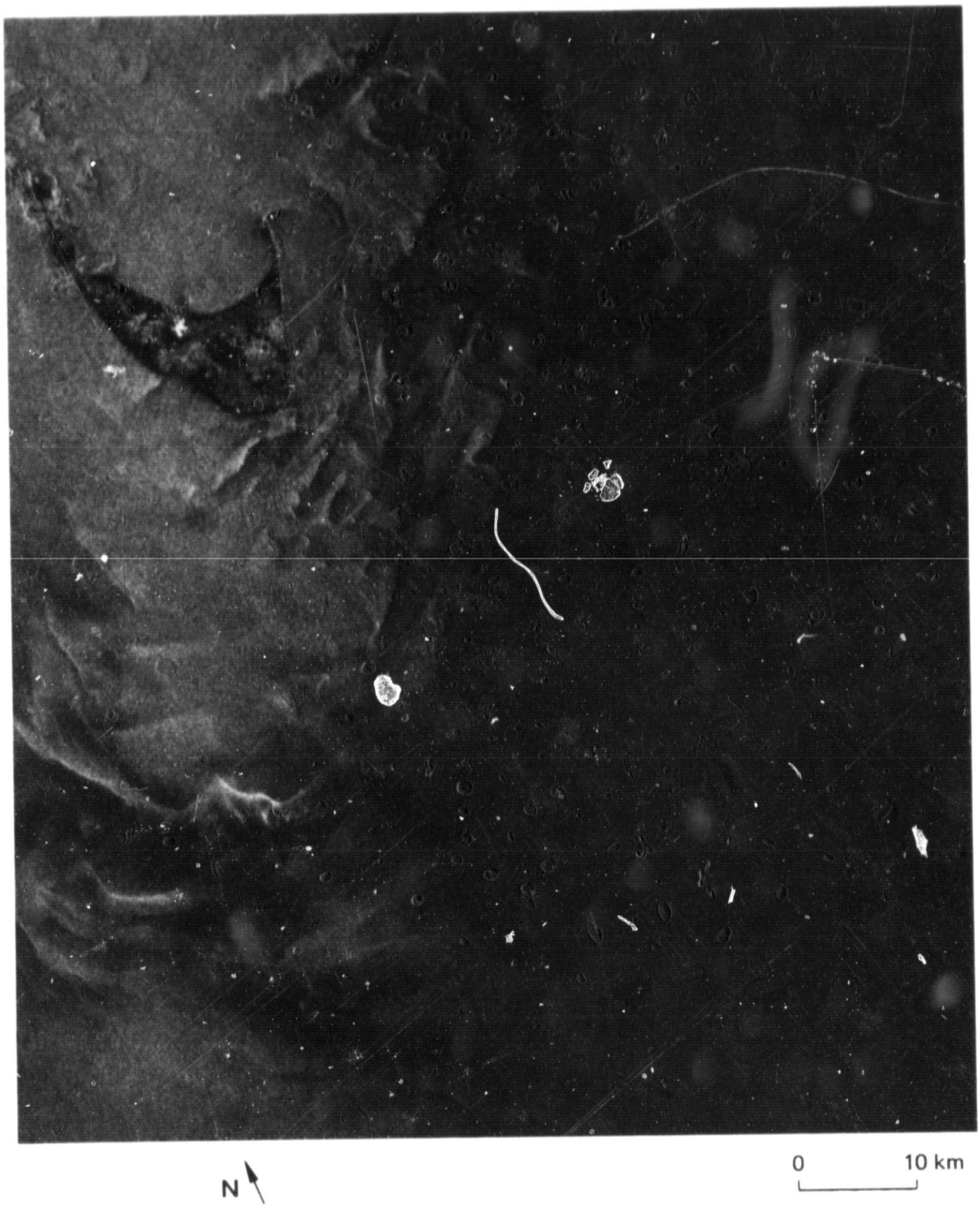

Fig. 3-5. Seasat SAR image showing ocean bottom signatures

3. **Internal structure, upwelling, currents, and fronts experiments.** The nature of experiments to observe all of these phenomena is the same, although the particular areas to be observed may be different. Candidate areas for SIR-B observation of internal waves should be selected and combined with suitable surface-truth experiments, including L-band scatterometer measurements. Upwelling, current, and front areas must be selected independently of the areas selected for internal-wave experiments, although selection of areas near each other would aid in conducting the surface-truth experimentation.

4. **Bottom morphology experiments.** The exciting possibilities of observations of bottom topography can be exploited with SIR-B. Sites where the evidence is already available from Seasat and/or SIR-A can be surveyed with SIR-B, with extensive surface-truth instrumentation in place. Since the surface manifestations of bottom topography in the near-shore environment are almost certainly tidal-current driven, the experiment should be planned, if possible, to observe the radar images at different points in the tidal cycle. In the deeper oceans, and possibly in some river mouths, the effects may be caused by more persistent currents, and sites should be selected to permit verification of this effect.

5. **Slicks and entrained material experiments.** Attention should be concentrated on areas of known natural slicks. The observation from space should be accompanied by simultaneous surface observations indicating the nature of the slicks and by scatterometer or spectrometer observations indicating the degree of suppression of the small waves. Landsat images of these areas could be part of a coordinated experiment.

6. **Coastal refraction and morphology experiments.** Coastal morphology sites for coastal refraction/diffraction experiments should be selected with a variety of shorelines, and where the effects are already well known, further surface observations should be made at the time of overflight to verify the conditions. Coastal morphology sites should be selected with a variety of shorelines. Recent aerial and Landsat photography should be available.

VI. Vegetation

A. The Objectives of Vegetation Remote Sensing Experiments

The ability to obtain accurate and timely assessments of the extent and condition of specific types of vegetation on the earth's land surface is fundamental to agriculture, forestry, rangeland, and land cover studies. Agricultural resource managers need estimates of crop area and yield for crop production estimation. In the case of forestry and rangeland studies, there is a need to map vegetation in specific regions. On a global scale, there is an ever-pressing need to measure the change in vegetation cover to be able to estimate the effect of deforestation and desertification rates for global ecology.

The use of optical region (visible, near-infrared, mid-infrared, and thermal-infrared) remotely sensed data to aid in crop production estimation, forest mapping, and rangeland mapping has been under investigation especially since the launch of Landsat. The MSS has proved quite useful for crop identification and area estimation. However, it has been necessary to use multidate data over a specific site to achieve the best and most robust results. Transformations of 4-band MSS data have been useful in developing features that can be used as vegetation indices. For example, the Kauth-Thomas Tasseled Cap Transformation produces four features called soil brightness, greenness, yellowness, and nonsuch. The use of the greenness values to form modeled profiles of the seasonal variations in greenness leads to the extraction of features (maximum greenness and the width of the greenness profile) that produced significantly low error estimates of the proportions of corn and soybeans without significant bias. Such data handling lends itself to automatic crop identification and area estimation. Other researchers have found that Landsat MSS data can be used to estimate crop condition parameters such as leaf area index (up to about 3.0), percent ground cover, and biomass. Also, crop growth stage can be estimated to about 10 percent accuracies. Numerous examples of using Landsat MSS data for mapping forest and rangeland also exist. The primary problem with MSS data or TM data has been the interference of clouds causing holes in the multidate data set needed for profiling.

Radar remote sensing should add significant information to that obtainable by MSS or TM. Of course, clouds would not be a problem. But, beyond that, the radar should provide complementary biophysical data about vegetation canopies such as plant water content, leaf area index (beyond 3.0), and canopy structural information. Most studies to date indicate that C-band or higher frequencies and the use of dual polarization will yield the best results. However, each frequency and polarization adds unique information. Combinations of frequencies and polarizations at various angles are needed for best results. It is expected that existing data transformations such as the Kauth-Thomas Transformation and profiling techniques and perhaps new transformations will be used for radar data.

With these applications in view, the scientific and research objectives of the SIR-B mission for vegetation can be considered. SIR-B should provide calibrated, digitally processed data over extended areas during the peak of the growing season of summer crops in the Northern Hemisphere. Also, during the 7-day SIR-B mission, the same areas will be covered from

angles of incidence ranging from about 15 to 60 deg. These two capabilities (quality of data and angle agility) and the time of year of the SIR-B mission are significantly better than the SIR-A mission in November 1981. The primary limitations of the SIR-B mission for vegetation studies are the use of a single, relatively long wavelength (L-band), the use of only one polarization combination (HH), and the short duration of the SIR-B mission. Nevertheless, with proper experiment design, the SIR-B data should be useful for research in vegetation surveying through remote sensing. Some important research questions are:

(1) What, if any, biophysical characteristics of vegetation canopies and the underlying soil are unambiguously sensed by an L-band HH SAR operating at incidence angles in the range of 15 to 60 deg from the nadir?

(2) How might these remotely sensed biophysical characteristics be used in vegetation canopy identification, mapping, area estimation, and condition assessment?

(3) What is the natural spatial variability of the active microwave backscatter from vegetation and soil over extended areas?

(4) What is the effect of weather, soil conditions, and row structure on the fundamental ability of an L-band HH SAR to sense vegetation canopy characteristics?

B. The Scientific Basis for SIR-B Vegetation Experiments

Over the past two decades, many investigations have been made of the microwave backscattering properties of vegetation and soils. Most of these studies were made from surface-based platforms using radar scatterometers that operated at frequencies of 8 GHz and above. In the case of soil moisture studies, 1- to 8-GHz bands were used. The vegetation experiments concentrated almost exclusively on agricultural crops. As a result of these experiments and a few aircraft-based experiments, a great deal is known about the active microwave properties of vegetation in the 8- to 18-GHz range and about the active microwave properties of soils in the 1- to 8-GHz range. In contrast, all active microwave data taken from spacecraft platforms (i.e., Seasat/SAR and SIR-A data) have been acquired at 1.275 GHz (L-band) using the HH-polarization combination and two angles on incidence (20 deg for Seasat and 50 deg for SIR-A). This interesting circumstance has led to the present problem of not knowing much about the L-band properties of vegetation.

The basic findings of past vegetation microwave remote sensing investigations are summarized below.

1. **Agriculture crops.** At X-band and higher frequencies, crops exhibit the characteristic temporal properties of rapid increases in phytomass early in the season followed by senescence. This biophysical characteristic produces similar seasonal changes in the radar backscattering coefficient especially for incidence angles near 50 degrees (Ulaby and Eger, 1982). The shape of the temporal profile is similar to that observed in the Landsat MSS data. There are differences, however, in that the MSS responds primarily to the leaf area index and the radar responds to the plant water content. For example, in a truck-based experiment, the backscattering of corn at 17 GHz K_u-band VV at 50-deg incidence was highly correlated to the plant water content (Ulaby and Bush, 1976). At L-band and C-band, the competing effects of volume scattering and absorption by various plant parts and surface scattering from the soil result in a complex temporal behavior mechanism for radar backscattering from crops over a season.

L-band and C-band radar scatterometry measurements have been made from aircraft on up to six dates in several agricultural sites. For the Colby data, no preferred band was found when single configurations were considered (Shanmugan, 1981). The best results were for HV polarization using either L-band or C-band with field classification accuracies as high as 100 percent. The depolarization ratio

$$\sigma^{o}_{HV}\,(\mathrm{dB}) - \sigma^{o}_{HH}\,(\mathrm{dB})$$

performed well, also. The use of multidate, single channel or multidate, multichannel data produced 100 percent correct classifications (Shanmugan, 1981).

Analyses of the Webster data on dry soil (Paris, 1982) showed classification accuracy of 100 percent by field and 98 percent by pixel for separating corn and soybeans (C-band HV at 50 deg). Good results were observed at L-band HH at 50 deg as well with 93 percent accuracy for discriminating corn from soybean fields. Also, the depolarization ratio produced excellent results for both the dry- and wet-soil flights. Separation was poor for C-band HH, L-band HV, and K_u-band VV. Interesting effects were observed due to differing soil moisture conditions in that the change in backscatter at 50 deg was significantly different between crop types. One study (Batlivala and Ulaby, 1975) has been made of the L-band backscattering properties of crops and cover (corn, soybean, woods) using an airborne SAR over Huntington County, Indiana, on September 13, 1973. Corn and soybeans were separable (71 percent accuracy) when both HH and HV polarizations were used. Using only HH polarization produced a classification accuracy of only 65 percent. Woods were confused with corn, a result also seen in the Webster study.

Studies have been made of the agricultural information in Seasat SAR data (Wu, 1982) registered with Landsat MSS data. As a result, additional landcover classes (wetlands) could

be identified compared to MSS alone. Early season (July 25) separation of corn and soybeans was observed compared to MSS data for the same sites and year. When it comes to radar crop identification, crop-canopy condition assessment, stage-of-growth assessment, and stress detection, many effects exist to confuse these applications. For row crops in either irrigated or dryland farming areas, row structure and row direction changes can cause variations in the backscattering of as much as 20 dB for bare fields, and as much as 10 dB (Paris, 1982), even through thick vegetation canopies. These effects are at a maximum for L-band HH data at incidence angles near the slope of the furrowed row sides (10 to 30 deg) and occurs only when the radar is looking across rows and is due to specular-like reflections from the row sides. Another confusing effect is caused by changes in soil moisture. Differences in backscattering coefficient as large as 10 dB may be observed at steep incidence (~15 deg), but at 50 deg the effect is only about 2 dB.

The revisit interval affects the vegetation identification ability of a SAR. In the case of SIR-B, the duration is too short to provide a meaningful time series of data except for such possible occurrences as the wetting and drying of soils and those effects and sudden events such as harvest or hail damage. Spatial resolution affects the ability of SAR (or MSS-type sensors) in that large ground resolution elements lead to a large number of boundary pixels. In the case of SIR-B for a 40-acre field, the boundary pixels would move up less than 10 percent of all pixels.

2. Forest and wetlands. The differences in backscattering returns that are related to forest-canopy density, arrangement, and vigor offers the potential to more effectively differentiate among various species and forest-cover types than may be possible with MSS data, even from the TM. For example, the results of an analysis of the integration of Landsat MSS and Seasat L-band SAR data (Wu, 1982) indicate that while MSS data could be used to delineate different forest types and would allow for some species separation, the Seasat L-band SAR data provide additional information related to plant-canopy configuration and vegetation density as associated with varying water regimes, and therefore allow further subdivision in the classification of forested wetlands. Better classification accuracy was also demonstrated in swamp forests that are flooded with water. Pine forest with partial clear-cutting which causes shrubs and native grasses to be exposed among the tall pine crown clusters can be accurately identified by Seasat L-band SAR data. In addition, the use of cross-polarization data in conjunction with linear-polarization data provides improvement in delineating woodland from other crop vegetation in the mixed vegetation area. A recent test was conducted over an area in France using the L-band JPL SAR system. For pine trees, the image intensity was found to be directly proportional to the height and age of the trees as shown in Fig. 3-6.

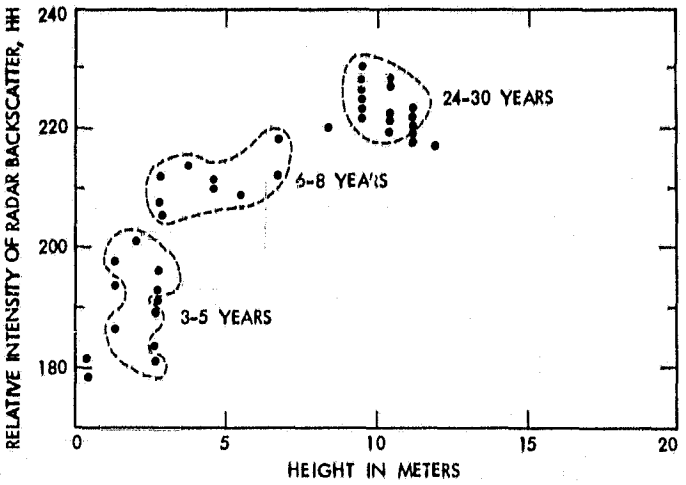

Fig. 3-6. Measured L-band radar backscatter dependence on height and age of pine trees (after Riom and LeToan, 1981)

The study was conducted by Riom and LeToan of Paul Sabatier University (Riom and LeToan, 1980). Although the few experiments conducted to date show that imaging radar has the potential to provide useful information with regard to forest biomass productivity, no concrete information exists with regard to optimum angle of incidence, frequency, or polarization configuration. The SIR-B provides an opportunity to evaluate the use of L-band imaging radar for forestry applications.

3. Rangelands. Essentially no research has been done on rangelands with microwave remote sensing. Some work has been done on grasses and pastures and could be extended to rangelands, but, the objectives of this work have not been directly driven by the range needs. However, the considerable amount of work that has been done on agricultural crop identification and soil moisture determination has provided a technical foundation on which the range experiments can build.

Very little is known about the microwave response of rangelands. Rangelands differ from many cultivated agricultural areas in ways that may affect microwave response. The vegetation types may be quite varied, the density of vegetation is generally lower per unit area than in mature croplands, and the effect of the soil background will probably have a larger relative effect on the microwave signal than over mature crops. It is not clear that these characteristics will show up in the L-band imagery, however, experiments to evaluate this potential could be coordinated with other vegetation experiments. Previous experiments in cultivated agriculture suggest that L-band measurements at various angles of incidence might provide experimental evidence for range areas, range types, and total biomass production.

C. SIR-B Vegetation Experiments

The following areas are suggested for SIR-B vegetation observation experiments.

1. **Agricultural crops.** Significant studies could be made of:

(1) The effects of crop-canopy morphology on the backscattering of crops by using several fields of crops having natural or induced differences in plant part sizes and angular distribution.

(2) The effects of soil background on the backscattering of crops by using fields prepared in various combinations of small-scale roughness, row structure, row direction, and surface (0 to 5 cm) soil moisture.

(3) The effects of wind on the backscattering of crops by using multidate data taken under different conditions of wind and precipitation (effects of change caused by wind and effects of having the surfaces of the canopy wetted by rain). This experiment will depend on cooperative conditions during the SIR-B 7-day mission.

(4) The effects of illumination geometry (incidence and azimuth angles) on the separability of croplands according to their backscattering properties or on the assessment of crop-canopy condition.

(5) The ability of SIR-B to detect the occurrence of specific stages of growth, as might be expressed through significant morphological differences (e.g., appearance of heads) by using several test sites for the same crops, distributed over wide latitude ranges to be able to view the same crop at various stages of growth during the same 7-day mission. The row aspect effect would have to be normalized or controlled using radar squint.

(6) The effects of having confusion crops in an area of interest on the performance of crop-classification and crop-proportions estimation algorithms.

(7) The effects of regional practices (planting, management) on the separability of croplands according to their backscattering properties.

(8) The effects of regional topography on the ability of the SIR-B to discriminate crop types or to assess crop-canopy conditions.

(9) The effects of day viewing vs night viewing for the applications above.

(10) The added usefulness of SIR-B data with respect of Landsat/MSS or TM data for the above applications.

(11) The usefulness of spatial data such as texture, pattern, size, shape, and shadow for cropland identification and mapping.

2. **Forestry and rangeland.** Forestry and rangeland experiments could study:

(1) The effects of tree and rangeland vegetation on backscattering by using sites containing vegetation with a wide range of health, growth, and pattern states.

(2) The effects of soil background (see Agricultural Crops Experiments) on rangeland backscattering and the additional effects of surface cover (grasses, bare soil, snow, standing water, etc.) on the backscattering from forests.

(3) The effects of angles of observation on the separability of forests and rangeland vegetation according to the backscattering properties.

(4) The ability of SIR-B to detect the occurrence of certain stages of growth in forest and rangeland vegetation.

(5) The effects of topography on the ability of SIR-B with regard to forest and rangeland vegetation mapping and condition assessment.

(6) The effects of time-of-day on the above applications.

3. **SIR-B performance requirements for vegetation experiments.** In most cases, the usefulness of the SIR-B data for vegetation applications is directly affected by the radiometric or tonal precision of the images. This is due to the fact that most vegetation of interest lies in relatively flat terrain and that spatial information is of minimal usefulness. Texture may be an exception since, for some vegetation types such as forests, the texture may be used to identify the type. Another exception might be that of pattern, where field sizes and shapes might be indicative of crop type in some regions (e.g., where strip fallow practices are used). However, the primary feature of interest in vegetation mapping is the tone of the image or the backscattering coefficient of a calibrated image. For many vegetation types, the temporal variation of backscattering coefficient for any given angle through the season is less than 10 dB. The maximum difference between vegetation types at any instant of time is usually less than 19 dB except for cases when no row-direction effects are present nor sloping terrain effects are evident (angles near nadir). Based on these considerations, the vegetation team recommends that the day-to-day repeatability and the across-the-image precision of the digital SIR-B data be no more than about ±1 dB (at the 90 percent confidence level).

a. Multiangle mode. Due to the angle agility of the SIR-B, it will be possible to image a test site at several angles during the mission. Based on radar scatterometer data gathered over vegetation from aircraft at angles of incidence from 5 to 50 deg, the team recommends that at least three angles of

incidence be available for use in the SIR-B experiment for typical mid-latitude test sites. These angles should be near 15 deg, 30 deg, and 45 deg. Multiangle data should be useful in sorting out some soil background effects. But, since soil moisture can change significantly over a few days, it will be difficult to unambiguously distinguish between changes in backscattering caused by changes in incidence angle and caused by changes in surface soil moisture.

b. Revisit interval. The use of multidate SAR data during the short-duration SIR-B mission for vegetation experiments is not expected to produce good results (compared to single-date studies) for most situations. There are exceptions, for example, if a field of vegetation undergoes a drastic change in condition (due to a change in stage of growth such as heading or harvest), then that event might be useful in the identification process. Another example is the fact that different canopies respond differently to changes in soil background such as the wetting of the soil by irrigation or rain. Thus, it will be useful to have frequent coverage during the mission for specific sites. A 1-day revisit interval is desirable. At a minimum, the site should be viewable at least two times during the mission. It would be more desirable to have the two views at the same incidence and azimuth angles to allow investigators to observe the changes caused only by changes in the canopy of background soil and not caused by the differences in viewing geometry.

Another revisit interval of interest is the twice-daily viewing afforded by day and night passes over the same site. This mode would allow investigators to study the effects of time of day. Time of day should cause differences in canopy and background soil conditions that may influence the information content of the data.

Section 4
SIR-B Sensor Experiments

I. Introduction

This section describes the SIR-B sensor characteristics and also outlines sensor experiments that can be conducted during the mission. It is important to understand both the capabilities and limitations of the SIR-B sensor in order to design geoscientific experiments which take full advantage of the mission but which are practical. A number of sensor-specific experiments can be conducted with SIR-B which will be very useful in the design of future SAR missions, and some of these are described here.

II. Sensor Characteristics

The characteristics of the SIR-B sensor are summarized and compared to SIR-A in Table 4-1. The major improvements from the SIR-A experiment include the addition of digital data recording capability, improved range resolution, and controllable incidence angle.

Additional features such as a variable number of bits per sample (3 to 6) and a radiometric calibrator have been added to enhance the flexibility of the system and improve the image product.

The ability to control the SIR-B look angle is a major step toward improving understanding the effect of illumination geometry on the information content inherent in SAR imagery. However, it should be pointed out that changes in look angle are accompanied by changes in range resolution, swath width, SNR, and dynamic range.

With a 12-MHz bandwidth and 20 percent degradation in the impulse response, the SIR-B slant-range resolution is 12.5 m; the ground-range resolution can be found by dividing the slant-range resolution by the sine of the incidence angle. At a 15-deg incidence angle, the ground-range resolution is 58 m; at 60 deg, it is 17.4 m, etc.

Table 4-1. SIR-B sensor characteristics

Parameters	SIR-A	SIR-B
Orbital altitude	260 km	225 km
Orbital inclination	38 deg	57 deg
Frequency	1.28 GHz	1.28 GHz
Polarization	HH	HH
Look angle(s)	47 deg	15 - 60 deg
Swath width	50 km	20 - 50 km
Peak power	1 kW	1 kW
Antenna dimensions (m)	9.4 X 2.16	10.7 X 2.16
Antenna gain	33.6 dB	33.0 dB
Bandwidth	6 MHz	12 MHz
Azimuth resolution	40 m (6 look)	25 m (4 look)
Range resolution	40 m	58 - 17 m
Optical data collection	8 h	8 h
Digital data collection	0	25 h
Digital link capability	N/A	46 Mbits/s

Figure 4-1 illustrates the dependence of the swath width on the look angle for various system parameters. At near-nadir look angles, the swath is limited by the SNR and at large look angles, it is limited by the data rate that can be accommodated by the digital link. The data rate limited swath is determined by the number of bits per sample (bps) and the pulse repetition frequency (PRF). The data rate limited swath is the maximum swath that can be transmitted through the 46-Mbit/s channel allocated for the shuttle-TDRS link. The SNR-limited swath is defined as that for which the mean backscattered signal is a certain number of dB above the noise. In Fig. 4-1, two SNR levels are plotted, one for 8 dB and the other for 3 dB. An 8-dB SNR produces a 4-look image that is

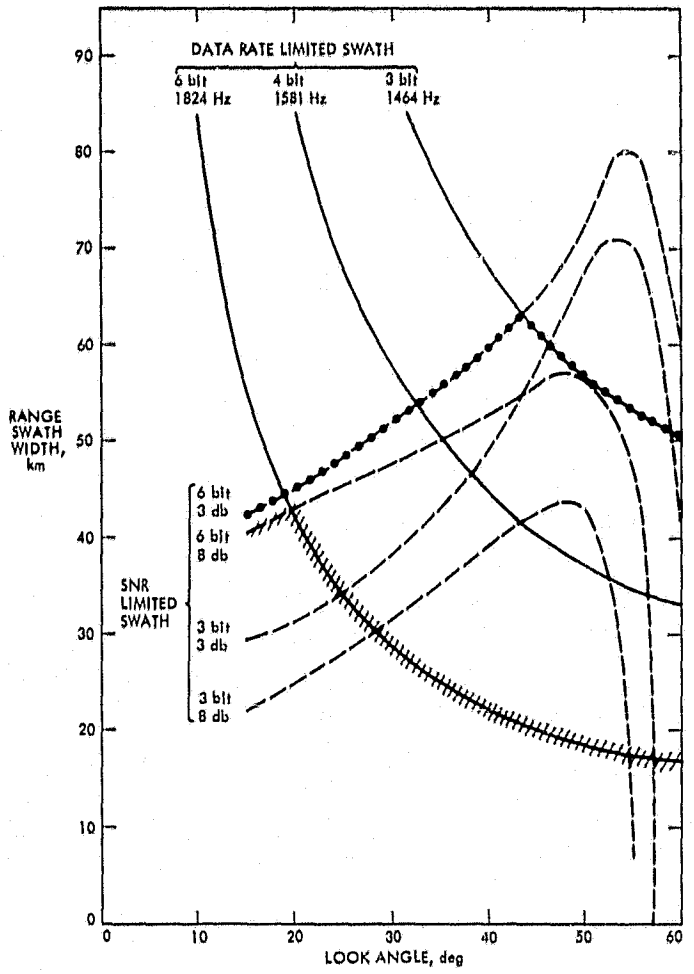

Fig. 4-1. SNR limited range swath as a function of look angle. The slash marks indicate a typical range of swath widths for the calibration experiments assuming 6-bit quantization and a minimum 8-dB SNR. The circles indicate the maximum swath widths for a mapping mode assuming a minimum 3-dB SNR.

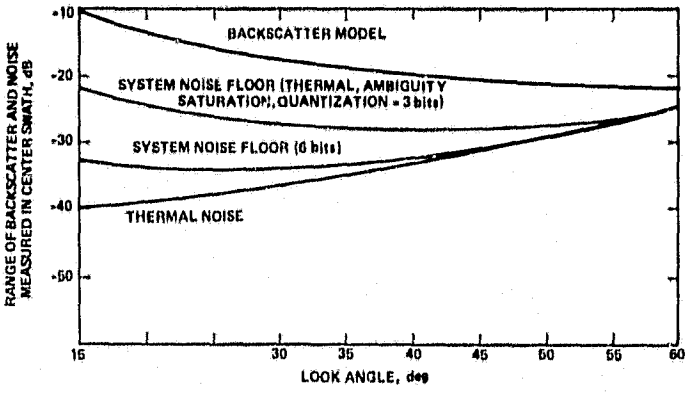

Fig. 4-2. Expected backscatter and system noise as a function of look angle

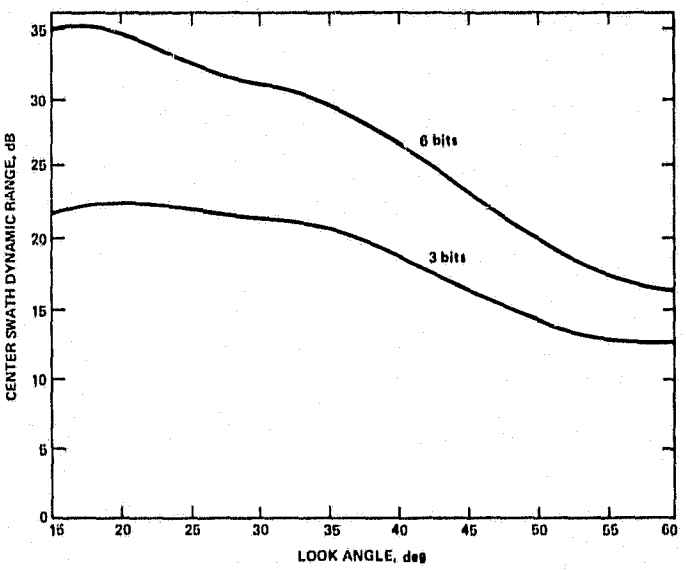

Fig. 4-3. Dynamic range as a function of look angle

subjectively good, whereas a 3-dB SNR produces an image that is subjectively noisy but still interpretable. An 8-dB SNR image is approximately equivalent to the standard Seasat digital image product. The 8-dB and 3-dB levels are the worst case for the swath edge and typically most of the image is much better than this value.

Figure 4-2 shows a plot of expected backscatter and system noise measured in the center of the swath as a function of look angle. For look angles below 35 deg, the SNR exceeds 20 dB and even in the worst case at 60 deg is 7 dB. The usable swath (3-dB SNR) exceeds 40 km at all look angles, although to achieve this swath the system may require a reduction in the number of bits per sample (accompanied by a reduction in dynamic range as shown in Fig. 4-3). The dynamic range within the imaged area is also a function of incidence angle, with a typical value of 10 to 12 dB for an agricultural scene. If the natural variability of radar backscatter intensity within the imaged area exceeds the system dynamic range, underflow and/or overflow will occur in the quantizer and the radiometric calibration will be correspondingly degraded. At 6-bps quantization, the dynamic range of the system should exceed the natural variability of the scene for nearly all of the data, while for a 3- or 4-bit setting, the dynamic range may be marginal.

III. Sensor Performance

A. Radiometric Calibration

Absolute calibration requires that a known relationship exist between the radar image intensity and the radar scatter-

ing coefficient. An ideal system would possess the following linear relationship:

$$I = K\sigma^{\circ}$$

where I is the image intensity, K is a known constant of proportionality, and σ° is the radar scattering coefficient. If the constant K is unknown but stable to a few tenths of a dB over a period of days or months, then the system is calibrated on a relative scale so that changes in the backscattering coefficient of the scene produce a proportional change in image intensity. For land areas, no models currently exist which require an absolute calibration, but all of them require a good relative calibration, i.e., to a few tenths of a dB. Since SAR images are acquired by a coherent system, coherent noise or speckle may degrade the calibration of an individual pixel; however, by incoherent or multilook averaging, this speckle can be reduced. SAR calibration can be further degraded by inaccuracies in antenna pointing, uncertainty in such system parameters as the transmitted power, antenna pattern, receiver gain, etc., and by environmental factors such as ionospheric scintillation, Faraday rotation, etc.

In this discussion, the term "radiometric calibration" refers only to uncertainties in the system parameters, i.e., the transmitted power, antenna pattern, etc. It does not include errors due to speckle, or system saturation effects such as produced by bright targets.

An analysis has been made of the relative radiometric calibration which can be expected of the SIR-B system. This includes an assessment of errors due to uncertainties in transmitter power, antenna gain, shuttle roll, slant-range position, and received power. At a 40-deg look angle, this analysis predicts a worst-case calibration of ±2.2 dB (at the swath edges), ±0.8 dB at the swath center, and the best possible relative calibration of ±0.6 dB.

The effects of speckle noise on the radiometric calibration have not been included in the above analysis. Speckle noise is a random process that can be modeled as a Rayleigh distribution. For the 4-look SIR-B image the speckle alone will produce a backscatter variance of 3 dB. The only effective way to reduce this variance is to use spatial integration. The variance will decrease proportionally to the square root of the number of spatially integrated resolution cells. To meet a ±0.5-dB relative calibration requirement, a uniform region of about 5 to 10 resolution cells would be integrated. This would give good relative calibration, although it would degrade the resolution to about 200 to 400 m.

B. Geometric Calibration

Geometric calibration refers to the absolute location accuracy of an image pixel and the geometric fidelity of the final image product. The sources of error in azimuth location include the platform position (along-track), data timing, and platform velocity. In range, errors result from uncertainties in platform position (cross-track), sensor hardware performance (timing and stable local oscillator (STALO) frequency), ionospheric group delay, and platform velocity (cross-track). Table 4-2 summarizes the expected geometric calibration for SIR-B. The minimum and maximum columns are derived from the refined postflight ephemeris data and the real-time data respectively.

Table 4-2. Expected SIR-B geometric calibration

Error Source, RSS Total	Location Error, m			
	Look Angle, max		Look Angle, min	
	15 deg	60 deg	15 deg	60 deg
Azimuth	1608	2591	60	79
Range	4145	1894	212	83
Overall	4446	3209	220	114

The largest error occurs at near-nadir look angles and is due primarily to uncertainty in the radial components of position and velocity. The overall error in absolute location using the high-precision postflight ephemeris is 220 m at 15 deg and 114 m at 60 deg. This ephemeris may not be available for all orbits and will not meet the stated accuracies if attitude maneuvers were conducted on the orbits before or after the desired time. In addition, these accuracies are relative to an assumed geoid model. Any deviation from the assumed geoid will result in an additional cross-track location error.

Table 4-3 illustrates the image registration error resulting from uncertainties in pixel location. For the high-precision ephemeris case, the cross-track misregistration will be less than one pixel, assuming a terrain without significant relief. This registration error is greater at near-nadir look angles due to the increasing location error.

Table 4-3. Cross-track registration error

Look Angle, deg	Range Location Error, m	Pixel Spacing Error, %	Misregistration, m
15	4145 (max)	6.5	3250 (max)
60	1894 (max)	0.1	50 (max)
15	212 (min)	0.02	10 (min)
60	83 (min)	0.0	0 (min)

IV. Sensor Experiments

In addition to those geoscientific experiments discussed in Section 3, a number of sensor experiments with SIR-B will be possible which explore the technological capabilities and limitations of spaceborne SAR. This section discusses those which are directly related to the spaceborne hardware and the next chapter summarizes SAR processing experiments.

A. Calibration Experiments

SIR-B radiometric calibration experiments are important in order to determine the degree to which the in-flight antenna pattern agrees with preflight ground measurements. These experiments, which would be performed during the mission, would include an orbital pass during which several sets of across-swath deployed corner reflectors would be imaged, another pass in which several receivers deployed across the swath would be monitored to obtain the antenna pattern, and several passes over a nominally homogeneous extended target zone (e.g., the Amazon rain forest) in order to independently ascertain the antenna pattern and also monitor the repeatability of the SIR-B imagery.

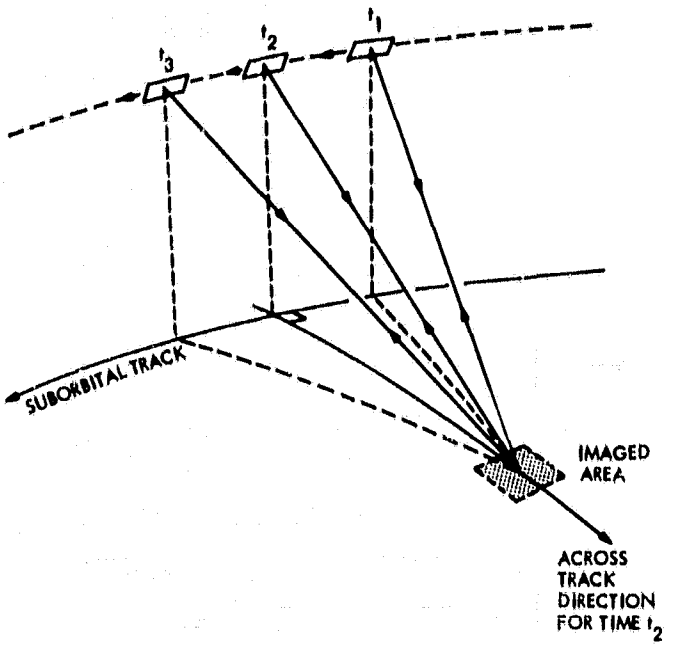

Fig. 4-4. Geometry for spotlight mode showing SAR position at three successive times t_1, t_2, and t_3

B. Target Statistics

It is important in radar design to understand the exact statistics of the raw data entering the synthetic aperture system as well as the statistics of the final imagery. It is therefore desirable to know the intrinsic dynamic range of the backscattered signal from an imaged area as a function of look angle and resolution. To collect a complete set of data the resolution should vary from the finest available in the SIR-B system up to resolutions approximating the size of the antenna pattern footprint, all for a full set of look angles from 15 to 60 deg. The results of such an experiment would be valuable to all future designers of spaceborne radars for earth observations.

C. Spotlight Mode

An increased SAR acquisition time can be used to increase the number of looks (thereby reducing speckle noise) for a fixed resolution. In the SIR-B spotlight mode, the shuttle would perform a controlled yaw maneuver so that a selected ground area remains in the antenna pattern for a much longer period of time than in the normal side-looking mapping mode. This maneuver is illustrated in Fig. 4-4, although the azimuth angle sweep is greatly exaggerated. For SIR-B there is a practical limitation on the number of degrees of yaw that can be processed in a single image. It is anticipated that for a maneuver greater than ±3-deg yaw, the change in range from spacecraft to target will be appreciable. The processing algorithms for this mode have not yet been implemented on the JPL IDP, although it is anticipated that they would be developed by mid-1984 with additional funding.

Although it is theoretically possible to improve the azimuth resolution using the spotlight mode, it is computationally easier and potentially more useful to employ the increased synthetic aperture length to increase the number of looks and maintain the resolution at 25 m in azimuth. This technique has the potential to produce images with 15 to 20 looks at this resolution. This would greatly reduce the speckle and enhance the radiometric quality of the imagery. It should be emphasized that the spotlight mode image is not a standard SIR-B data product being planned and only a very limited test of the concept is being considered.

D. Squint Mode

In this mode the shuttle would yaw in the positive or negative direction to a fixed azimuth angle (see Fig. 4-5) and image a strip at this squint angle as contrasted to the spotlight mode where the squint angle is constantly changing. This mode could be useful as a means of classifying scenes which have a strong azimuthally dependent radar signature, such as plowed fields with a row-direction modulation or sea surfaces with a strong azimuth dependence of wind-induced backscatter. This mode would also provide the capability to detect scenes whose fading pattern has a null in one azimuth direc-

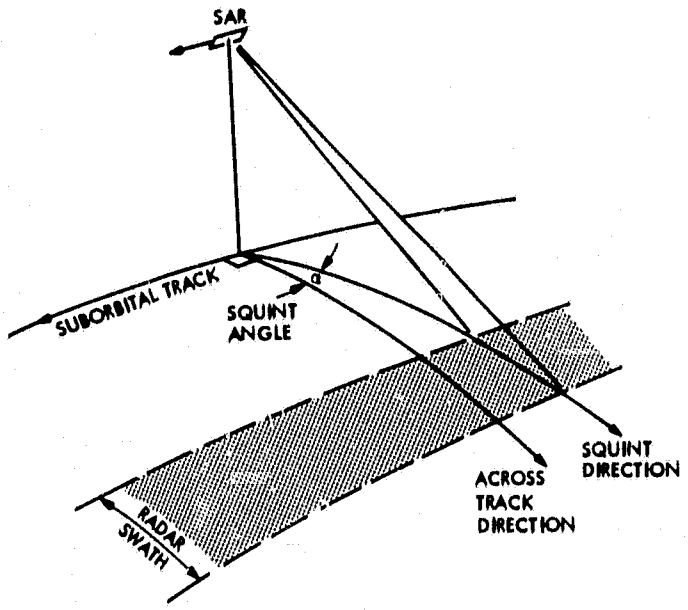

Fig. 4-5. Squint-mode geometry

tion, but produces a bright return at other directions. The reader is cautioned that the squint mode is not a standard SIR-B data configuration and that no plans are being made to support requests for SIR-B squint mode images except for possible limited tests of the concept.

E. Ocean Current Detection

New techniques are being studied for ocean current detection utilizing special Doppler centroid processing of Seasat data. Unfortunately, the Seasat data taken at a 20-deg look angle is not optimal for current detection since a relatively small Doppler shift results from a moving current. However, as the look angle is increased, this shift becomes more pronounced thus improving the accuracy of the estimator algorithm for ocean currents. The addition of the SIR-B variable look angle data would be very helpful to this investigation. Also, the SIR-B squint mode could be helpful in resolving uncertainties in the angular backscatter characteristics of ocean current boundaries.

Section 5
SIR-B Image-Processing and Information Extraction Experiments

I. Introduction

The extraction of useful information from SAR imagery presupposes not only a good understanding of the physics of backscattered microwave energy from the earth's surface, but also that the SAR data have been properly processed. SAR data processing involves two stages, the first being signal correlation and the second, image processing. Signal correlation is that process which generates a focused image from raw signal data, while image processing refers to post-correlation operations.

This section describes image-processing products envisioned for SIR-B, various image processor options, and special experiments in the technology of signal correlation and image processing.

II. Image-Processing Products

Table 5-1 gives the specifications for various standard image-processing products envisioned from the SIR-B mission. Each of these are further described in the following paragraphs.

A. Quick-Look Digital Processing

Quick-look digital images are to be generated during the mission from data relayed through the TDRS link. Signal data will be transmitted to JPL from GSFC and JSC via courier or transmission link. The signal data will then be processed by a quick-look low-resolution algorithm and placed on either film or video tape for viewing. The purpose of these images is to ascertain the general health of the radar and the general data quality. The goal is to complete the images within 24 hours after acquisition to support any necessary adjustments to the radar for subsequent data acquisition.

B. Survey Processing

The survey optical images are generated from the digital data by the optical processor. The high-density digital tapes are converted to film through a digital to analog converter and processed in a manner similar to the flight optical images. In order to speed processing, the images will not be processed to the same degree of quality as the flight optical data. The potential also exists to perform the survey processing digitally at a reduced resolution of about 100 m.

This data will give experimenters an early look at their data sets in order to verify coverage and provide an indication of the image quality. It will also aid in the selection of data to be digitally processed to standard product form. Although a complete set of this survey data will be kept at JPL, experimenters will receive only their specific data sets because of the large quantity of film involved.

C. Flight Optical Processing

The flight optical images are to be generated from the optical signal film recorded onboard the shuttle. This onboard recording capability can be used as a backup to the TDRS link in the event the shuttle is in a link blind spot. These images will be very similar to the SIR-A data with variations in range

Table 5-1. Standard product specification

Product \ Parameter[a]	Ground-Range Resolution, m	Azimuth Resolution and Number of Looks	Radiometric Calibration	Image Geometry	Image Location	Image Media	Dynamic Range Point Targets, dB	Distributed Targets, dB	Data Quantity and Processing Period
Quick-look digital	100	100 m 1 look	None	Slant range with Doppler	None	Print on TV monitor	30	10	Several frames during mission
Survey optical	30 – 100	50 m 4 look	None	Slant range with Doppler	None	Positive film and print, 5 in.	17	12	All 25 h (digital) during first 6 mo
Flight optical	30 – 100	40 m 6 look	None	Slant range within 38 of 500,000:1 map	None	Positive film and print, 5 in.	17	12	8 h during first 12 mo
Standard digital	15 – 55	25 m 4 look	~1 dB (relative)	Correct to within ~100 m, 10-m pixels sampled cross-track and along-track	To ~1 km[b]	100-km frames on 1600 bpi and 8 × 10 film and print	45	10-30 dependent on look angle and number of bits	Minutes; first 6 mo 4 h: 1985 6 h: 1986

[a]Variations are functions of look angle.
[b]Location and geometric errors are primarily due to shuttle orbit knowledge errors.

resolution due to the different incidence angles possible with SIR-B.

D. Standard Digital Processing

The standard digital images are those processed on the IDP from the High Density Digital Tape (HDDT) data. Most of the geoscientific experiments discussed in Section 3 will be conducted using these images as they have the best spatial resolution and are the only images with radiometric and geometric calibration.

III. Image Processor Options

Several image processor options could be implemented as part of the SIR-B mission if there is sufficient justification. These are described below.

A. Selectable Dynamic Range

Some geoscientific experiments may require an enhancement of various parts of the dynamic range. This optional processing involves both the correlation process and output image representation. The current Seasat processor limits the output after range compression to 8 bits. At this point it would be desirable to allow arbitrary selection of the "exponent," i.e., which of the 8 bits are retained. The image output is again limited to 8 bits. Various selectable output representations such as amplitude intensity, amplitude squared intensity, etc., may be of use for different applications. It may also be desirable and possible to retain more than 8 bits at the output, although throughput and tape storage capability will be reduced.

B. Complex Output

This processing option for either I-Q or polar form of the complex output is related to the previous one since it involves output data representation. The output images could be recorded without the detection process. For multilook processing, either one of the center looks or all of the looks would be represented, but the latter case would require larger tape storage. If desired, the complex pixels could be added although this would slow the processor. The I-Q form would be the normal output, and the polar form would require additional computations.

C. Uncorrected Output

Some experimenters may wish to perform their own geometric and/or radiometric corrections. Although the standard data products will already be corrected, it is possible to process the data without these corrections. As an example, a cartographic rectification experiment may require data in a slant-range rather than a ground-range format.

IV. Correlation and Image-Processing Experiments

Several data processing experiments are possible with SIR-B which would be very valuable in future spaceborne radar designs. These experiments include both correlation and image processing.

A. Multilook Processing

The standard SIR-B image product will be processed to 4 looks at 25-m resolution. However, a very useful correlation experiment would be to process the images to a larger or smaller number of looks with an increase or decrease in the resolution cell size. Implementing several different algorithms for various numbers of looks would not be possible, due to funding limitations. A single-look 6-m resolution mode may be desirable. Looks would then be taken in the image domain by spatial filtering as an image-processing experiment. This multilook technique provides more speckle noise reduction by up to a factor of two over the multilook correlation technique. However, single-look processing reduces throughput by about a factor of three over 4-look processing.

B. Cartographic Rectification

This image-processing experiment would correct the layover distortion in the image caused by altitude variations. A digital topographic map is required to determine the necessary corrections. The data will normally be corrected for geometry and location at a single altitude. This process will be necessary before extensive pixel by pixel comparisons can be made between different phases or different data sets.

C. Latitude-Longitude Resampling

This process would resample the data to lines of constant latitude and longitude as opposed to the standard cross-track and along-track representations. This could facilitate merging with other data sets such as Landsat–4 TM. This process might also be useful for comparing ascending to descending passes.

D. Data Merging

The process of overlaying various digital data sets is of considerable interest to the remote sensing community. If this is to be done on a pixel by pixel basis, geometric and cartographic corrections will be required. Errors in the STS orbit will preclude geometric corrections at accuracies of a pixel or less, so that "rubber-sheeting" processes will be required for pixel by pixel data merging.

E. Image Domain Filtering

This is intended as an image-processing experiment for processes which alter the resolution, spectral content, amplitude distribution speckle characteristics, etc. As previously mentioned, speckle reduction can be achieved most effectively by image domain filtering. Other experiments include high-pass filtering to emphasize boundaries and directional filtering to enhance periodic structures such as ocean waves.

Section 6
SIR-B Ancillary Data Support Requirements

I. Introduction

This section outlines requirements for ancillary data necessary to support the SIR-B mission.

II. Ancillary Data Needed for Verification and Assessment of Imaging Radar Studies

In order to assure the successful completion of the proposed experiments, it is necessary that ancillary data, in the form of *in-situ* ground truth and other remote sensing data, be obtained or readily available for the study areas. Some of the basic needs for ancillary data are suggested in the following subsections. Although the listing does not emphasize in detail the simultaneity of these data, it is obvious that for studies dealing with rapidly changing phenomena (oceans, hydrology, vegetation, etc.), these data need to be obtained within a time frame which is compatible with the stated experiment objectives.

A. Geography

Geography experiments will require accurate mapping information for experiment sites and can benefit from satellite and aircraft photographic and radar scatterometer data as well. A moderately detailed table (Table 6-1) is provided as an example of how each of these ancillary data resources might apply to experiments in geology.

B. Geology

SIR-B geology experiments will utilize ground-based and other ancillary remotely sensed information. Ground-based measurements will include digital topographic data, field survey information, soil moisture measurements, and dielectric constant measurements for field samples. Aircraft measurements would include radar scatterometry, multispectral scanner data, SAR imagery, photography, and profilimetry. Satellite remote sensing ancillary data sources would include the Landsat-4 TM and MSS, thermal infrared imagery from civil or military meteorological satellites, and the shuttle-based large format camera.

C. Hydrology and Oceanography

Hydrologic and oceanographic experiments will require many of the same satellite and airborne measurements as the previous experiments but for the express purpose of viewing surface wave and wind/wave structure. Special emphasis should be given to airborne scatterometer measurements at L- and X-band and possibly short-pulse wave spectra measurements. Hydrologic and oceanic measurements are very sensitive to near simultaneous measurement coordination.

In-situ measurements include current, wind, and wave spectral information, at the experiment site, coordinated with SIR-B overflights. Bottom topography (bathymetry) sedimentation and subsurface flow information are important to several suggested experiments.

D. Vegetation

In the case of the vegetation experiments, the standard of comparison for evaluating the performance of any procedure to extract information from the SAR data will be the corresponding performance with Landsat/MSS or TM data. It is not likely that the SIR-B and Landsat/MSS or TM image data would be collected over a given site on the same day, or at the same time of day even if collected on the same day. Such synoptic data are not required and are certainly not practical in an operational sensor where MSS or TM data are gathered at nadir and SAR data are gathered off nadir. Nevertheless, investigators will want to have both SIR-B data and Landsat/

Table 6-1. Ancillary data sets needed for successful completion of candidate experiments

Experiment	Cartography[a]	Deforestation/ Clear-Cutting[b]	Geomorphology[c]	Land Cover/ Land Use[d]
Gestalt photomapper/digital terrain models	X		X	X
Ground control points	X		X	X
High-altitude black and white aerial photography		X[f]	X[f]	
High-altitude color infrared (CIR) aerial photography	X	X[e]	X[e]	X
Landsat data		X	X	X
1:24,000-1:50,000 topographic maps	X[h]		X	X[h]
1:50,000-1:100,000 topographic maps		X[g]	X[g]	X
1:100,000-1:250,000 topographic maps		X	X	X
Aircraft SAR imagery		X	X	X
Aircraft scatterometer data		X		X
Large format camera data (from SIR-B)	X	X	X	X
Ground truth		X	X	X
SIR-B spotlight mode				X
SIR-B squint mode			X	X

Notes:

[a] U.S.

[b] U.S. and tropics.

[c] Worldwide.

[d] U.S. and developing countries.

[e] Preferred aerial photography.

[f] Acceptable aerial photography.

[g] ±2 years of SIR-B data acquisition.

[h] ±7 years of SIR-B data acquisition.

MSS or TM data taken over their test sites within the same general period of time.

Aircraft ancillary data are also important. As stated above, the configuration of SIR-B is quite limiting especially for vegetation experiments. SIR-B will not be able to gather data at multiple wavelengths using multiple polarizations, and it will be limited to only a 7-day period of time. To provide a basis for understanding SIR-B data in the context of general radar data, it will be necessary to conduct aircraft-based experiments over at least some of the same test sites with multifrequency, multipolarization, and multiangle radar scatterometers. These flights should take place throughout the growing season. Such joint experiments between aircraft and spacecraft radar sensors are necessary to provide a basis for the calibration of the spacecraft SAR and to provide a basis for understanding the SIR-B data in the context of more extensive radar data collected over the same test site.

References

Batlivala, P. P. and Ulaby, F. T. *Crop Identification From Radar Imaging of the Huntington County, Indiana Test Site*, RSL Technical Report 177-58, November 1975.

de Loor, G. P. and Hoogeboom, P. Radar Backscatter Measurements From Platform Noordivyk in the North Sea, *IEEE Journal of Oceanographic Engineering, OE-7*(1), pp. 15-20, January 1982.

Eagleson, P. S. *Dynamic Hydrology*. McGraw-Hill Publishing Co., N.Y. 1970.

Paris, J. F. Crop Classification With Multifrequency, Multipolarization, and Multiangle Radars, *8th International Symposium on Machine Processing of Remotely Sensed Data*, Purdue University, 1982.

Riom, J. and LeToan, T. Relations Entre des Types de Forêts de Pins Maritimes et la Rétrodiffusion Radar en Bande L, *Digest of ISP*, Spectral Signatures of Objects in Remote Sensing, Avignon, France, September 8–11, 1981.

Shanmugan, K. S., et al. Textural Features for Radar Image Analysis, *IEEE Transactions on Geoscience and Remote Sensing, GE*-19(3), July 1981.

Ulaby, F. T. and Bush, T. F. Corn Growth as Monitored by Radar, RSL Technical Report 177-57, *IEEE Transactions on Antennas and Propagation*, November 1976.

Ulaby, F. T. and Eger, F. *A Three-Part Geometric Model to Predict the Radar Backscatter From Wheat, Corn, and Sorghum*, RSL Technical Report 360-18, April 1982.

Wu, S. T. Analysis of Results Obtained From Integration of Landsat Multispectral Scanner and Seasat Synthetic Aperture Radar Data, *National Space Technologies Laboratories Report 189*, Earth Resources Laboratory, February 1982.

Appendix A
Principles of Radar Backscatter

Figure A-1 demonstrates some of the principles used to describe radar backscatter. A radar wave obliquely incident on a large electrically smooth conducting surface will be reflected away at an angle equal to the incidence angle. If the surface becomes slightly rough then the energy is scattered in all directions, although it will still be concentrated along the reflected angle direction, i.e., the specular direction. If the surface is quite rough, then the scattered energy will show little dependence on angle and will appear along all directions. Surface roughness depends on the rms height H with respect to a wavelength λ and also the incidence angle θ_i. A convenient rule of thumb is the Rayleigh criterion which states that a surface can be considered rough if the rms height exceeds one-eighth of a wavelength divided by the cosine of the incidence angle. This means that the surface becomes smoother at near-grazing incidence and that at any angle the surface becomes rougher at higher frequencies. Table A-1 provides a comparison of surface roughness as a function of λ, assuming normal incidence.

At normal incidence, this would mean that at the SIR-B L-band frequency (23-cm wavelength), a surface with an rms roughness greater than 8 cm would appear to be rough. It should be noted that the rms roughness is with respect to a horizontal plane and that the above criterion does not consider large-scale slope or topography.

The radar cross section σ is a fundamental measure of the intensity of radar backscatter from a point target, such as a corner reflector. The radar cross section of a point target is the area of an equivalent isotropic scatterer which produces the same power density at the radar receiver as does the actual target. The radar scattering coefficient σ° is used to characterize the backscatter intensity from extended scenes such as agricultural fields or an oceanic surface; it is the average radar cross section per unit area. This dimensionless

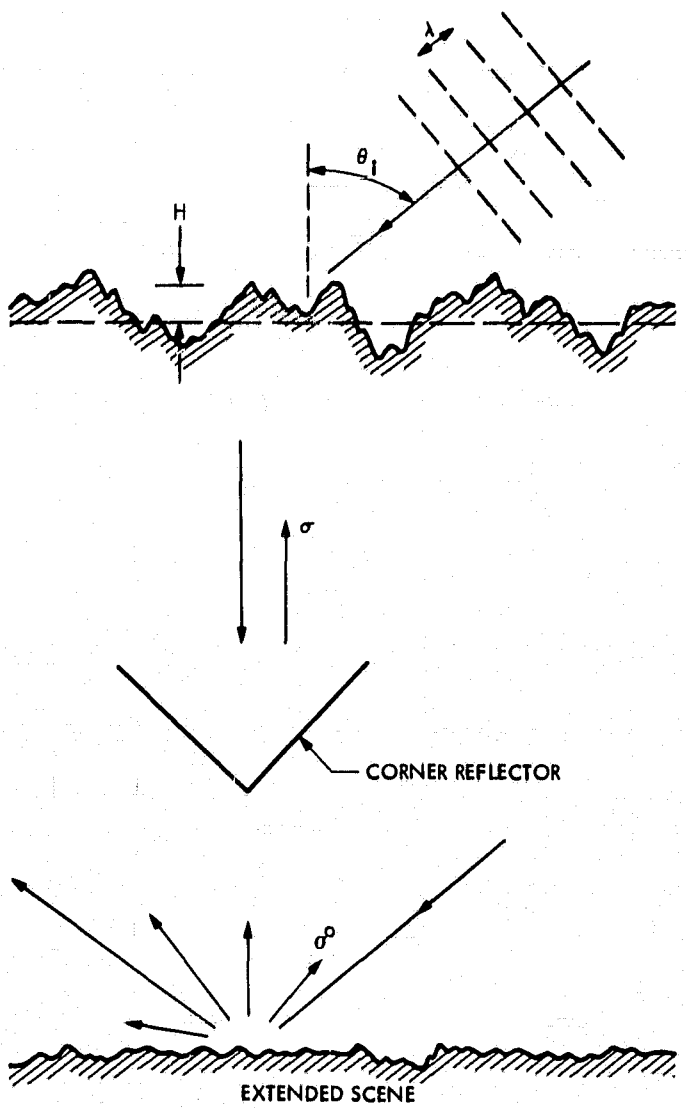

Fig. A-1. Radar backscatter principles

Table A-1. Surface roughness

Roughness Category	K_u-band, cm (λ = 0.86 cm)	X-band, cm (λ = 3 cm)	L-band, cm (λ = 25 cm)
Smooth	$h < 0.05$	$h < 0.17$	$h < 1.41$
Intermediate	$h = 0.05 - 0.28$	$h = 0.17 - 0.96$	$h = 1.41 - 8.04$
Rough	$h > 0.28$	$h > 0.96$	$h > 8.04$

quantity σ° may vary over several orders of magnitude and is therefore usually expressed in dB as ten times the logarithm of the average radar cross section per unit area.

The radar scattering coefficient is the fundamental measure used to characterize quantitatively the backscattering from extended scenes. It depends on two kinds of factors:

(1) Scene parameters (e.g., surface geometry, near-subsurface granularity, soil moisture, vegetation cover, and moisture content, etc.).

(2) Illumination parameters (incidence angle, azimuth angle, wavelength, and polarization).

Hence, the general problem in radar remote sensing is to select the illumination parameters so that the desired scene parameters can be inferred. This is accomplished by the use of signature models that can be analytical, empirical, or a combination. Figure A-2 illustrates the general dependence of the radar scattering coefficient on the small-scale surface roughness (and subsurface characteristics) and the incidence angle. Surfaces that are smooth relative to the wavelength show a rapid decrease in scattering coefficient with angle of incidence, whereas surfaces that are rough have a scattering coefficient that varies little with angle.

In reality, surfaces are not as simple in form as described above. Composite surfaces are the most common type of rough surface at microwave frequencies, and many geological surfaces are good examples of composite surfaces. Large-scale features scatter specularly in a facet-like manner. The return from many facets could be almost completely incoherent. The smaller scale roughness variations on top of them further redistribute the scattered energy and might fill in where specular scattered power is at a minimum. This contribution is sometimes referred to as the "diffuse component" by radar

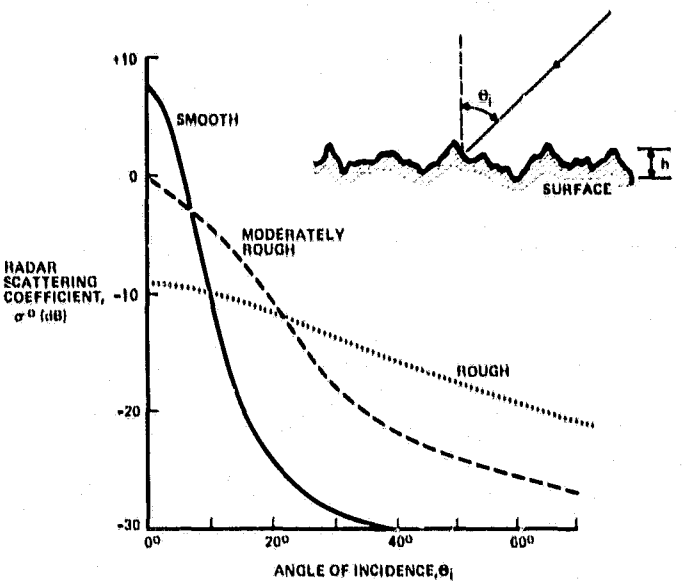

Fig. A-2. Dependence of radar scattering coefficient on surface roughness

experimentalists. Both types of roughness scatter only incoherently since the coherent component is suppressed by the large-scale random roughness. Both types of roughness are for the most part statistically independent in nature.

For backscattering, the large-scale roughness produces a maximum in the energy along the normal to the planar surface, while the smaller scale roughness backscatters most near the grazing angle. The reason for this is that the largest scales of roughness in natural surfaces are usually the most gently sloping and their local normal deviates little from the mean surface normal.

SIR-B is the first major space imaging radar designed specifically so that the illumination parameter of incidence angle can be controlled for inferring scene parameters sensitive to illumination geometry; although SIR-B uses a fixed wavelength and polarization, it will allow a major advance in quantitative analyses of extended scene signatures which can be used for inference of such scene parameters as geological structure, soil moisture, or urban/rural boundaries. Future NASA imaging radar missions will provide variable wavelength and polarization imagery for additional illumination parameter control.

Appendix B

SIR-B Data Acquisition Scenarios

I. Orbit Configuration

STS-17 will be launched into a nominally circular orbit at an inclination of 57 deg and an average altitude of 337 km for the first 26 to 28 hours and 229 km for the duration of the mission. For the majority of the mission at the 229-km altitude, this will result in a 1-day repeat cycle with a westward drift of 216 km at the equator each day. From one orbit to the next, the ground track will drift westward by 2500 km. This orbit configuration will allow SIR-B to image a given site at six different look angles, one for each day at latitudes between ±60 deg. It will however result in a 10-deg gap between the first and last ground tracks at the equator (see Fig. B-1).

On OSTA-3, MAPS has a coverage requirement of approximately 5-deg intervals. It is in order to satisfy this requirement that STS-17 will first fly at an altitude of 337 km for the first 26 to 28 hours after OMS-4. This altitude results in a 2-day repeat cycle on the ground and will fill in the gaps between the first and last orbits of the nominal 229-km, 1-day repeat cycle mode (see Fig. B-1). After these 26 to 28 hours at 337 km

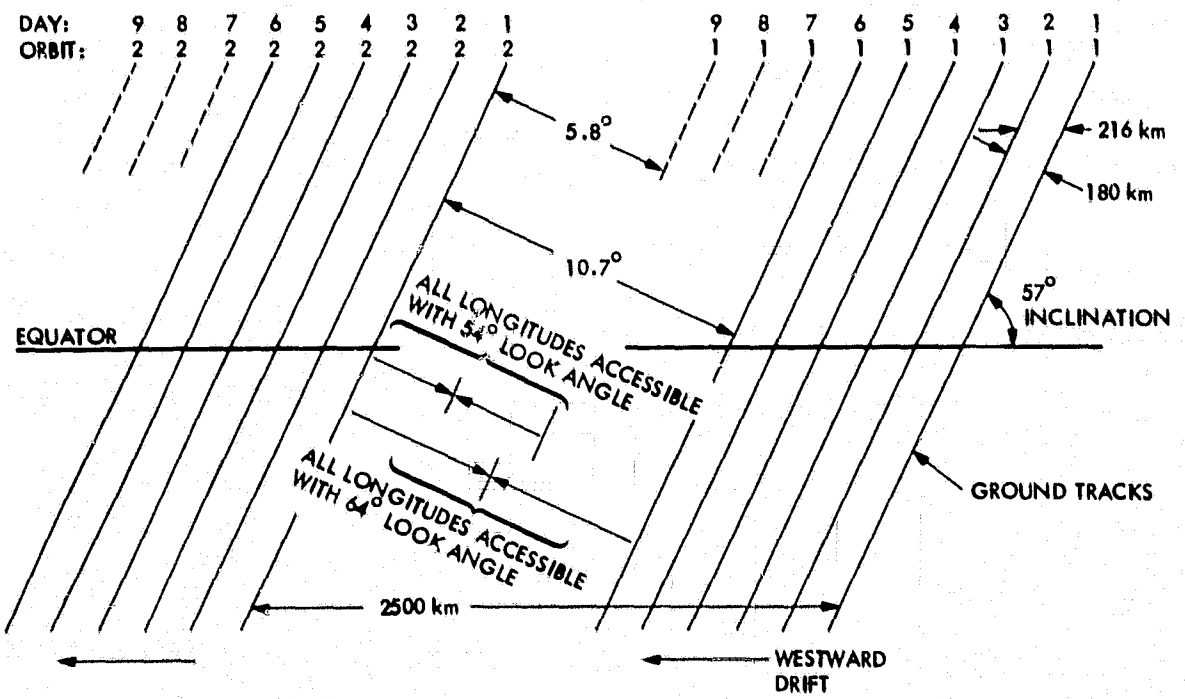

Fig. B-1. OSTA-3 orbit plan

have been completed, an OMS burn will decrease the altitude of the shuttle to 229 km. The time required to change altitude from 337 km to 229 km is about 45 minutes (half an orbit) during which time no data taking will be possible. The SIR-B antenna will be folded and the payload bay doors will be closed.

Figure B-2 shows the ground tracks at the two altitudes. These tracks have not been correlated with the actual OMS-4 burn, therefore the node may shift left or right. Figure B-2(a) shows the first 28 hours after OMS-4 at an altitude of 337 km. Figure B-2(b) shows the next six days at an altitude of 229 km. Figure B-2(c) is a superposition of Figs. B-2(a) and (b) showing the sound tracks for the entire mission. Note that the 337-km tracks do indeed fill in the gaps between the 229-km tracks.

II. TDRS Coverage

All digital data acquired by SIR-B on the OSTA-3 flight will be sent to the ground through the TDRS K_u-band antenna. There is only one K_u-band antenna on the shuttle and it is mounted in the payload bay; therefore, in the nose forward, -ZLV attitude, TDRS access is limited to about 30 percent of the time due to blockage by the orbiter itself. It is also possible to fly in a tail forward, -ZLV attitude without impacting the other experiments. In this mode, TDRS access is again about 30 percent, although with an increase in coverage of sites in the U.S. and Africa. The tail forward, -ZLV attitude has been chosen as the nominal mode for STS-17. The SIR-B antenna will be looking on the south side of the shuttle ground track in this attitude.

In order to acquire digital imagery over scientifically interesting sites, several maneuvers may be carried out which do not impact SIR-B data acquisition. The simplest is a roll of 90 deg such that the SIR-B antenna is imaging on the north side of the shuttle ground track (see Fig. B-3). This maneuver requires about 15 minutes to accomplish and would be conducted over the ocean whenever possible. In this attitude, all other experiements (LFC, MAPS, FILE) will not be able to acquire data.

In many cases, TDRS is still inaccessible even in the rolled attitude. A 180-deg yaw or a 180-deg yaw plus a 90-deg roll may also be done (see Fig. B-3). These maneuvers require about 30 minutes to accomplish and would also be conducted over the ocean. In the yawed attitude, SIR-B will be imaging north of the shuttle ground track, and in the yawed and rolled attitude, data will be acquired south of the ground track. In the yawed attitude, the LFC will not be able to acquire data due to the mechanics of its motion compensation technique. In the yawed and rolled attitude, all experiments are out of attitude except SIR-B.

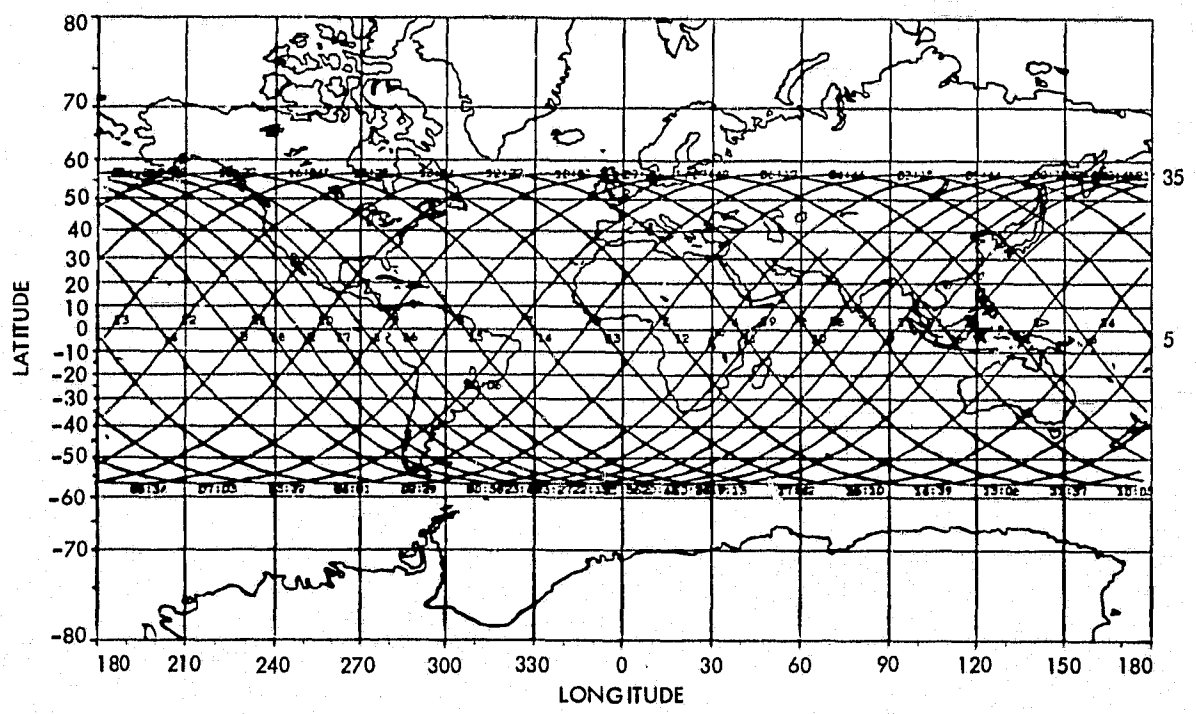

Fig. B-2(a). Shuttle ground track for first 28 hours after OMS-4 at 337-km altitude

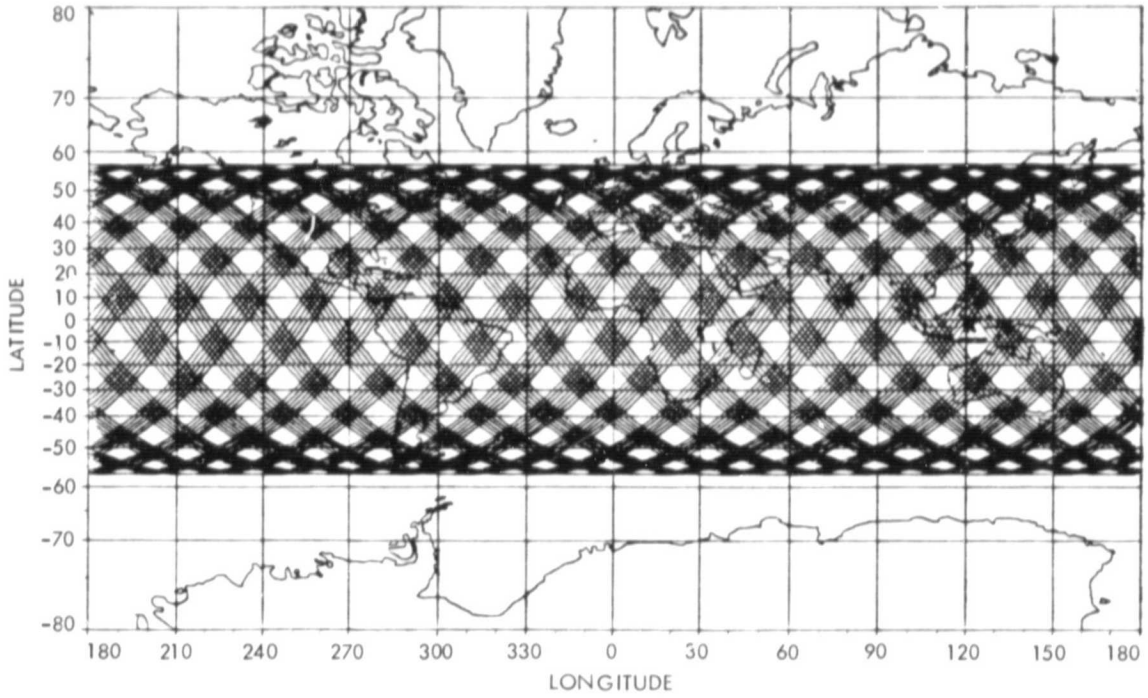

Fig. B-2(b). Shuttle ground tracks for six days after altitude decrease maneuver

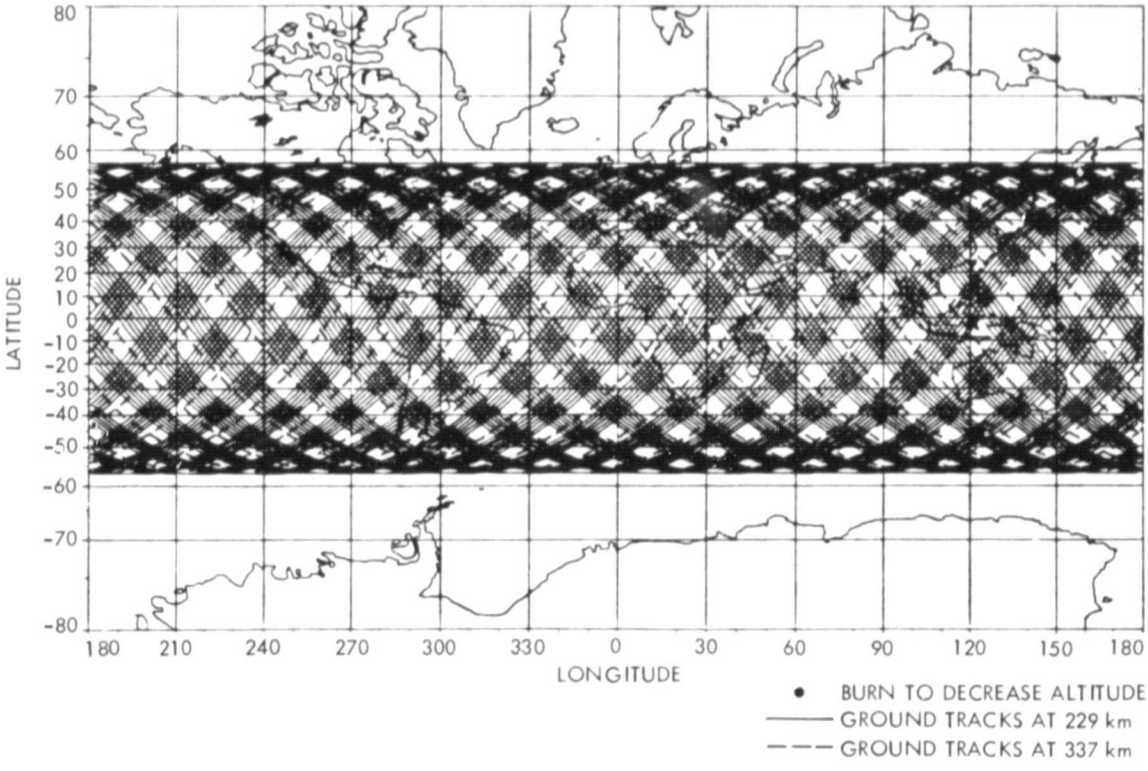

Fig. B-2(c). Ground tracks for entire mission after OMS-4 burn

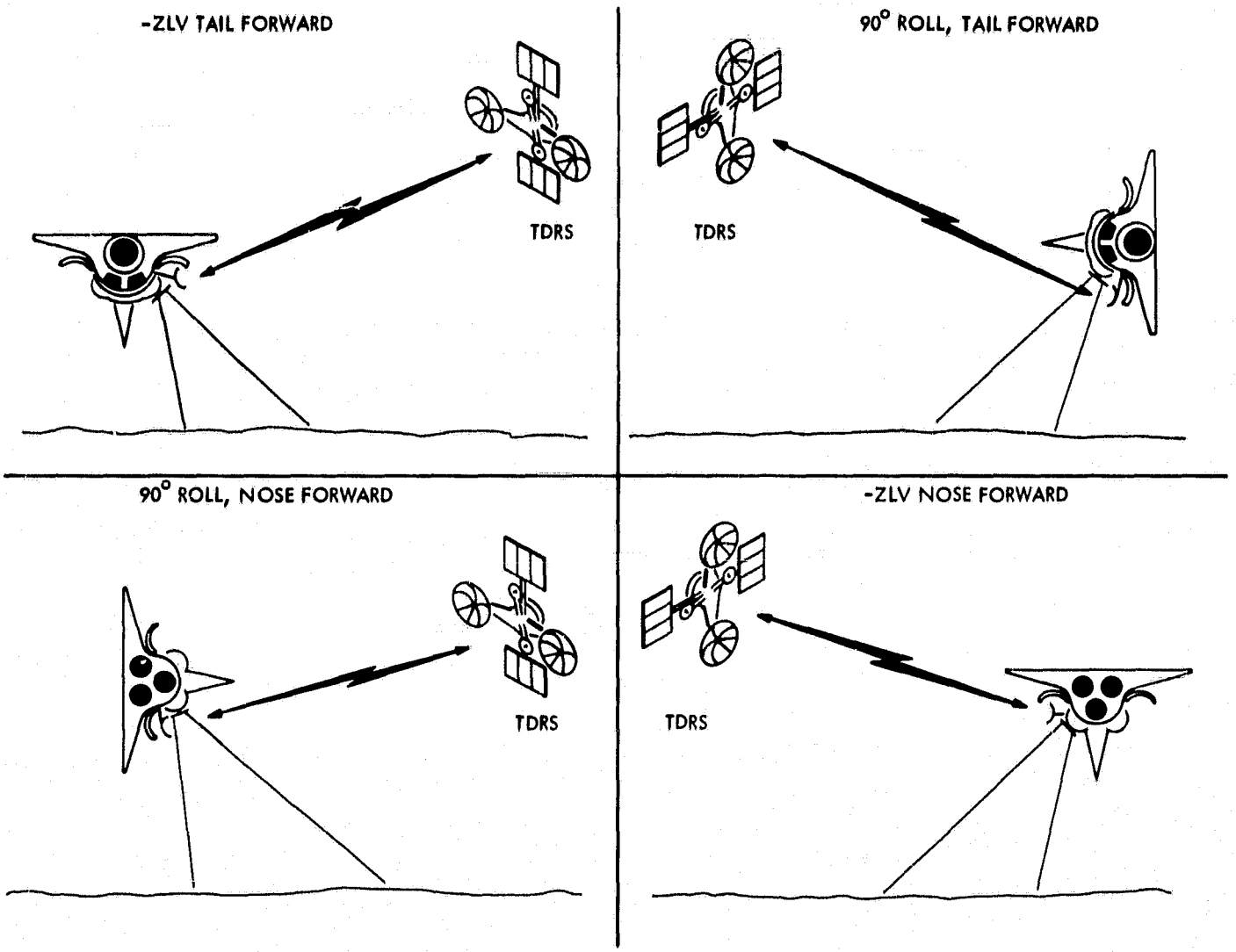

Fig. B-3. SIR-B data acquisition attitude

Figures B–4(a) through (d) show the TDRS access in each of the above attitudes for a 24-hour period at a 229-km altitude. Orbit tracks with dots have access to TDRS; those tracks without dots indicate TDRS blockage by the shuttle. Since the node location is not necessarily correct, the ground tracks may shift left or right for the actual missions.

An attempt was made to develop a mission in which data could be acquired by SIR–B over all landmasses within the 57-deg latitude limits. The results are shown in Fig. B–5. When TDRS was inaccessible in the nominal tail forward, -ZLV mode, a 90-deg roll was chosen because it requires the least maneuvering time. As a second choice, a 180-deg yaw was chosen and the yawed and rolled attitude was selected only as a last resort.

This is a very preliminary mission scenario. As more accurate TDRS coverage maps are available and specific sites are selected the mission plan will be adjusted accordingly. Tradeoffs will need to be made with the other experiments (LFC, etc.) such that each instrument will be able to obtain its required data.

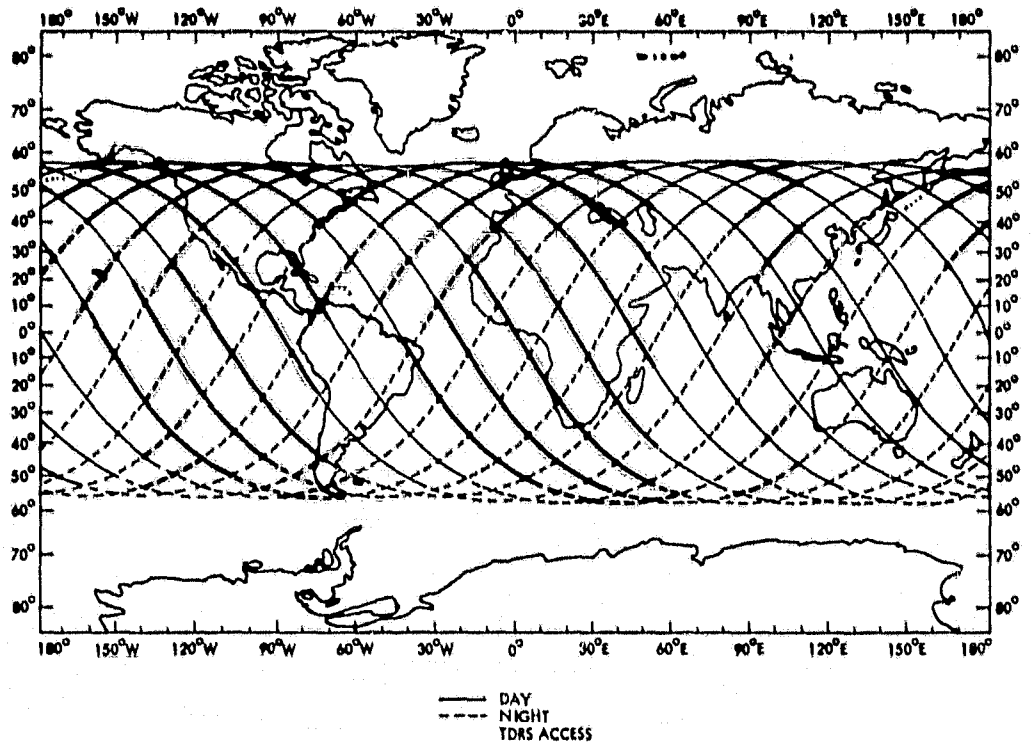

Fig. B-4(a). Shaded area indicates TDRS access in the nominal tail forward, -ZLV attitude. Sixteen orbits or 24 hours of the mission are included. Node will shift for actual mission.

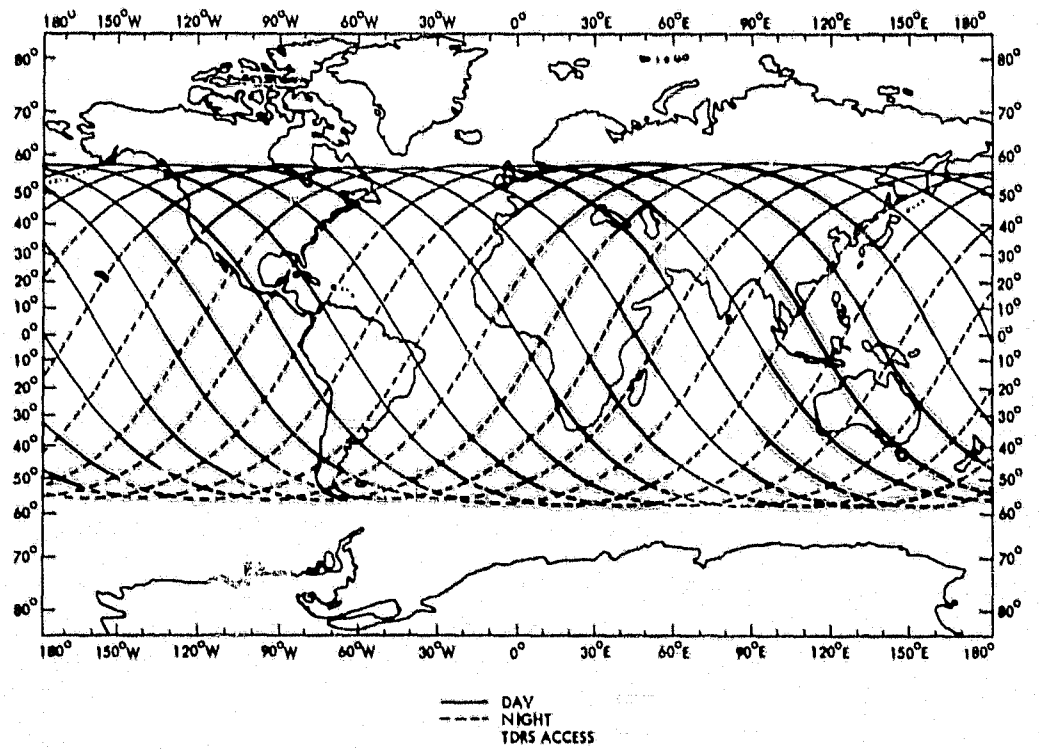

Fig. B-4(b). Shaded area indicated TDRS access in the tail forward, 90° roll attitude. Sixteen orbits or 24 hours of the mission are included. Node will shift for actual mission.

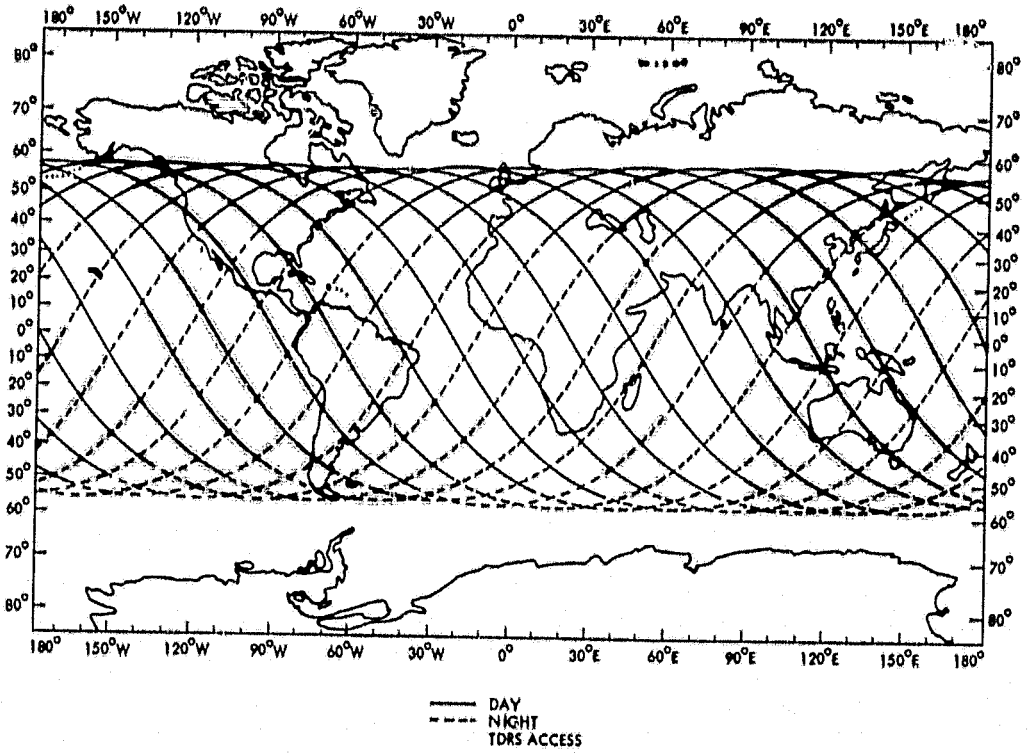

Fig. B-4(c). Shaded area indicates TDRS access in the nose forward, -ZLV attitude. Sixteen orbits or 24 hours of the mission are included. Node will shift for actual mission.

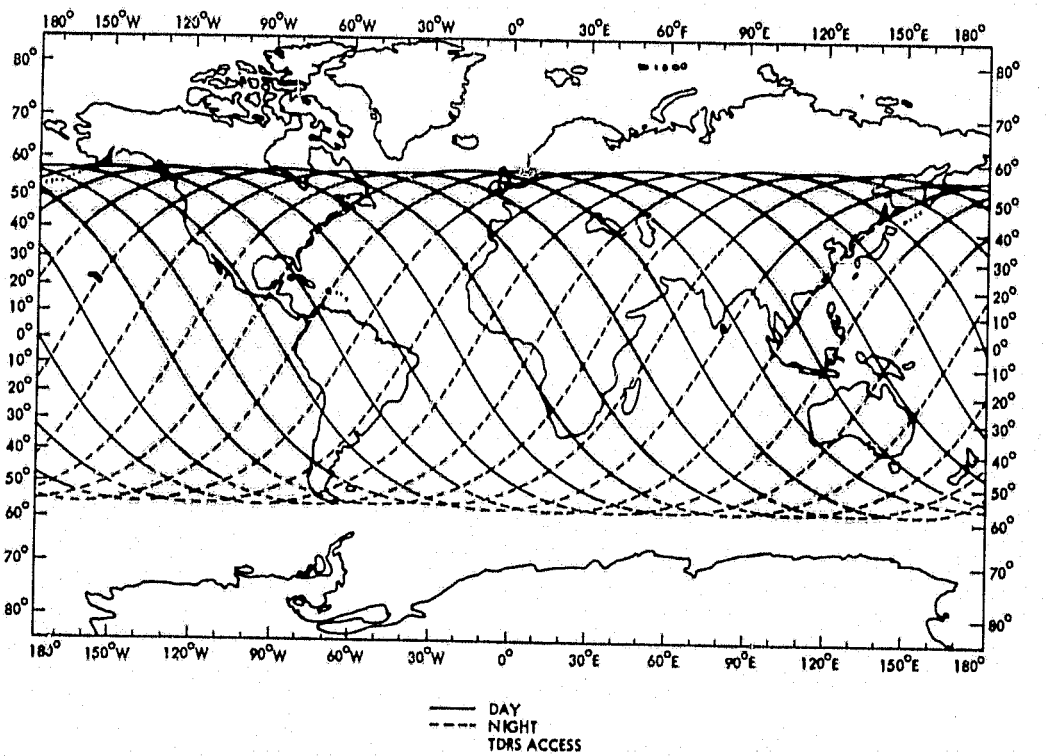

Fig. B-4(d). Shaded area indicates TDRS access in the nose forward, 90° roll attitude. Sixteen orbits or 24 hours of the mission are included. Node will shift for actual mission.

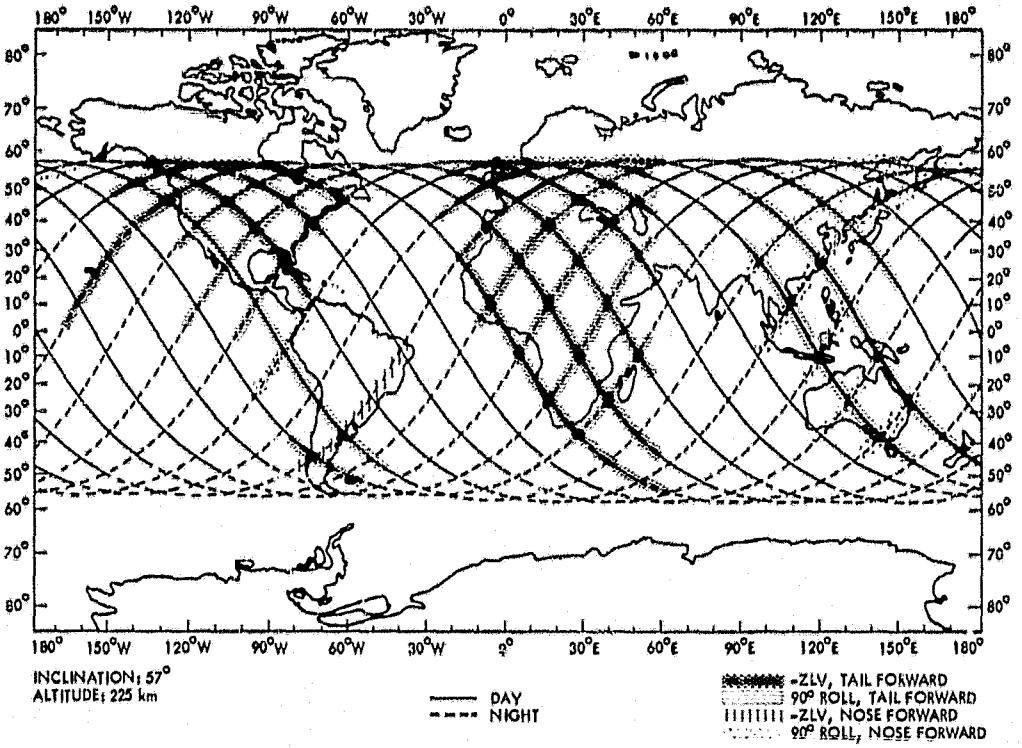

Fig. B-5. SIR-B mission requirements. Preliminary mission scenario for first 16 orbits (1 day) at 229-km altitude. Successive days will have similar TDRS coverage and therefore a similar mission scenario will apply.

Appendix C

Bibliography

_____. Advances in Instrumentation for Processing and Analysis of Photogrammetric and Remotely Sensed Data, *Proceedings, Commission II Symposium*, International Society for Photogrammetry and Remote Sensing (ISPRS), August-September 1982.

_____. Application of Remote Sensing Data on the Continental Shelf, *EARSEL-ESA Symposium Proceedings*, ESA SP-167, May 1981.

Beal, R. *The Seasat SAR Wind and Ocean Wave Monitoring Capabilities*, Johns Hopkins University, September 28, 1978.

Brisco, B. and Prontz, R. Manual and Automatic Crop Identification With Airborne Radar Imagery, *Photogrammetric Engineering and Remote Sensing, 48*(1), 1982.

Bryan, M. L. Extraction of Urban Land Cover Data From Multiplexed Synthetic Aperture Radar Imagery, *Proceedings, 9th International Symposium on Remote Sensing of Environment*, April 1974.

Bryan, M. L. The Effect of Radar Azimuth Angle on Cultural Data, *Photogrammetric Engineering and Remote Sensing*, August 1979.

Bryan, M. L. Analysis of Two Seasat Synthetic Aperture Radar Images of an Urban Scene, *Photogrammetric Engineering and Remote Sensing*, March 1982.

Bryan, M. L. Urban Land Use Classification Using Synthetic Aperture Radar, *Proceedings, Pecora VII Symposium*, October 1981.

Bryan, M. L. The Use of Radar Imagery for Surface Water Investigations, *Satellite Hydrology*, American Water Resources Assoc., 1981.

Bryan, M. L. Analysis of Two Seasat Synthetic Aperture Radar Images of an Urban Scene, *Photogrammetric Engineering and Remote Sensing, 48*(3), March 1982.

Bush, T. F. and Ulaby, F. T. *Remotely Sensing Wheat Maturation With Radar*, KU-CRES RSL, University of Kansas Center for Research, Inc., Remote Sensing Laboratory, 1975.

Bush, T. F. and Ulaby, F. T. *Radar Return From A Continuous Vegetation Canopy*, KU-CRES RSL, TR 177-56, 1975.

Bush, T. F., et al. *Radar Backscatter Properties of Milo and Soybeans*, KU-CRES RSL, TR 177-59, 1975.

Chang, A. T., et al. L-band Radar Sensing of Soil Moistures, *IEEE Transactions of Geoscience and Remote Sensing, GE-18*(4), October 1980.

Eagleson, P. S. *Dynamic Hydrology*. McGraw-Hill Publishing Co., N.Y. 1970.

Elachi, C. and Apel, J. R. *Internal Wave Observations Made With an Airborne Synthetic Aperture Imaging Radar*, Jet Propulsion Laboratory; NASA, Remote Sensing Laboratory.

Ford, J. P., et al. Seasat Views North America, the Caribbean, and Western Europe With Imaging Radar, *JPL Publication 80-67*, Jet Propulsion Laboratory, Pasadena, California, November 1980.

Frost, V. S., et al. Radar Image Pre-Process, *Remotely Sensed Data Symposium*, 1980.

Fu, L. and Holt, B. Seasat Views Oceans and Sea Ice With Synthetic Aperture Radar, *JPL Publication 81-120*, Jet Propulsion Laboratory, Pasadena, California, February 1982.

Goldfinger, A. D. Space Systems Seasat SAR Processor Signatures; Point Targets, *JHU/APL, CP 078*, April 1980.

Hardaway, G., et al. Cardinal Effect on Seasat Images of Urban Areas, *Photogrammetric Engineering and Remote Sensing*, May 1, 1981.

Henderson, F. M. and Wharton, S. W. Seasat SAR Identification of Dry Climate Urban Land Cover, *International Journal Remote Sensing, 1*(3), pp. 293–304, April 1980.

Kasischke, E. S., et al. *Detection of Bathymetric Features Using Seasat Synthetic Aperture Radar–A Feasibility Study*, ERIM Final Report No. 135900-2-F2, 1980.

Latterman, L. H. Evaluation of Remote Sensors for Exploration Geomorphology, *American Association of Petroleum Geologists Bulletin, 57*(4), April 1973.

Leberl, F. Metric Properties of Imagery Produced by Side-Looking Airborne Radar and Infrared Linescal Systems, *ITC Journal*, Series A/No. 50, 1971.

Leberl, F. Accuracy Analysis of Stereo Side-Looking Radar, *Photogrammetric Engineering and Remote Sensing, 45*(8), August 1979.

Lee, J. Speckle Analysis and Smoothing of Synthetic Aperture Radar Images, *Computer Graphics and Image Processing 17*, pp. 24–32, 1981.

Leighty, R. D. Terrain Information From High Altitude Side-Looking Radar Imagery of an Arctic Area, *Proceedings, Fourth Symposium on Remote Sensing of the Environment*, 1966.

LeToan, T. and Riom, J. Effet de la Direction des Rangs de Semis de Mais sur la Response Radar en Bande L. *Teledetection Hyper-frequences Journale*, G.D.T.A., 1980.

Levine, *Radargrammetry*, McGraw-Hill Publishing Co., N.Y. 1960.

MacDonald, H. C. and Waite, W. P. Imaging Radars Provide Terrain Texture and Roughness Parameters in Semi-Arid Environments, *Modern Geology, 4*, 1973.

MacDonald, H. C., et al. Use of Seasat Satellite Radar Imagery for the Detection of Standing Water Beneath Forest Vegetation, Technical Papers, *American Society of Photogrammetry Fall Meeting*, N.Y., October 1981.

McCandless, S. W. Radar Remote Sensing and Offshore Technology, *Offshore Technology Conference*, OTC 3718, 1980.

McCandless, S. W. and Mader, G. L. Space-Based Topographic Mapping Experiment Using Seasat–Synthetic Aperture Radar and Landsat–3 Return Beam Vidicon Imagery, *IEEE Conference, International Geoscience and Remote Sensing Symposium (IGARSS)*, July 1981.

Mattie, M. G. and Harris, D. L. Chapter 8–The Use of Imaging Radar in Studying Ocean Waves. *Proceedings of the 16th Coastal Engineering Conference*, ASCE/Hamburg, West Germany, August–September 1978.

Montgomery, D. R. Seasat Data Applications by Commercial Users, *Marine Geodesy, 4*(4), 1980.

Moore, R. K. and Thomann, G. C. Imaging Radars for Geoscience Use, *IEEE Transactions on Geoscience Electronics, GE-9*(3), July 1971.

Moore, R. K. and Simonett, D. S. Potential Research and Earth Resource Studies With Orbiting Radars: Results of Recent Studies, AIAA Paper No. 67-767, *AIAA 4th Annual Meeting and Technical Display*, October 1967.

Mullins, R. A. Urban Area Analysis From Tonal Signatures on Side-Looking Airborne Radar Imagery, *Multi-Sensor Signatures of Urban Morphology Function and Evolution: Remote Sensing Environment*, UCLA, August 1968.

Nunnaly, N. R. Integrated Landscape Analysis With Radar Imagery, *Remote Sensing of Environment, 1*(1), 1969.

Paris, J. F. Crop Classification With Multifrequency, Multipolarization, and Multiangle Radars, *8th International Symposium on Machine Processing of Remotely Sensed Data*, Purdue University, 1982.

_____. Radar Geology: An Assessment—Report of the Radar Geology Workshop, *JPL Publication 80-61*, Jet Propulsion Laboratory, Pasadena, California, September 1, 1980.

Riom, J. and LeToan, T. Relations Entre des Types de Forêts de Pins Maritimes et la Rétrodiffusion Radar en Bande L, *Digest of ISP*, Spectral Signatures of Objects in Remote Sensing, Avignon, France, September 8-11, 1981.

Schaber, G. C., et al. Variations in Surface Roughness Within Death Valley, California: A Geomorphological Approach, *ITC Journal*, 1978.

_____. Seasat Special Issue I Geophysical Evaluation, *Journal of Geophysical Research, 87*(C5), American Geophysical Union, April 1982.

Shanmugan, K. S., et al. Textural Features for Radar Image Analysis, *IEEE Transactions on Geoscience and Remote Sensing, GE-19*(3), July 1981.

Shuchman, R. A. and Kasischke, E. S. The Detection of Oceanic Bottom Topographic Features Using Seasat Synthetic Aperture Radar Imagery, *Proceedings, Thirteenth International Symposium, Remote Sensing Environment*, 1979.

Shuchman, R. A., et al. Contour Strip Mine Detection and Identification With Imaging Radar, *IEEE International Radar Conference*, Ann Arbor, Michigan.

_____. Spaceborne Synthetic Aperture Radar for Oceanography, *The Johns Hopkins Oceanographic Studies, Number 7*, 1981.

Thompson, T. W., et al. Seasat SAR Cross-Section Modulation By Surface Winds: GOASEX Observations, *Geophysical Research Letters, 8*(2), February 1981.

Ulaby, F. T. and Bush, T. F. *Corn Growth As Monitored By Radar*, KU-CRES RSL, TR 177-57, 1975.

Ulaby, F. T. and Bush, T. F. Monitoring Wheat Growth With Radar, *Photogrammetric Engineering and Remote Sensing, 42*(4), pp. 577-578, 1976.

Ulaby, F. T., et al. Microwave Backscatter Dependence on Surface Roughness, Soil Moisture, and Soil Texture, *IEEE Transactions on Geoscience Electronics, GE-16*(4), pp. 286-295, 1978.

Ulaby, F. T., et al. Microwave Backscatter Dependence on Surface Roughness, Soil Moisture, and Soil Texture: Part II—Vegetation-Covered Soil, *IEEE Transactions on Geoscience Electronics*, 1979.

Valenzuela, G. R. *An Asymptotic Formulation for SAR Images of the Dynamical Ocean Surface*, Ocean Services Division, Naval Research Laboratory, May 1979.

Vesecky, J. F. and Stewart, R. H. *The Observation of Ocean Surface Phenomena Using Imagery From the Seasat Synthetic Aperture Radar: An Assessment*, Paper (2C0061).

Waite, W. P., et al. Wetland Mapping With Imaging Radar, *International Geoscience and Remote Sensing Symposium (IGARSS)*, 1981.

Wu, C., et al. An Introduction to the Interim Digital SAR Processor and the Characteristics of the Associated Seasat SAR Imagery, *JPL Publication 81-26*, Jet Propulsion Laboratory, Pasadena, California, April 1981.

Wu, S. T. *Analysis of Results Obtained From Integration of Landsat Multispectral Scanner and Seasat Synthetic Aperture Radar Data*, Report No. 189, Earth Resources Laboratory, National Space Technology Laboratories, 1981.

NASA—JPL—Comm., L.A., Calif.